Characterization of Rocky Flats and Oak Ridge Glass Containing Mixed Wastes

by

Anthony Lawrence Brinkley

B.S., Mechanical Engineering
Virginia Military Institute, 1992

Submitted to the Department of Nuclear Engineering in Partial Fulfillment of the Requirements for the Degree of

MASTER OF SCIENCE
in Nuclear Engineering
at the

Massachusetts Institute of Technology

June 1994

Signature of Author _____
Department of Nuclear Engineering
May 12, 1994

Certified by _____
Scott A. Simonson
Assistant Professor, Department of Nuclear Engineering
Thesis Supervisor

Certified by _____
Daniel R. Cohn
Senior Research Scientist & Acting Assistant Director, Plasma Fusion Center
Thesis Reader

Accepted by _____
Allan F. Henry
Professor, Department of Nuclear Engineering
Chairman, Departmental Committee on Graduate Studies

Characterization of Rocky Flats and Oak Ridge Glass

Containing Mixed Wastes

by

Anthony Lawrence Brinkley

Submitted to the department of Nuclear Engineering
on May 6, 1994 in partial fulfillment of the
requirements for the Degree of Master of Science in
Nuclear Engineering

ABSTRACT

Vitrification of radioactive and RCRA listed hazardous materials is an excellent technology for effectively immobilizing these mixed wastes. In this thesis, mixed waste from Rocky Flats plant sludge and Oak Ridge plant sludge was vitrified for this purpose. In order to understand the factors influencing glass degradation, several experiments were performed on the Rocky Flats vitrified waste: 1) a hot (KOH) fusion determined post-furnace glass compositions; 2) MCC-1 leach testing defined leach rates and degradation trends; 3) curve fitting determined the degradation mechanism; 4) SEM-EDAX analysis confirmed non-crystalline growth on the most chemically durable batches; and 5) the multivariate analysis statistically determined which variables improved or worsened chemical durability.

This thesis conducted the first MCC-1 test ever performed on low level radioactive Rocky Flats glass by testing chemical durability in room temperature and 90°C environments. Glass compositions were analyzed for 3, 7, 14, 28, 90, and 180 days in an aqueous environment. Non-radioactive glass was tested at room temperature conditions only. Rocky Flats glass was assumed to contain 16 ppm plutonium at 100% waste loading. This amount of Pu-239 was equivalent to the TRU limit of 100 nCi/gram. Thorium was used as a surrogate for plutonium.

Data were fit to diffusion and saturation limit controlled equations to better define the degradation mechanisms of various Rocky Flats compositions. Results showed that the most chemically durable glasses followed solubility limit controlled leaching and that the poorest of the glasses followed diffusion controlled leaching at room temperature and 90°C tests. It was determined that high melting temperatures (1350°C) and high levels of Fe_2O_3 (8 wt%) increased chemical durability the greatest. Leach rates of Rocky Flats glass were within one order of magnitude to that of lead-iron-phosphate glass and two orders of magnitude lower than Savannah River borosilicate glass.

Thesis Supervisor: Dr. Scott Simonson

Title: Assistant Professor of Nuclear Engineering

Table of Contents

List of Tables

List of Figures

ACKNOWLEDGMENTS

I would like to acknowledge Pacific Northwest Laboratories for giving me the opportunity to fulfill research in one of the most exciting fields today, nuclear waste management, and more specifically, vitrification of mixed nuclear wastes. The person I owe the most thanks to is my advisor, Scott Simonson, who's sagacity kept the project focused, interesting, and most of all, fun. Professor Simonson also had faith in my abilities to complete the numerous tasks set out for this research.

I would also like to thank Toni Korzan, Dave Freed, and Mark Sautman of the waste management group, who helped me learn the deep dark secrets of Microsoft word and to Mark for the help on the ICP spectrometer. To Tim Lawrence and Dan Doney, I would like to thank you for the many pranks you inspired me to commit. I would like to thank John Thomas, for purely selfish reasons, for introducing me to Objectivism.

My final gratitude goes to Virginia Military Institute (and the professors there who prepared me for solid, consistent work), the Southern Conference Athletics Committee, and the U.S. Air Force, who each provided me with a graduate scholarship.

Chapter 1

INTRODUCTION

1.1 Thesis History

This thesis was made as a result of cooperation between Pacific Northwest Laboratories (PNL) and the Nuclear Engineering department at MIT. The purpose of this particular research was to design a glass which immobilized mixed wastes from two radioactive waste sites: Rocky Flats and Oak Ridge. PNL provided the direction of the research and the composition of the wastes to be vitrified. The goal at MIT was to vary the waste loadings of these compositions and then test the chemical durability using the MCC-1P static leach test. This thesis represents the first low level Rocky Flats glass tested by the MCC-1 leach test. The facilities at MIT provided a furnace to melt the reagent chemicals into a glass, and room temperature and 90°C environments for leach testing. MIT also provided an ICP-AES to analyze leachate, and a SEM-EDAX for surface crystalline identification.

1.2 Thesis Summary

This section gives a description of the upcoming chapters in the thesis. There are five chapters in total in the following order: 1) introduction; 2) background; 3) experimental; 4) discussion and results; 5) conclusions and future work. There are seven appendices which discuss or give results on the following subjects: a) vitrification technology; b) multivariate analysis; c) graphs; d) data compilation; e) safety, f) RS/1 curve fitting results, and g) SEM-EDAX results.

The Background chapter gives an overview of literature relative to the work done on this thesis. The basics of glass properties are discussed using binary and ternary diagrams to study the effects of certain glass making oxides. Liquidus temperature is emphasized along with oxide percentages for each Rocky Flats glass composition. Following the discussion on glass properties, the basic leaching mechanisms of glass are presented in a manner that will facilitate the explanation of Rocky Flats glass leach rates. A discussion on some of the different leach tests available is given and reasons are given for preferring one leach test over another.

Following the Background chapter, the Experimental chapter looks at the procedures followed in order to produce the data for this thesis. The first step in creating glass was the batch calculation process and furnace melting. Next, the Experimental chapter shows how the glass composition was verified by using a fusion technique while

leach tests were performed on the glass samples. The final part of this chapter discusses techniques used in the inductively coupled plasma spectrometer (ICP) and SEM-EDAX analysis.

The Discussion and Results chapter is separated into five main parts. The first section discusses the glass compositions and issues and trends that were observed. The second section determines why leach rates existed as they did by using the Background chapter information. Two of the best glasses were analyzed using the scanning electron microscope (SEM) and energy dispersive auger x-ray analyzer (EDAX) before leaching and a section is devoted to these observations. The final section used the results from the multivariate analysis to reinforce past knowledge on glass oxide effects and attempts to explain any discrepancies found in these results.

This first part of the Conclusions and Future Work chapter discusses the main points of the previous chapter and draws the main conclusions of the thesis. The second part of this chapter looks at the possibility of any future work which may aid in better defining Rocky Flats glass and any other glass which may undergo similar tests.

Appendix A discusses the vitrification technology of the past and present relevant to the Rocky Flats glass compositions. A description of several vitrification plants is given and the difference in each of them discussed.

Appendix B presents the data from the multivariate analysis which were used to reinforce past knowledge on glass oxides and other information important to glass durability. The graphs which were not shown in the results chapter, and any graphs relative to the thesis but not otherwised referenced are displayed in Appendix C.

Appendix D shows how the data was manipulated for fusion results and leach test results. Appendix E was made specifically for students at MIT continuing work in the glass area. In it, a description of safety procedures for working with glass, furnaces, and acid baths are given. Curve fit values of T, F, and R^2 generated by RS/1, are presented in Appendix F. Appendix G shows micrographs and the resulting EDAX charts for two of the best glass compositions, batch 37 and 61.

Chapter 2

BACKGROUND

2.1 Chapter Summary

Wastes that contain both radioactive and RCRA listed hazardous wastes are known as mixed wastes. These wastes are being considered for vitrification in order to effectively immobilize the waste for a long period of time and/or eliminate the toxic component. This, incidentally, may reduce the volume of waste by orders of magnitude. In doing so, a vitrified waste, i.e. glass, is produced that when optimized by methods such as those presented in this study will produce a superior waste form for a repository or for potential unrestricted release.

This chapter discusses the basic characteristics of Rocky Flats and Oak Ridge mixed waste glass investigated in this thesis. The main constituents of glass, silicon, sodium, calcium, and other elements are discussed relative to their properties and effects on glass. The two types of glass made were tailored to incorporate waste compositions from Rocky Flats plant sludge and Oak Ridge plant sludge. Rocky Flats wastes were generated from the reprocessing of americium out of plutonium-239 weapons. The effects of the major oxides in these glasses are discussed in this chapter. Following this analysis is a description and history of the different theories of glass dissolution. The dissolution of glass may be measured with many different tests and the following three types of tests each have a specific purpose which will be discussed: the MCC-1P Static Leach Test; the Product Consistency Test (PCT); and the Toxicity Characteristic Leaching Procedure (TCLP). Of these three tests, the MCC-1 Leach Test was selected for use to analyze the mixed waste glass.

2.2 Glass Properties

Glass can be divided into three types of oxides: network formers, network modifiers, and intermediates. Each group has a particular function in glass making. Binary and ternary graphs of several different oxide combinations used in Rocky Flats and Oak Ridge glass are analyzed for their effects on the melt viscosity, liquidus temperature, and chemical durability. Fig. 2-1 shows the general properties of specific oxides in glass making with a more detailed description to follow. The only oxide not shown is Fe_2O_3 which would most likely be located near the Al_2O_3 line. The weight percentage of different oxides present in Rocky Flats and Oak Ridge glass are presented in Table 3-1.

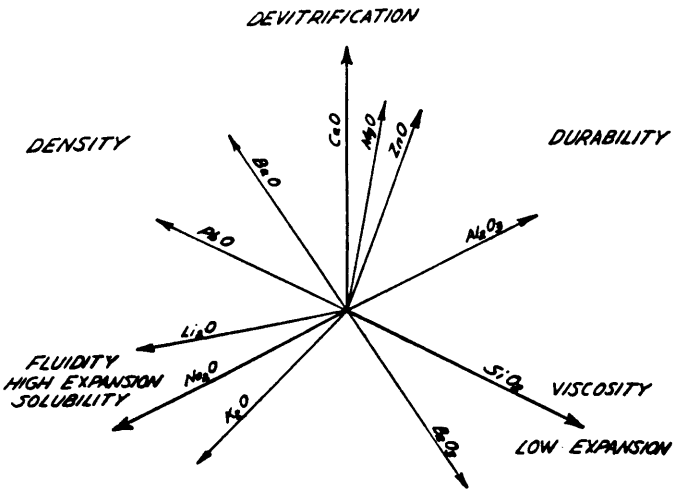

Fig. 2-1. Function of important glass oxides [1].

2.2.1 Network formers

Glass is defined as an inorganic product of fusion which has cooled to a rigid condition without crystallizing [1]. Glass atoms exhibit a random nature and do not exhibit the patterned structure of crystalline solids as shown in Fig. 2-2. The three network formers used in Rocky Flats glass were SiO_2, B_2O_3, and P_2O_5. Silicon forms a tetrahedral structure, $\equiv SiO_4$, and is surrounded by four oxygen atoms as shown in Fig. 2-3. The smaller spheres represent silicon atoms and the larger spheres are oxygen atoms. As the percentage of Silicon in glass compositions increases, so does the temperature required to melt the glass. As can be seen from Fig. 2-1, SiO_2 adds viscosity to the melt and keeps the glass from thermally expanding. Silica is the most important glass oxide as it gives molten glass viscosity and cold glass its vitreous state, as well as generally imparting chemical durability.

The oxide of boron, B_2O_3, was only used in limited attempts to reduce the melting temperature of the glass compositions studied. B_2O_3 acts as a small flux to reduce the melting temperature of the glass. At low temperatures (500-600°C), boron forms $\equiv BO_4$ groups in the glass structure. At higher temperatures, boron reduces to a trigonal plane coordination with three oxygens and becomes a network modifier and thus lowers the viscosity of the melt. The ternary diagram of CaO-B_2O_3-SiO_2 in Fig. 2-4 shows that even small additions of B_2O_3 such as that used in Batch 56 (~10% B_2O_3) reduce the liquidus temperature significantly. Because many of the Rocky Flats glass had approximately 50% SiO_2 and 20% CaO, an addition of 10% B_2O_3 should decrease the melting temperature from above 1400°C to 1200°C.

In Fig. 2-5, small additions of B_2O_3 expand the field of devitrite, a highly chemical

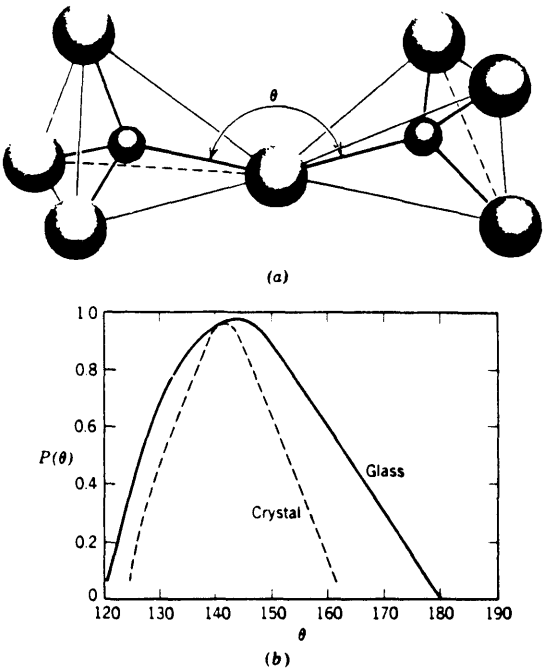

Fig. 2-2. Schematic representation of (a) ordered crystalline from and (b) random-network glassy form of the same composition. From W.D. Kingery, Bowen, and Uhlmann [10].

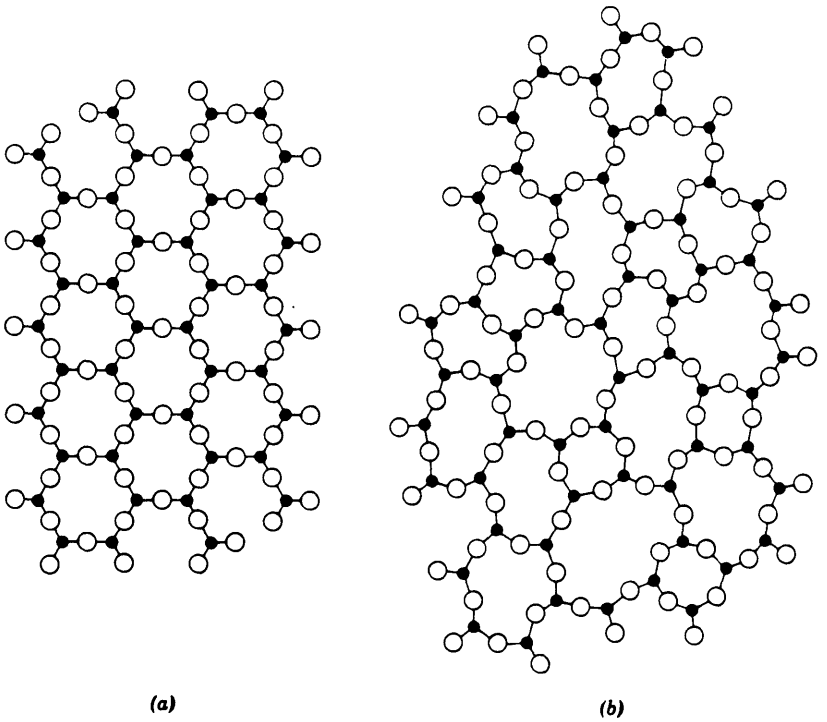

Fig. 2-3. (a) Schematic representation of adjacent SiO_4 tetrahedra showing Si-O-Si bond angle. (b) Distribution of Si-O-Si bond angles in fused silica and crystalline crystobalite. From R. L. Mozzi, Sc.D. thesis, MIT, 1967 [11].

durable phase of glass in the SiO_2-CaO-Na_2O network which is extremely reluctant to devitrify [1]. Furthermore, boron reduces the expansion of the glass and helps to give it a glassy state. It is rarely found in devitrification products and may help to stabilize other elements contained in the glass and thereby increase the chemical durability of the glass[2]. P_2O_5 was used in very small percentages in the glass and was judged to have essentially no effect on the glass properties.

2.2.2 Intermediates

Intermediates are not glasses on their own, but in the presence of network formers may act as a network former[1]. Intermediate oxides of importance used in Rocky Flats compositions were Al_2O_3, and Fe_2O_3. These oxides act as network formers in low concentrations, and increase the viscosity of the melt [3]. Al_2O_3 occurs as $\equiv AlO_4$ tetrahedra in glass. According to Fig. 2-6, small additions of Al_2O_3 between one and three percent actually decreases the viscosity of the melt by lowering the liquidus temperature. The thorium doped glass compositions (Batches 52-61) made for Rocky Flats contained an average of one to three percent. Al_2O_3 is ideal for lowering melting temperatures. This particular oxide retards crystallization and increases the chemical durability of glass when added [1].

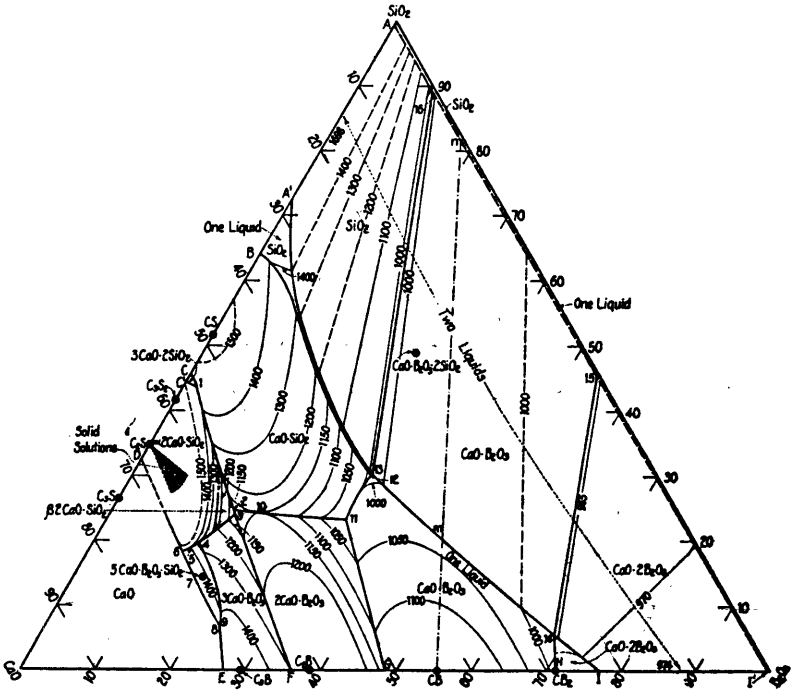

Fig. 2-4. Ternary phase equilibrium diagram of the system CaO-B_2O_3-SiO_2 with isotherms showing temperatures of complete melting. From Flint and Wells, Journal of National Bureau of Standards, Vol. 17 [12].

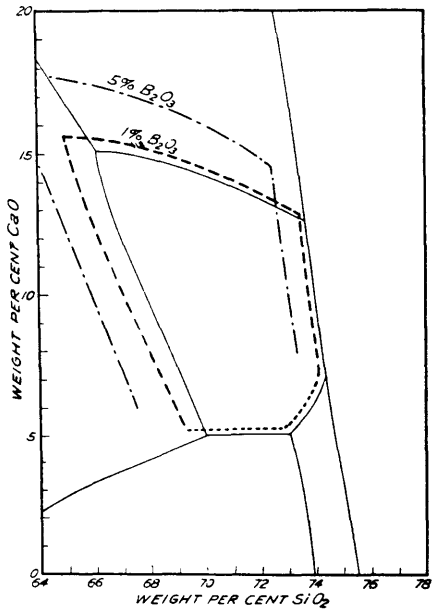

Fig. 2-5. Effect of boric oxide on the field of devitrite, $Na_2O{\cdot}3CaO{\cdot}6SiO_2$ in the Na_2O-CaO-SiO_2 system. From Morey, page 470 [13].

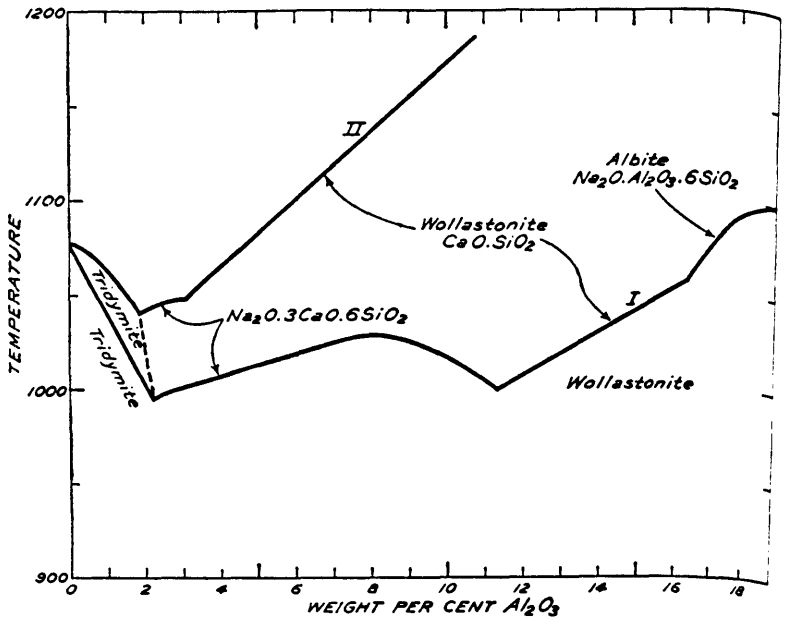

Fig. 2-6. Effect of alumina on the liquidus temperatures of some glasses in the Na_2O-CaO-SiO_2 system. From G.W. Morey, J. Am. Ceram. Soc., 15, 457 (1932) [14].

2.2.3 Network modifiers

Network modifiers are characterized by oxides which tend to decrease the liquidus temperature of melts and add favorable processing properties to the glass although other

properties may degrade. The balance of the oxides may be considered to act as network modifiers in the Rocky Flats and Oak Ridge system and are only considered when present in significant amounts: Na_2O, MgO, CaO.

Na_2O, also known as soda, acts as a network modifier by weakening the silicate structure in the glass and increasing its solubility in water. It is the main flux used in glass production. When present in glass, Na^+ ions are sandwiched in between the SiO_4 tetrahedral structure as shown in Fig. 2-7. No one unit in this structure is repeated at regular intervals in this system. When other network modifiers are added to glass, they also take up a position similar to that of sodium ions. Fig. 2-8 is a binary phase equilibrium diagram of the Na_2O-SiO_2 system. The dark line represents the melting point at various compositions. The minimum temperature (788°C) is reached at a 74% SiO_2-26% Na_2O composition. Any additional silicon added at this point increases the melting temperature sharply to the melting point of pure silica, 1713°C. However, no less than 46% SiO_2 can be added before the temperature starts to climb again. Rocky Flats and Oak Ridge glass silicon to sodium ratios averaged from 1.67 to 3.97 which corresponds to approximately 62% SiO_2 (melting point at 837°C) and 80% SiO_2 (melting point at 1100°C), respectively.

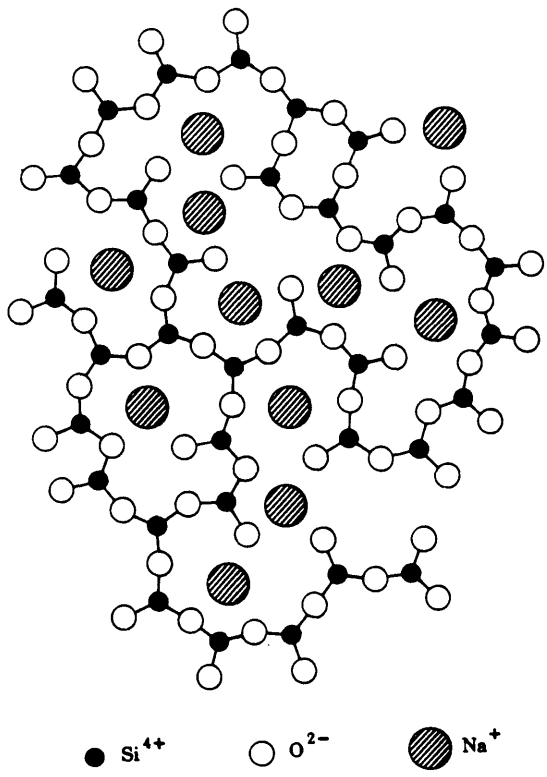

Fig. 2-7. Schematic representation of the structure of the sodium silicate glass. From W.D. Kingery, Bowen, and Uhlmann [10].

CaO, also known as lime, acts as a modifier and lowers the melting temperature of glass (but only in a certain range of wt%) by weakening the structure of the melt at high temperatures (1000-1300°C) which decreases the viscosity. The binary phase equilibrium diagram of the CaO-SiO_2 system is shown in Fig. 2-9. The range where calcium is most effective in reducing temperatures is from 43% to 63% SiO_2. The melting temperature at these concentrations ranges from 1455°C up to a maximum of 1544°C (51% SiO_2) and back down to 1436°C. Above and below these percentages, the melting temperature shoots up to above 2000°C. The addition of small amounts of CaO helps to retard devitrification [1, 2]. Large amounts of calcium oxide cause devitrification probably because there is not enough silica present to form a strong coherent network. At low temperatures (400-600°C), the double charge of the ion pulls the network together which increases the rigidity and chemical durability of the glass [1].

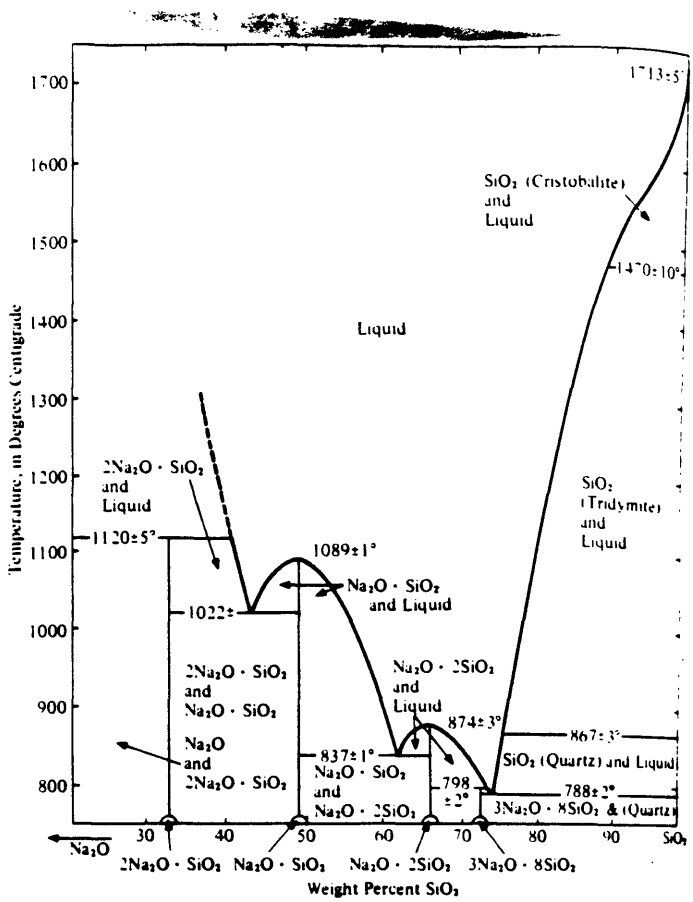

Fig. 2-8. Binary phase equilibrium diagram of the Na_2O-SiO_2 system. Based on Moray and Bowen (1924); Kracek (1930); Schairer and Yoder (1970) and Shahid and Glasser (1971). (Modified from "Professional Paper 440-L, "Geological Survey, U.S. Department of the Interior, Reston, Virginia.) [15].

With the addition of Na_2O to the binary CaO-SiO_2 system, the melting temperature is decreased significantly as can be seen from Fig. 2-10. A small amount of calcium added to the system on the order of two to three wt% decreases the melt temperature. Most of the glass made for this project fell into the $Na_2O{\cdot}2CaO{\cdot}3SiO_2$ composition range. Thus with the CaO wt% ranging from 10 to 40 wt%, melting temperatures ranged from 1050°C to

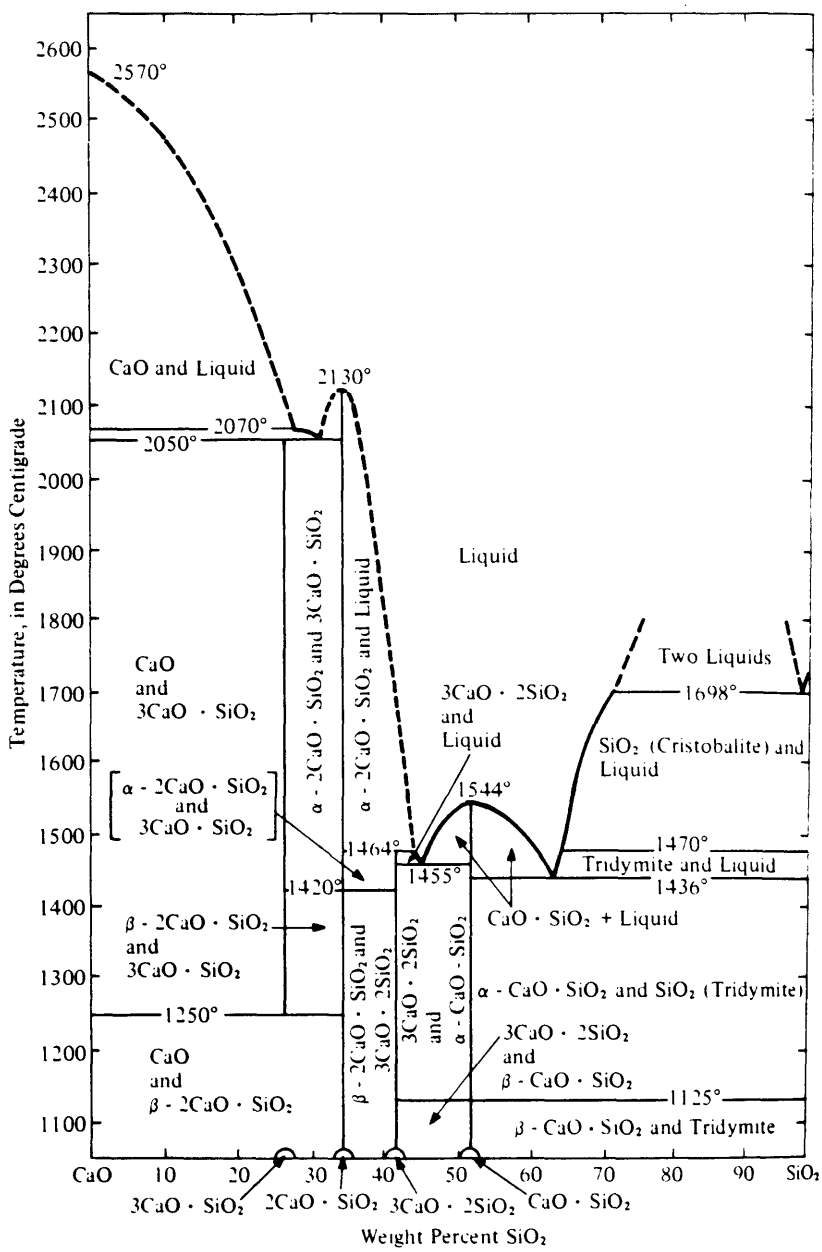

Fig. 2-9. Binary phase equilibrium diagram of the CaO-SiO_2 system. From Rankin and Wright (1915) and Welch and Gutt (1959). (From "Professional Paper 440-L, "Geological Survey, U.S. Department of the Interior, Reston, Virginia.) [16].

1300°C* . After this, any additional calcium increases the melting temperature. Based on the knowledge of these diagrams, it is possible to become accurate when predicting melt temperatures for Rocky Flats and Oak Ridge glass.

MgO as stated earlier has very similar properties and effects on glass as that of CaO but has a larger effect on glass temperature in small quantities. Fig. 2-11 shows these effects. Any addition of MgO decreases the melting temperature of the Na_2O-CaO-SiO_2 glass system until 3 wt% is added. After this point, the melting temperature rises to the original point of 1080°C at 7 wt% MgO. Whereas a the maximum temperature drop of the CaO addition was only 20°C or so, the drop for MgO is near 200°C. The amount of MgO added for glass in this project ranged from 5 wt% to 12 wt% which corresponds to a 100°C drop in melt temperature or a 100°C increase in melt temperature, respectively.

2.2.4 SiO_2-CaO-Na_2O ternary system

Now that the binary phase equilibrium diagrams of the Na_2O-SiO_2 and the CaO-SiO_2 have been shown, they can be combined into a ternary diagram (Fig. 2-12). All temperatures are in degrees Celsius. The ternary diagram is valuable because it can be used

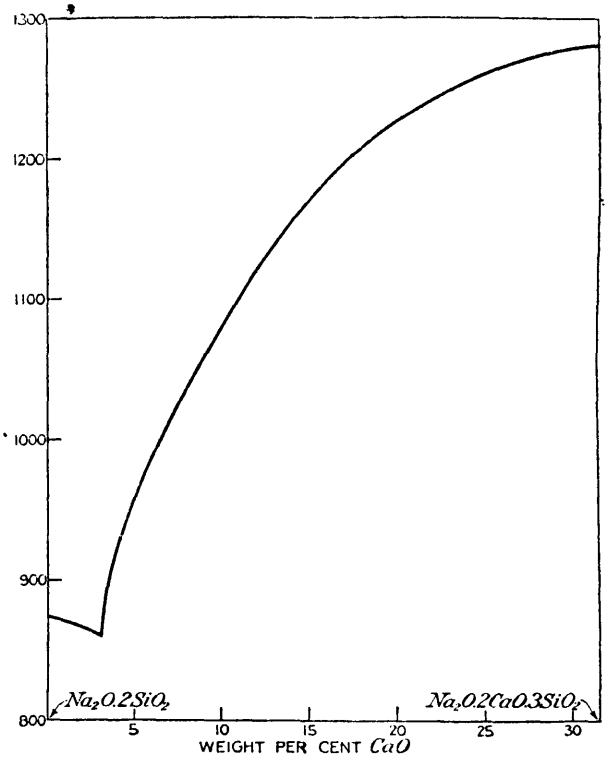

Fig. 2-10. Melting point diagram of the binary system Na_2O, $2SiO_2$-Na_2O, 2CaO, $3SiO_2$. From Journal of the Society of Glass Technology p. 248 [17].

* Because MgO has similar properties to that of CaO, both oxides were added together when reporting CaO wt% in Fig. 2-12. The amount of MgO was about half that of CaO for most samples.

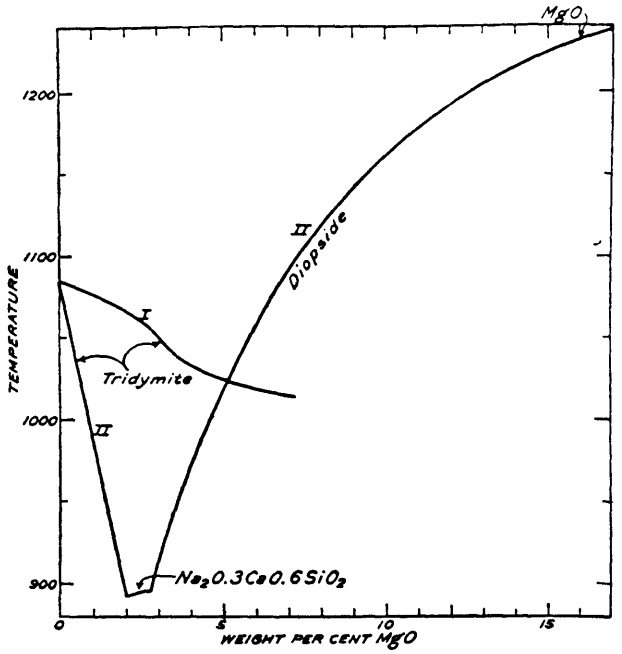

Fig. 2-11. Effect of Magnesia on the liquidus temperature of some glasses in the system Na_2O-CaO-SiO_2. From W.D. Kingery, Bowen, and Uhlmann [10].

to indicate trends in the minimum temperature required to melt the glass. Once this is known then, it can be used to predetermine if the glass is worth attempting.

Many of the glasses had a SiO_2 wt% below that of 50% which does not read on the available ternary diagrams. Batch 31 has a liquidus temperature (LT) of 1150°C according to the diagram, and 32 (LT of 1100°C), and 59 (LT of 1040°C) also fall within the Na_2O-$2CaO$-$3SiO_2$ phase. If the diagram is extended, it is possible that batch 35 (estimated LT of 1280°C) and 52 (estimated LT of 1270°C) fall within that phase also. The phase for batch 29 is unknown as there is no diagram found to compare with that composition. Batch 37, 56, and 61 conglomerate together in the phase of $\propto CaO{\cdot}SiO_2$ and a similar LT near 1275°C. The various Rocky Flats glass compositions are shown on a ternary diagram in Fig. 2-13. In the Discussion and Results chapter, the location of these batches in reference to their leaching characteristics, liquidus temperature and melting temperature are analyzed.

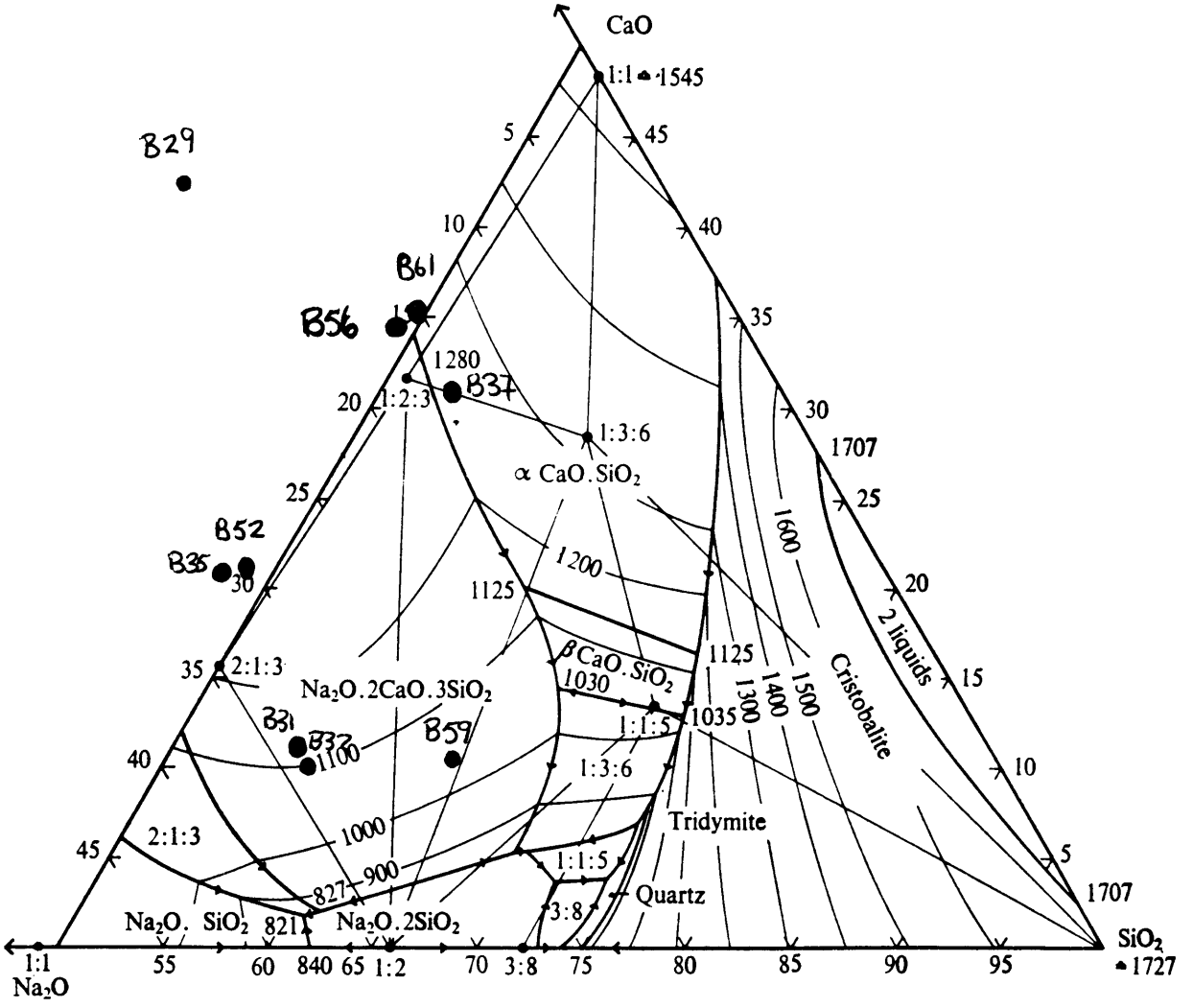

Fig. 2-12. Phase equilibrium diagram of the Na_2O-CaO-SiO_2 ternary system. Temperatures are in degrees Celsius. Compositions are in wt%. Straight lines indicate subsolidus compatibility joins. From K. A. Shahid and F.P. Glasser, Physics and Chemistry of Glasses Vol. 13 No.2 April 1972 [18].

Fig. 2-12. Rocky Flats Glass Compositions

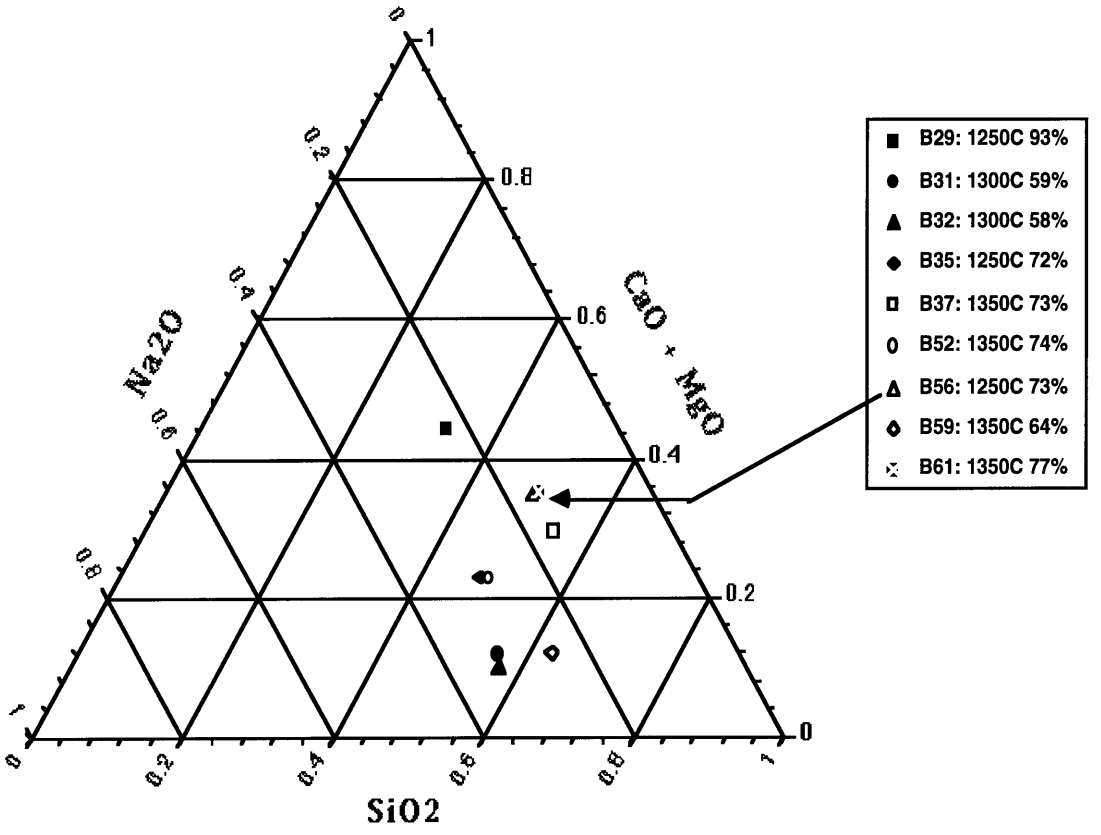

Fig. 2-13. Ternary diagram of Rocky Flats glass compositions made in this thesis. Percentages are in mol%.

2.3 Leaching mechanisms and chemical durability

The chemical durability of a glass refers to its ability to resist decomposition in the environment. The fact that glass will degrade is not the problem as virtually every substance degrades to some extent in the environment. The problem is measuring how fast the glass degrades. The rate of degradation, a.k.a. leach rate, is affected by environmental conditions, glass composition, and glass structure. The mechanism of glass degradation has been described by several theories: 1) classical interdiffusion; 2) chemical ion exchange; 3) water transport; 4) network hydrolysis mechanisms, 5) free energies of hydration; and 6) solubility effects [4]. These models will be discussed along with experiments which have incorporated these theories to explain their results.

2.3.1 General glass degradation principles

Degradation rates are affected by several factors: glass composition; chemical composition and ionic strength of leachant; pH of leachate; redox potential; flow rate; repository temperature; waste package components; surface layers; devitrification; and radiolysis [2]. Lutze has made the following conclusions on the chemical corrosion of high-level waste (HLW) glass:

(1) Different glasses have different corrosion rates. The corrosion rate can be related to the free energy of hydration of the glass.

(2) The corrosion rate decreases with time in a closed system by several orders of magnitude, relative to its initial value.

(3) The corrosion rate is constant in a flowing water, if transport through surface layers is not rate controlling. The corrosion rate is typically on the order of 0.5 to 5.0 g m^{-2} d^{-1}, at 90°C in deionized water.

(4) The corrosion process is likely to proceed at a low rate over long periods of time. Long-term rates are on the order of 0.01 to 0.001 g m^{-2} d^{-1}, at 90°C.

(5) Solid reaction products form as layers on the surface of the pristine glass. Theses layers, which may contain elements from the glass and from solution, consist of crystalline and non-crystalline phases (e.g., $NaAlSi_2O_6 \cdot H_2O$, analcime, with Al and Si from the glass, Na and H_2O from an NaCl leachant solution) [2].

Network formers are covalently bonded in the glass network and along with intermediates are released by the hydrolysis of metal-oxygen bonds. Intermediates as discussed before, may act as a glass former in the presence of other network formers. Modifiers are ion exchangeable cations in the network which are removed from the network selectively via ion exchange reactions.

If flow rates in the repository are fast enough so that glass leaching does not affect the solution chemistry then dissolution kinetics are initially proportional to $t^{\cdot 5}$ and over time become proportional to t^1. If the flow of the water is slow enough, the glass constituents could saturate the solution and leaching could come to a halt. When predicting long term leach rates and the transition time between diffusion, $t^{\cdot 5}$, and t^1 is unknown and is assumed, predicted leach rates could be poor representations of the real values. Furthermore, changes in pH values between 3 and 12 can change the leach rates by a factor of 10. If network formers form insoluble products, the change in pH could change leach rates by a factor of 10^4 [4]. The following six theories attempt to describe effects of the kinetics, glass structure, and pH changes into their models.

2.3.2 Classical interdiffusion

In this theory, the modifiers in the glass are selectively leached by an ion exchange process:

$$\equiv Si - O^{-}Na^{+} + H_3O^{+} - - > \equiv Si - OH + Na^{+} + H_2O$$

The model states that the transition from $t^{.5}$ to t^{1} is a change from selective glass dissolution to uniform glass dissolution. The model overestimates the actual leach rates by a factor of 10^{2}-10^{5}. Assuming that the hydronium ion is the rate limiting factor, then it must move slower than the alkali ions which makes the prediction of leach rate even worse. When elements leach from a glass, experiments show that the following order prevails Cs, Rb>K>Na whereas classical interdiffusion predicts the reverse. It has been shown that selective leaching can occur during the transition and full implementation of the t^{1} leach rate, which this theory contradicts. This model also fails to explain solution chemistry effects [4].

2.3.2 Chemical ion exchange

Assuming all water molecules have access to all ion exchange sites, an effective diffusion coefficient can be found for leaching:

$$D_{eff} = \frac{D/\propto^{2}}{1+\rho K_D/\varepsilon}$$

where D is the ionic diffusion coefficient in water, a is the tortuosity factor, K_D is the distribution coefficient, ρ the density of the glass, and ε the void fraction of the solid. Although the $t^{.5}$ to t^{1} transition is not explained in this model, it does accurately describe the chemical ion exchange qualitatively. The prediction turns out to be 10^{2} to 10^{4} faster than actual leach rates [4].

2.3.4 Water transport

Glass has pore sizes the same size or smaller than water molecule sizes. It can thus be assumed that most of the leach rate is controlled by reversible hydrolysis reactions. The predicted results agree to within one order of magnitude to the real results. The second part of this theory states that if the structure of the glass changes, then pore sizes increases and the diffusion layer does not stop or slow leaching and the rates follow the t^{1} curve. An explanation of network hydrolysis mechanisms is needed to understand reversible hydrolysis reactions [4].

2.3.5 Network hydrolysis mechanisms

In this theory, reactions cause dissolution and restructuring of the silicate network. Under most pH conditions the following reaction is dominant:

$$\equiv Si-O-Si(OH)_3 + OH^- \Leftrightarrow \equiv Si-O-Si(OH)_4^- \Leftrightarrow \equiv Si-O+Si(OH)_4$$

In this reaction, hydroxide ions attack non-bridging oxygen (nbo) sites and form unstable 5 coordination intermediates. The intermediates can then decompose to break the Si-O-Si bonds. This explains why alkali silicates with a high nbo content dissolve faster than tetrahedral or borate sites. Soda-lime glasses consist of high field strength modifiers which phase separate into silica rich and modifier rich regions. Silica rich regions provide hydrolysis barriers to protect modifier regions. Low field strength modifiers (Cs, K) have randomly separated regions and as a result can not form a protective layer.

In explaining the $t^{.5}$ to t^1 transition, these glasses have a high number of silanol molecules after leaching which results in a porous aggregate structure of colloidal silica particles that do not act as a diffusion barrier [4].

2.3.6 Free energies of hydration

The structure of glass is ignored in this model and only the free energy of hydration is concerned. For Silicon, results have been within one order of magnitude of real leach rates. This model works well only with durable glasses that dissolve uniformly and do not saturate the leachate with saturation products. Problems occur with the oversimplification of the chemistry and pH effects [4].

2.3.7 Solubility effects

This model works well for simple oxide minerals dissolving uniformly. The dissolution rate is strongly influenced by the degree of solution saturation. The equation used for this model follows the following pattern:

$$K = C(1-[M]/[M]_s)^p$$

where [M] is the solution concentration of dissolved elements and $[M]_S$ is the concentration of M in a saturated solution. This model shows what the maximum concentration of elements in the solution can ever be. The kinetics of elemental release are based on short term tests. Unfortunately, the quickness with which a glass dissolves can not be predicted.

Even though the silicon concentration may be at saturation limits in the solution, the glass can continue to react with the water. The result is the glass becoming a mass of colloidal particles of amorphous silica which may or may not be retained in leached layers. Also, protective oxide layers may form on the glass layers.

As a result of the different glass dissolution theories, it is possible to predict leach rates within one order of magnitude of the actual rates provided that the structure, composition, and chemistry of both solid and solution phases are known [4].

2.3.8 Application of theory to experiments

In tests done by Carrol et al. (1993), it was found that glass dissolution rates of SRL-165 glass (18.2% Na, 5.97% Ca, 11.68% Al_2O_3, 8.43% B_2O_3, 55.73% SiO_2) were directly proportional to the amount of hydrogen and hydroxide ions in solution. A combination of network hydrolysis theory, and water transport theory, was used to explain the results. Pure silicon gel tests showed that very little reaction occurred between the gel and the DI water leachant which supports the fact that there were very few nbo's present in pure silicon gel. The manner in which sodium leached from the glass was unsure as to whether it enhanced dissolution or if it was a part of the depolymerization of the framework bonds.

The dissolution rate of glass is controlled by the breaking of bonds in the metal-oxygen framework. This is accelerated by H^+ and OH^- ions adsorption at the reaction sites. The rate limiting step is the detachment of the cation from the mineral/solution interface:

protonation: >MOH + H^+<=> >MOH_2^+ $\quad K_{a1} = \dfrac{[> MOH_2^+]}{[> MOH]\{H^+\}}$

deprotonation: >MOH<=>>MO^- + H^+ $\quad K_{a2} = \dfrac{[> MO^-]\{H^+\}}{[> MOH]}$

>M represents the metal surface species, K_{a1} and K_{a2} represent the conditional constants for mass balance expressions for absorption reactions. [i] and {i} are the concentration and activity of the i^{th} surface of the aqueous species. Thus the dissolution rate is,

$$R = K_H[> MOH_2^+]^n + K_{OH}[> MO^-]^m$$

where K_i is the dissolution rate constant attributed to the i^{th} adsorbing ion. The number of ions absorbed prior to the detachment of the metal ion into the bulk solution are represented by n and m. The chemical durability of the glass is decreased if there are more non-bridging silanol bonds following the network hydrolysis mechanism theory. H^+ adsorption or dissolution at these sites accelerates the dissolution of the glass [5].

A study by Van Isegham et al. showed that leach rates increased one order of magnitude when the surface area to volume ratio was decreased from 1.0 cm^{-1} to 0.1 cm^{-1}. The basic theory behind this test supports the solubility limit theory. This glass had a composition of 66-70% SiO_2, 6-4% Na_2O, and <10% Fe_2O_3 or Fe_2O_2 and when

Al_2O_3 was used to replace Fe_2O_3, the chemical durability of the glass was improved. Leach tests were performed at 200°C, 90°C, and below 90°C. Results were presented by using the normalized leach specific weight loss (NSWL) found by the following equation,

$$NSWL = \frac{q}{Q/100}\frac{1}{SA}$$

where q is the amount of element in the leachant, Q the weight percent of the element in the glass, and SA the surface area of the glass. The glass tested at 90°C and at a SA/V ratio of 1 cm^{-1} showed diffusion controlled leaching which is represented by, $Q_i \approx t^{0.5}$ for Si, Na, and K. The following relationship in glass dissolution quantities was found: NSWL => Na, K > Si, Ca > Mg, Al > Fe. Tests below 90°C showed rapid decreases in corrosion rates with time. The 200°C tests showed crystallization of the glass and corrosion rates remained constant with time. At 190°C, the solubility limit of Si, Na, and K are ten times greater than at 90°C and therefore it would be expected under saturation limit controlled leaching that the leach rate would be one order of magnitude larger than at 90°C. Also, the pH increased greatly at higher temperatures [7].

Depending on the various repository conditions and properties of any glass, diffusion or saturation limit controlled rates would be the most likely mechanisms for leaching. Chick and Pederson (1984) [8] proposed three theories for glass dissolution as follows:

(1) The layer is a diffusion barrier for either water transport to the reaction zone and/or transport of reaction products away from the reaction zone (Hench 1977).
(2) The layer has little or no effect on the transport of any critical species [9].
(3) A passive layer forms on the glass surface (Harvey and Jensen 1982).

For case one, the corrosion rate is proportional to the square root of time. For case two, the rate of corrosion decrease is due to the saturation effects of the leachate and the rate does not depend on the surface layer thickness. The creation of a solid reaction product can control the leaching of silica from the glass and solution. In case three, the rate basically comes to a halt as soon as the surface layer forms [2]. In the test to confirm one of the theories, there were three leach tests carried out with four different glasses. The first test studied the influence of pre-formed reaction layers on elemental release. The second test replaced glass specimens with fresh specimens. The third test replaced leachant at fixed intervals for analysis of reaction layer thickness. The overall findings were that the leach rate was saturation controlled and that the reaction layer had a very small effect in some cases but not all. Chick and Pederson reinforced the Grambow tests on gel layer effects and glass dissolution by Grambow. This effect was investigated in the Results chapter.

Tests by Grambow et al. (1984), were done to determine what effect the reaction layer on glass has during dissolution. There are two schools of thought in gel layer protection: the gel layer is protective; the gel layer is water permeable and is made of absorbed species and "sparingly soluble solids". In the first theory, the overall leach rate is limited by the growth of the surface layer and saturation effects. MCC76-68 and C31-3 glasses were tested in DI water and 0.001 M $MgCl_2$ leachate for up to 158 days. It was found that the surface layer added no protection to the glass tested in DI water. However, when the reaction layer was removed in the $MgCl_2$ solution, the leach rates increased.

As silicon reached its saturation level, the density of the silicon/oxygen crosslink bond increases at the glass/surface layer transition zone, thus a decrease in leaching. In brine leachates, the glass continued to dissolve because of magnesium silicate formations. In DI WATER, the leach rates went to zero because the silicon became saturated. The basic results for the DI WATER with the surface layer removed were the same as those samples with the surface layer left intact. Furthermore, glass was preleached for 57 days, had the gel layer removed, and replaced back into the container with no gel layer forming even with testing up to 100 days. Thus reinforcing the saturation limit theory of glass dissolution [9].

2.4 Leach Tests

A leach test attempts to simulate potential waste storage conditions and the effect of the conditions on the ability of a material to contain its hazardous/radioactive components. In addition to simulating environmental conditions, the test must be rigorously performed by placing a certain amount of glass with a specific surface area into a certain volume of leachate in an inert container. The type of leachate used can either by deionized (DI) water or some type of brine solution which is representative of a repository. The length of the leach test can vary from hours to months and the temperature can vary from room temperature to 200°C. The longer a test is run under prototypical conditions, the more reliable the predictions of future durability become. There are three major leach tests used for glass dissolution and they are discussed in this section.

2.4.1 MCC-1P static leach test

The MCC-1 leach test matrix consists of a 3, 7, 14, 28, 90, and 180 day test. The temperature range of the tests were room temperature, 40°C, and 90°C. Leachant was made of DI water or some type of brine solution. This thesis performed tests with DI water to conservatively estimate durability. Glass cubes were contained in PFA Teflon bottles and supported with Teflon PTFE tubing held by a Teflon basket.

Monolithic glass cube test specimens of approximately 13 mm per side were cut and polished from an original glass billet. The surface area to volume of leachant ratios were kept within 0.0005 of 0.01 mm^{-1}. The glass used in the project had an average surface area of 10 cm^2. Therefore, the amount of volume of leachant used averages 100 ml. Glass surfaces were finished by polishing the surfaces with a 320 grit SiC paper. Leachants were acidified with HNO_3 to one percent before being analyzed with an ICP-AES.

The MCC-1 test is not required for regulatory compliance, but is used as a tool to develop mechanistic understanding of material degradation behavior. Once the mechanism of degradation has been identified, a long term prediction about a particular glass can be determined using the results from the MCC-1 leach test. The other two tests, TCLP and PCT are used more for product and regulatory compliance and are more difficult to use when predicting leach mechanisms and therefore long-term durability assumptions.

2.4.2 Toxicity Characteristic Leaching Procedure (TCLP)

The TCLP is the primary test required by the EPA for compliance with its waste form durability requirements. Because this is the only "required" test for waste forms, the Department of Energy (DOE) has widely adopted the test as a comparator of different wastes. The TCLP was designed for use in municipal landfill conditions, which may not be typical of DOE hazardous/radioactive disposal environments.

Several methods exist for conducting this test but the basic concept behind these various methods is the same. Glass is crushed into two sizes, 1 mm<d_p<4 mm and d_p<1 mm, and mixed with a hydrochloric acid solution, heated, and cooled. The pH is recorded and if it is >5.0 extraction fluid #2 is used otherwise extraction fluid #1 is used. Extraction fluid #1 is made with acetic acid, DI water, and sodium hydroxide and has a pH of 4.98±0.05. Extraction fluid #2 is made with acetic acid and DI water and has pH of 2.88±0.05. New glass powder is mixed with the extraction fluid to a 10:1 ratio of liquid mass to glass weight. The bottle with this solution is placed into a tumbler and mixed for 18 hours. The leachant is then analyzed accordingly.

The drawback of this test is that only one time period is required, 18 hours. A time period of 18 hours is not sufficient to determine what mechanism is occurring with the glass corrosion. Also, only one temperature is used and even with a high surface area to volume ratio, glass leach rates will not represent accurate repository results. In effect, a leach rate may be low and pass the government standards for the short term but in the long term, the glass may corrode far differently than predicted. Some glasses may be much better than another glass but will yield the same results for the test once the solubility limit is reached.

2.4.3 Product Consistency Test (PCT)

This test was made for DWPF Savannah River site borosilicate glass. Although the test is highly reproducible and yields rapid results, the test is designed as a quality control check and is usually conducted for one length of time, usually seven days. This test has a high surface area to leachate volume and the entire purpose of the test is to determine the maximum solubility limit of the glass in solution. Glass is crushed into 100-200 mesh size and a temperature of 90°C during the test is used. The ratio of volume solution to solid solution is 10 ml per gram. A single leachant, ASTM Type I water is used. Again, this test will not determine corrosion mechanisms because it automatically brings the glass to its solubility limit. This does not represent actual repository conditions for glass and may be too conservative as a predictor for underground glass disposal.

Chapter 3

EXPERIMENTAL

3.1 Chapter Summary

This chapter discusses the procedures that were followed in order to create and test the glass made specifically for this thesis and Pacific Northwest Laboratory (PNL) master agreement No. 206005-A-L2. An in depth description of the following procedures is given: batch calculations; furnace melting; fusion/glass verification; MCC-1P static leach test; ICP-AES analysis; and SEM-EDAX analysis. Glass forming chemicals were first mixed according to batch calculations, and melted in a furnace. Once the melt was homogeneous, the molten glass was poured into a graphite mold and annealed. A large portion of the glass billet was sectioned and tested using the MCC-1P Static Leach Test while the glass composition was verified using a KOH fusion process. At the end of the leach test, the leachant was prepared for the ICP spectrometer. Glass samples were analyzed in the SEM-EDAX for crystallinity, structure and surface composition.

3.2 Batch Creation

Waste compositions were supplied by Pacific Northwest Laboratories and originated from two major nuclear waste producers: Rocky Flats and Oak Ridge

Table 3-1. Composition of Rocky Flats and Oak Ridge Glasses (wt.%)

	Sample	Rocky Flats	Oak Ridge
Major Constituents	SiO_2	28.51 - 54.85	44.37 - 59.17
	Al_2O_3	0.79 - 8.31	11.09 - 14.79
	Na_2O	10.27 - 25.82	4.43 - 5.91
	K_2O	1.31 - 6.54	0
	P_2O_5	1.40 - 4.47	0
	CaO	4.93 - 15.23	19.36 - 38.72
	Fe_2O_3	2.13 - 14.76	0
	MgO	2.82 - 8.80	0
Minor Constituents	B_2O_3	0 - 6.97	0 - 5.00
	SO_3	0.09 - 0.44	0
	ThO_2	.00051 - .00193	0
	ZnO	0	0.018 - 0.036
	PbO	0	0.098 - 0.196
	Cr_2O_3	0	0.15 - 0.31
	NiO	0	0.15 - 0.31
	BaO	0	0.098 - 0.196
	CdO	0	0.098 - 0.196
	Waste Loading	17.09 - 99.77 %	20 - 40 %

Laboratories. The glass termed Rocky Flats sludge was made of contaminated low level waste which was created during plutonium purification processes. The glass termed Oak Ridge sludge originated from depleted uranium manufacturing operations. Table 3-1 shows the range of glass compositions developed in this thesis along with their waste loading percentages.

3.2.1 Batch calculations

Waste compositions were given as oxide percentages for Rocky Flats and Oak Ridge glasses. Thus, the oxide percentage was exactly the gram amount needed if creating a 100 gram glass batch. For example, if a particular glass contained 40% by weight SiO_2, then 40 grams of SiO_2 would be the amount required to produce a 100 gram batch of glass.

To determine the number of grams of each chemical needed to create the glass, the chemical oxide mass desired was divided by the glass making oxide fraction of the chemical used in preparing the batch (see below). For example, in batch 52, the following calculations were performed:

OXIDE	Wt. of Oxide	÷	Fraction	=	Wt. of Chemical	Chemical Used
SiO_2	41.7	÷	1.00	=	41.7	SiO_2
Al_2O_3	2.96	÷	1.00	=	2.96	Al_2O_3
Na_2O	20.57	÷	0.369	=	55.74	$NaHCO_3$
P_2O_5	2.37	÷	0.50	=	4.74	Na_2HPO_4
CaO	9.92	÷	0.562	=	17.65	$CaCO_3$
Fe_2O_3	13.10	÷	1.00	=	13.10	Fe_2O_3
MgO	5.79	÷	0.1572	=	36.83	$Mg(NO_3)_2{\cdot}6H_2O$
SO_3	0.22	÷	0.5882	=	0.374	$CaSO_4$
K_2O	3.35	÷	0.465	=	7.20	KNO_3
ThO_2	0.0014	÷	0.470	=	0.00298	$Th(NO_3)_4{\cdot}4H_2O$
Total	99.98				180.30	

Some chemicals produced two oxides after decomposing such as Na_2HPO_4 which produced the oxide P_2O_5 and a small amount of Na_2O. In this case, the amount of $NaHCO_3$ was reduced so that the final composition compensated for the correct amount of Na_2O. Once all of the weights were ascertained, each chemical would be measured out to $\pm$ 0.01 grams on an OHAUS TP2KS scale and placed into a single DFC Fused Silica 120 gram crucible. Hygroscopic chemicals were measured under a nitrogen atmosphere in a plastic glove bag to ensure that no moisture or CO_2 were adsorbed[+]. Once all of the

[+] Adsorption of CO_2 or H_2O would erroneously provide less of the desired metal oxide.

chemicals were placed into the crucible, they were thoroughly mixed with a spoon or spatula.

If a particular glass sample was to be doped with thorium, such as RF-52, thorium (as $Th(NO_3)_4 \cdot 6H_2O$) was in dissolved in HNO_3 and added to the batch. For all Th-doped batches, the Th was added last and then mixed in with the rest of the sample. Thorium solutions were carefully droppered into the center of the powder mix so that the liquid would not be adsorbed by the crucible walls.

3.2.2 Furnace melting

Mixed waste samples to be vitrified were placed in a Lindberg/Blue M furnace, model 51333 (rated to 1500°C), at or below 1000°C to ensure that no rapid chemical reactions took place and also for the decomposition of certain elements, i.e. $CaCO_3$, to proceed slowly. The furnace, shown in Fig. 3-2, was controlled with an OMEGA PHB-47 bench microprocessor. Crucibles remained at 1000°C for at least thirty minutes before raising the furnace to the desired melting temperature of the glass. In some cases, the desired temperature produced non-homogeneous melts and the furnace would be raised to a higher temperature until the molten glass was homogeneous and had no gas bubbles. The majority of Rocky Flats glass and Oak Ridge glass became homogeneous when temperatures were above 1250°C and almost always at 1350°C. Typically, the higher the waste loading, the lower the temperature needed to create a homogeneous melt because the majority of the wastes acted as network modifiers.

Once the prescribed temperature was reached, the molten glasses were held at that temperature for two to three hours to ensure complete homogeneity. The molten glasses were then poured onto a graphite block mold, 13.5 mm by 13.5 mm by 84 mm, and cooled inside a fire brick housing shown in Fig. 3-1.

Generally, about 30 minutes was needed to cool the glass prior to removing it from the graphite block. If the glass survived the cooling process by remaining as one complete ingot, it would then be annealed in the furnace at 500°C for at least one hour and then furnace cooled. If the glass fractured while cooling, it would either be discarded, crushed and re-melted again in the same crucible, have flux added to it, or archived for later use. If re-melting failed twice, several things would usually be done to the composition, furnace temperature, or melt time in order to keep the glass from cracking in the fire brick housing while cooling[$]. After the annealing process, the glass would be used for three purposes:

[$] Many homogenous melts consistently cracked in the mold and there were no glass chunks large enough to facilitate a leach test. The mass of the graphite mold was reduced in order to lower the heat transfer from the glass to the graphite thereby avoiding stress cracking.

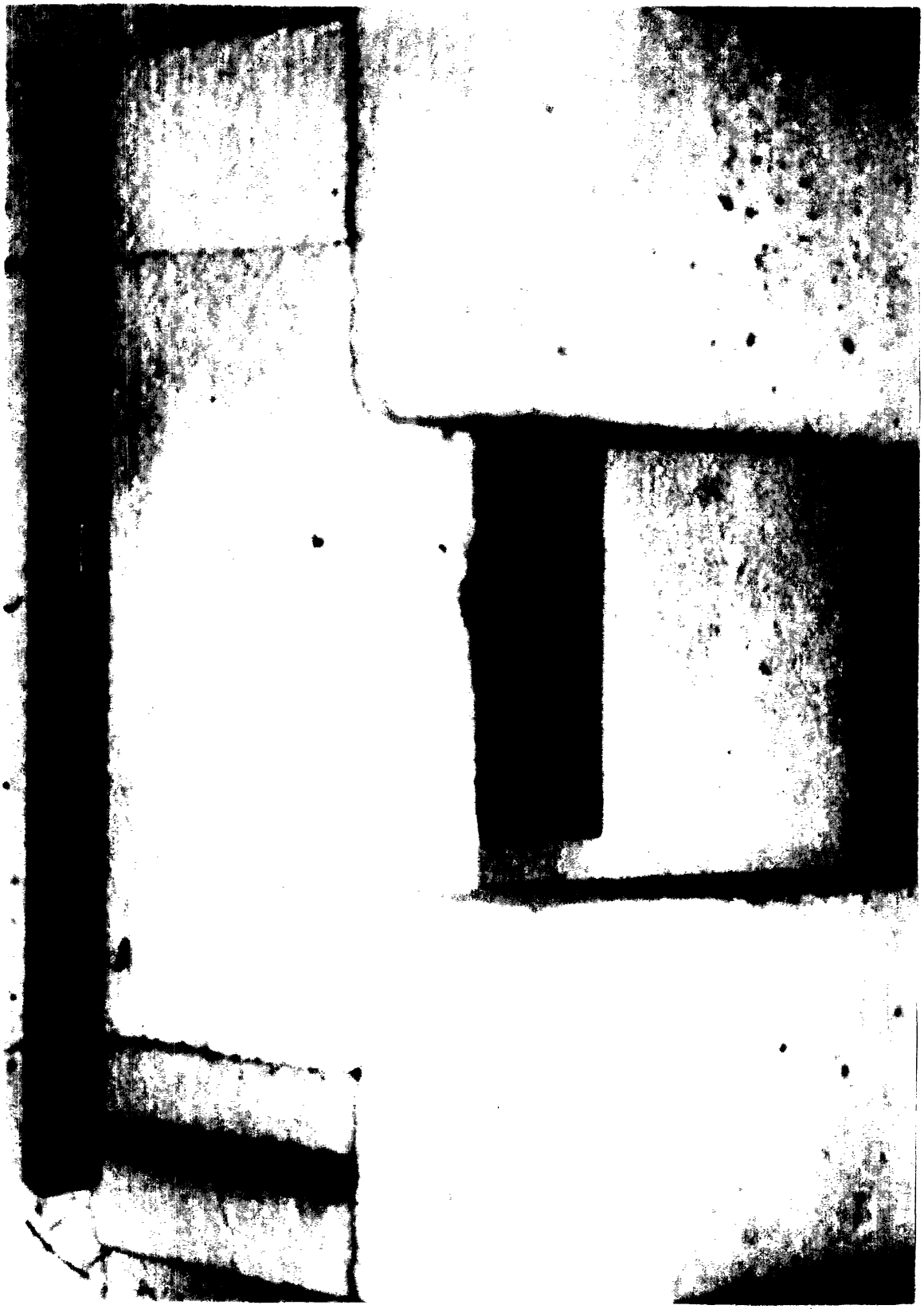

Fig. 3-1. Fire brick housing used in glass pouring and cooling.

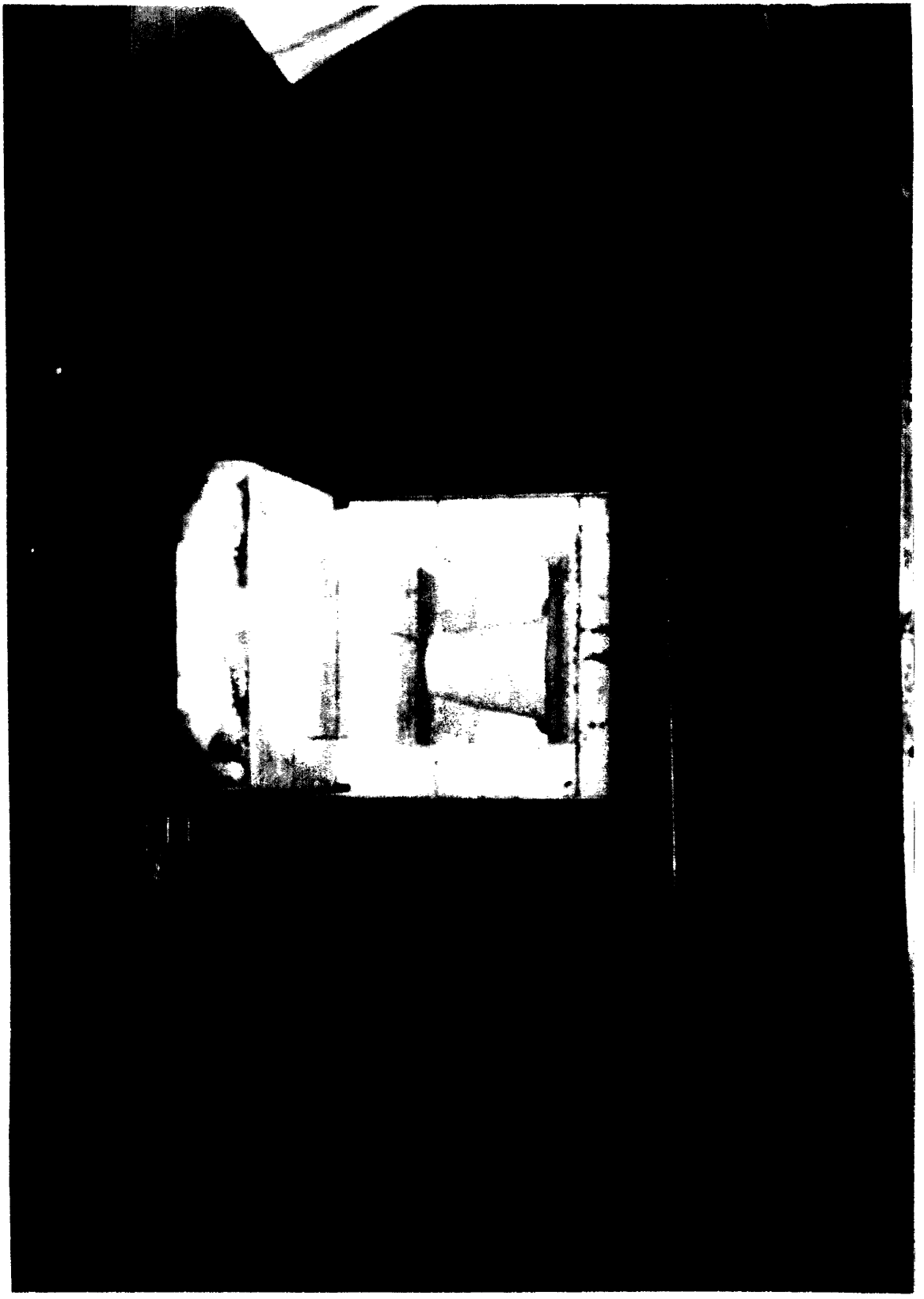

Fig.3-2. Lindberg/Blue M oven in which reagent grade chemicals are melted into a glass.

1) A fusion/ICP analysis in order to find the exact composition of the glass,
2) MCC-1 static leach tests and,
3) SEM-EDAX/microscopic analysis.

3.3 Glass Composition Verification

The final glass compositions were determined by using a fusion process described in PNL procedure no. APSL-03. This procedure uses an alkali caustic (KOH) to dissolve the glass. This would require that two fusions occur to determine all of the elements composing the glass. Potassium hydroxide fusions were performed in a nickel metal crucible which determined all elements present except potassium.

The glass was crushed using an alloy tool steel mortar and pestle then passed through a 140 mesh sieve. If the glass did not pass through the sieve, it was crushed until it became small enough to pass. The crushed glass was weighed out to 0.25 ± 0.075 grams and placed into a nickel crucible.

Approximately 1.8 ± 0.4 grams (about 20 pellets) of KOH was weighed and transferred into the Ni crucible. To further facilitate dissolution of the glass in the fusion, 0.2 ± 0.1 grams of potassium nitrate was added to the crucible. The contents were swirled until the ground sample was mixed with the flux. An electric Bunsen burner (model number BA 6101, 120V, 400W, fuse 3.5A, 1000°C max.) was preheated. About three minutes was needed to melt the KOH pellets and the total melt time was ten minutes. The crucible was removed from the burner and cooled to room temperature.

Approximately 10 ml of DI water was slowly added to the crucible in order to dissolve the cake-like crystalline melt. Once dissolved, the liquid was transferred to a 250 ml volumetric flask. If all of the melt in the crucible was not completely dissolved, another 10 ml of de-ionized water was added until all of the melt dissolved. After the transfer was completed, the solution in the flask was diluted up to 100 ml. The solution was then acidified with 25 ± 5 ml of concentrated hydrochloric acid. The solution was swirled, and if any precipitate remained approximately 0.3 ± 0.1 grams of oxalic acid crystals were added. The flask was then filled to the 250 ml mark on the neck. Because a KOH fusion was performed on the glasses the potassium concentrations were not determined from ICP analysis. The concentration of elements in the flask were typically near 1000 ppm.

ICP standards were created for the fusion analysis and were separated into two groups. One group contained the elements Si, Al, B, Na, and Ca, and the other group contained S, P, K, Fe, Mg, and Th. The strength of the standards were 10 ppm, 1 ppm, 100 ppb, and 10 ppb.

A problem was encountered in following the strict letter of the PNL fusion procedure. When the tool steel mortar and pestle set was used, a higher concentration of Fe_2O_3 was found. Thus, this quantity was artificially entered in the data compilation by using the amount of original grams of oxide placed in the crucible and then corrected for the extra silicon present due to the corrosive molten glass/fused silica crucible reaction. For example, if 5 grams of Fe_2O_3 were added to a 50 gram oxide sample originally, and the melt/crucible reaction added more silicon to the final composition, i.e., 20 extra grams of SiO_2, then the new percentage of Fe_2O_3 in the glass would be:

$$\frac{5\ gms\ Fe_2O_3}{(50\ gms\ Oxide\ +\ 20\ gms\ SiO2)} \times 100\% = 7.14\%\ Fe_2O_3$$

This procedure was also used when the ICP detected elements at their limit of detection.

3.4 MCC-1P Static Leach Test Method

MCC-1 leach testing was selected as a method for determination of the glass durability. The background chapter discusses the merits of two other testing procedures for environmental durability. The MCC-1 procedure requires that specimens of known volume and surface area be immersed in a leachant without agitation for defined time periods and temperatures. The SA/V used in this experiment was $0.0100 \pm 0.0005\ mm^{-1}$, where SA is the surface area of the waste form and V was the volume of the leachant. Three temperatures, 90°C, 40°C, and room temperature (20±5°C) along with specific times (3, 7, 14, 28, 90, and 180 days) were used to develop a matrix to compare and contrast different waste loadings and temperatures. Although different leachants can be used, deionized water (DI) was used in all the leach tests because it has been shown to be a conservative medium for durability determination.

Data in the form of ppm by weight quantities from ICP analysis from these tests were used to calculate normalized elemental mass loss (gm-solution/gm-glass) from specimens exposed to aqueous solutions at temperatures less than 100°C. Elemental mass loss (g/cm^2) was used as a comparison between different glass types. These quantities are found by performing the following calculations:

$$\frac{\#\ ppm_{element}}{1,000,000} \times \frac{Leachate\ Volume}{(Glass\ weight \times Element\ \%)} \times \rho_{leachate} = \frac{grams_{element}\ in\ solution}{grams\ of\ glass}$$

$$\frac{\#\ ppm_{element}}{1,000,000} \times \frac{Leachate\ Volume}{(Surface\ Area)} \times \rho_{leachate} = grams/cm/cm$$

3.4.1 Leach container

The leach containers used in this project were made of PFA Teflon (rated from -196 to 260°C). Each container had a capacity of six ounces, an inner diameter of 60 mm, and a height of 70 mm (74 mm with the cap screwed on). Teflon baskets made of folded strips with holes cut in the sides for Teflon PTFE tubing were used to hold the glass samples in the centroid of the leachant as shown in Fig. 3-3. The basket was used to maximize the surface area of glass in contact with the leachant. New Teflon containers and supports were heated at 200°C for one week prior to cleaning. Between uses, the Teflon containers and supports were re-used after cleaning them with the following procedure,

1. Soaked for 1 h in 6 M HNO_3-0.2 M HF.
2. Rinsed with three container volumes of high-purity H_2O.
3. Soaked in 6 M HNO_3 for 4 h at 50°C.
4. Soaked for 30 min. in >60°C, high-purity H_2O.
5. Soaked for at least 8 h in fresh high-purity H_2O at 80°C.
6. Boiled for 30 min. in fresh high-purity H_2O.
7. Rinsed with successive container volumes of high-purity H_2O until the pH of two successive rinse solutions was within 0.5 pH unit of the original high-purity H_2O. A minimum of three rinses was required and often more were used.

3.4.2 Test specimen preparation

After the glass was annealed, it was cut into cubes approximately 13.5 mm per side using a MARK V PCS-400 sectioning saw with a diamond blade. The glass cubes were sanded with 120 grit SiC paper and then followed up with 320 grit SiC paper on all sides. Only non-defective, visually homogeneous glass samples were used. Following the grit stages, the surface area of each glass sample was calculated. The samples were cleaned in the ultrasonic cleaner as follows,

1. Five minute ultrasonic wash in high-purity water.
2. Three five minute ultrasonic washes in fresh absolute ethanol.
3. Samples were dried to a constant mass for one hour at approximately 110°C which was sufficient for nonporous waste forms.

The samples were weighed and the surface area was calculated. Once the surface area was known, the volume of leachant needed to reach a SA/V ratio of 0.01 m^{-1} was determined. All handling of the specimens was done with lint free gloves and Teflon tongs.

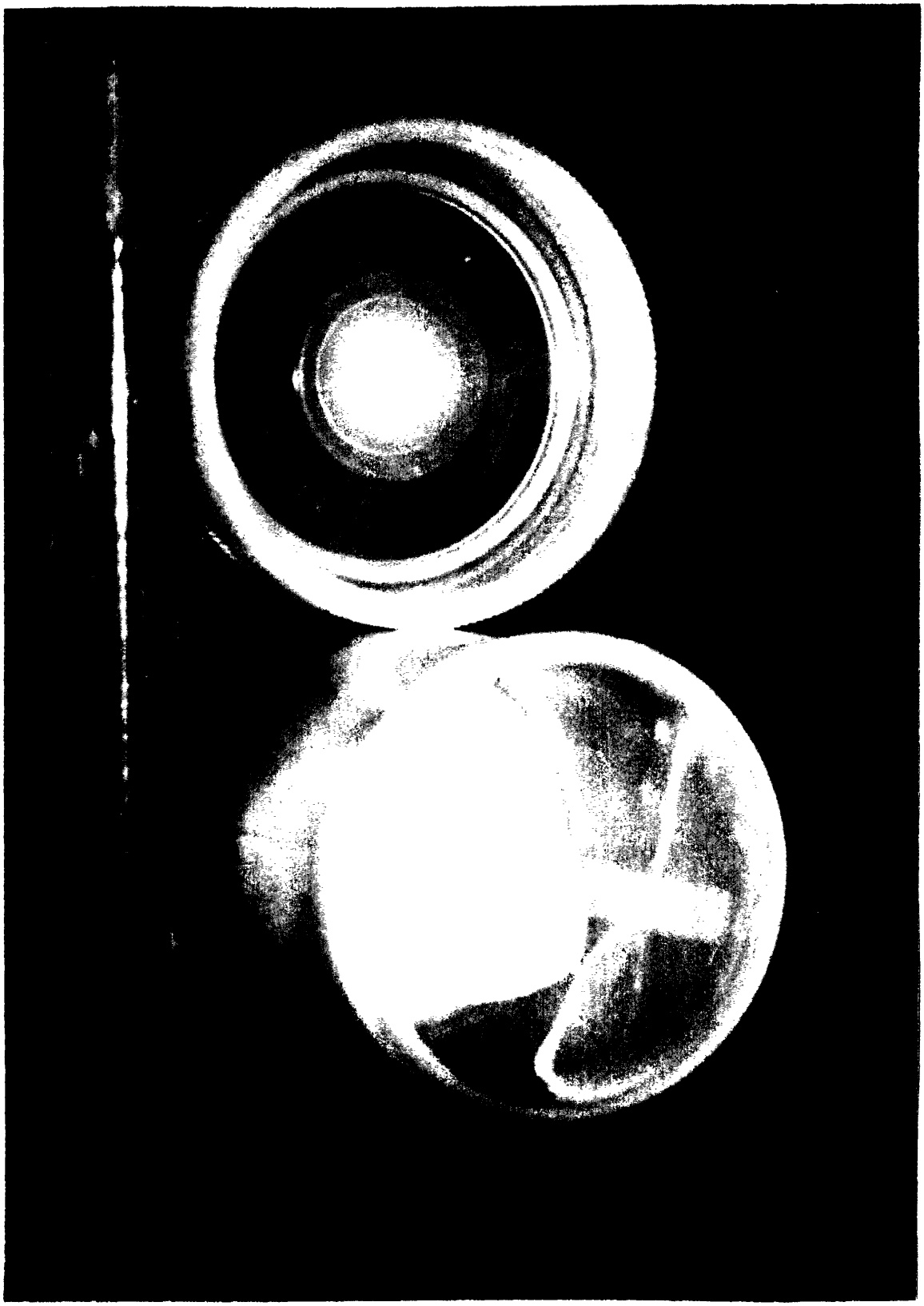

Fig. 3-3. Teflon Container with Teflon basket inside.

3.4.3 Volume measurement and surface area measurement

Leachant for the tests were measured with volumetric flasks and burettes accurate to within one percent. The surface area of the glass samples were measured after polishing and before cleaning. To ensure no contamination, talc-free gloves were used when handling the specimen, or any part of the Teflon container. A Manostat 6" dial caliper was used to measure each side length of the glass cube with an accuracy up to 0.1 mm. Only three lengths were needed because the opposite sides of the glass cube had the same lengths. From these lengths the surface area and volume of the glass were determined.

3.4.4 Environmental chamber

MCC-1 leach tests at 90°C were performed in a Mermmert oven which had a temperature range from 35°C to 220°C (±1%). The oven had a capacity of 1.1 cubic feet and can fit approximately forty Teflon containers. The testing remained within ± 1°C of the required temperature. Fluctuations beyond this range were not allowed to exceed 5% of the total time period and the maximum fluctuation allowed for any amount of time was 5°C. After opening the oven, the temperature decrease ranged from 89°C to 85°C and the recovery rate was usually one degree per twenty minutes. To minimize this transient, containers were placed into a separate oven until the container and contents reached a temperature near 90°C. They were then placed into the 90°C oven containing the leach tests which is shown in Fig. 3-4. Leach tests performed at room temperature were done in a cabinet which had a steady temperature of 20±2°C. [Calibration not done yet]

3.4.5 Leaching an individual specimen[@]

Specimens were placed inside Teflon containers using Teflon tongs. Leachant was poured into the containers and the containers were tightly closed. Specimens were submerged in leachant within the containers as close to the centroid of the holding basket as possible. The weight of the entire vessel, including the glass, and leachant were recorded. The time of placement into the oven was recorded and the samples were placed into the environmental chamber within thirty minutes of the glass being submerged into the leachant. The test period started when the container was placed into the environmental chamber. Testing at room temperature was done in a dry and dark cabinet with an average temperature of 22°C ± 2°C.

Lids were re-tightened on the containers approximately one hour and again at twenty-four hours after placement into the environmental chambers. Approximately 0.01

[@] This procedure applies to blanks as well, except that the specimen was omitted and the volume of the leachant was similar to that used with the samples. The pH of the liquid before testing was not tested.

Fig.3-4. Mermmert oven where 90°C tests were performed.

ml/day of water was observed to be lost through the Teflon containers. For long term tests, the weight of the containers were checked at least every three months. If water loss was 10% or greater the test was continued and data taken were highlighted for being out of compliance with MCC-1P requirements. If the water loss was greater than 5% and less than 10%, the leach container was opened and the loss was made up with fresh DI water under room temperature conditions. Water additions were limited by the MCC-1P procedure to a total of 15% per year. No additions were allowed after three months before the end of the test.

The testing period was within 2% of the times specified in MCC-1P. At the end of the test, the containers were removed from the environmental chamber. The weight of the containers were recorded. If the mass of a container was less than 90% of the original mass, the test was highlighted for non-compliance with MCC-1P* . The glass sample was taken out of the leaching solution as soon as the container was removed from the oven and then re-closed and cooled to room temperature. However, in the 90°C, 90 day tests, the containers cooled to room temperature with the glass samples present. Once cooled to room temperature the lid was opened and the pH was tested immediately. In all cases, once the specimen was taken out of the container it was rinsed with high-purity water for five seconds with the rinse going into a Teflon beaker. The reacted glass specimen was dried in an oven for one hour at 110°C. The leachate was filtered using neutral sterile filters and syringes and placed into a polyethylene bottle. One ml of concentrated HNO_3 was added to acidify the leachate for ICP analysis. The neutral filter was a 0.45 micrometer Cellulose Acetate filter. The acid filter was a 0.45 micrometer PTFE filter. Both have a maximum operation pressure of 75 PSI.

The inside of the Teflon container was rinsed along with the Teflon basket and inner portion of the lid. The rinse water was also placed into the Teflon beaker along with the neutral filter. One to two ml of concentrated HNO_3 was then added to dissolve any glass particles which may have become lodged in the neutral filter or stuck to other surfaces. This runoff liquid was then filtered using the acid filter and placed into a polyethylene bottle and the volume recorded. Once the leachant was extracted, new tubing was woven into the Teflon baskets and the cleaning process described in section 3.3 was started again. Leachants were analyzed by using an inductively coupled plasma (ICP) spectrometer, model Spectroflame-ICP D.

---

* Leach tests volume losses for 180 day tests lost up to 45% leachant. This amount was replaced for the remaining three months of the test. Although duplicate leach tests lost varying amount of volume, no significant difference in results was observed.

3.5 ICP Procedure

The results from quantitative ICP analysis give the concentration, on a mass basis, of elements in the leachant. Quantitative ICP analysis are made relative to known standards with an interpolation algorithm. Standards were bought from NIST in concentrations of 1000 ppm of the desired element in one percent nitric acid. The silicon standard also contained one percent hydrofluoric acid. The standards were diluted from 1000 ppm to the following ppm levels: 100, 25, 10, 1, 0.1, and 0.01 ppm. Dilution's were made using an automatic pipette (OXFORD Benchmate model #8885-500036, 1.00 to 5.00 ml) in a volumetric flasks and then acidified 1% with HNO_3.

Filtered liquid samples were analyzed using either an ultrasonic nebulizer, which gives extremely enhanced sensitivity, or a less sensitive cross-flow nebulizer both shown in Fig. 3-5. Diagram 3-6 shows the flow chart for the ICP analysis.

A peristaltic pump pumped the leachant to the cross-flow nebulizer where argon was pumped in to create a misted liquid. The mist was mixed with more argon in the bottom of the torch and went through the argon flame. The flame was magnetically contained in the glass torch for a flame shape conducive to the "eye" of the machine. As the elements in the mist were burned, they gave off characteristic wavelengths identified by the spectrometer. The spectrometer generates an emission spectrum for the sample in question and compares that spectrum with the standards previously entered into the computer to get a concentration number. The computer uses a linear polynomial calibration equation of up to three orders to calculate ppm values.

The accuracy of the ICP changed daily so that the calibration curve for the standards was reviewed before and after each set of analysis. The crossflow nebulizer was used for all leach test results. The ultrasonic nebulizer has more sensitivity but was not used due to the large amounts of sodium, silicon, and calcium present in the leachant. Large amounts of these elements in the leachate may overexpose the instrument when the ultrasonic nebulizer is used.

3.6 SEM-EDAX

A scanning electron microscope (SEM) equipped with an energy diffusive X-Ray micro-analyzer (EDAX) was used to determine if crystalline phases were present on the surface of the glass and to conduct quantitative elemental surface analysis. A TOPCON dual stage scanning electron microscope model ABT-150S used a tungsten electron source and is shown in Fig. 3-7. The illumination stage consisted of five stages,

1. A 40KV electron gun
2. A first stage condenser lens with double gap

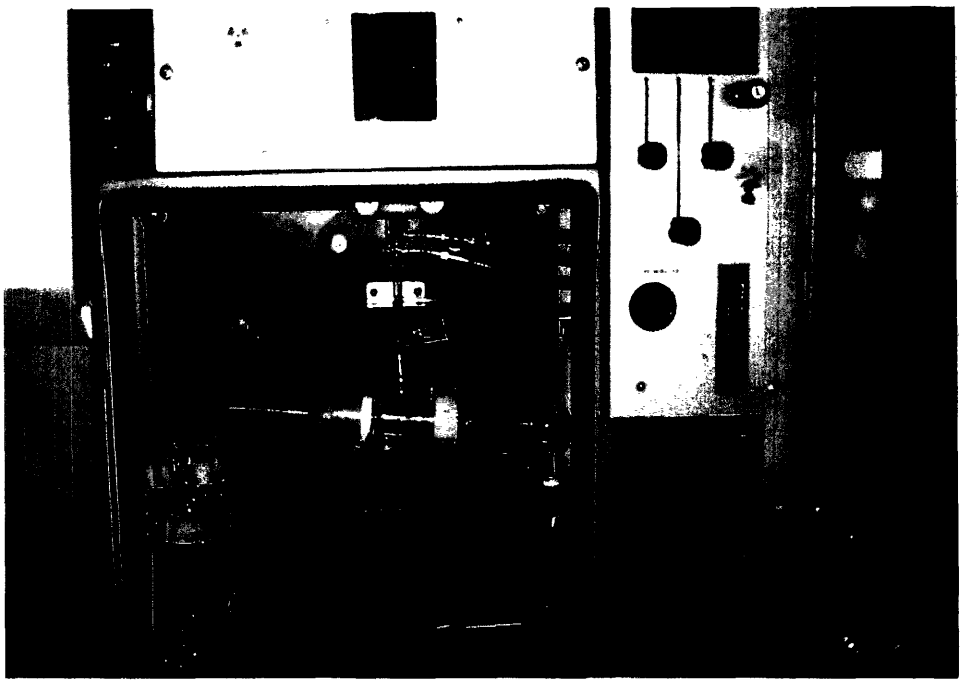

(a)

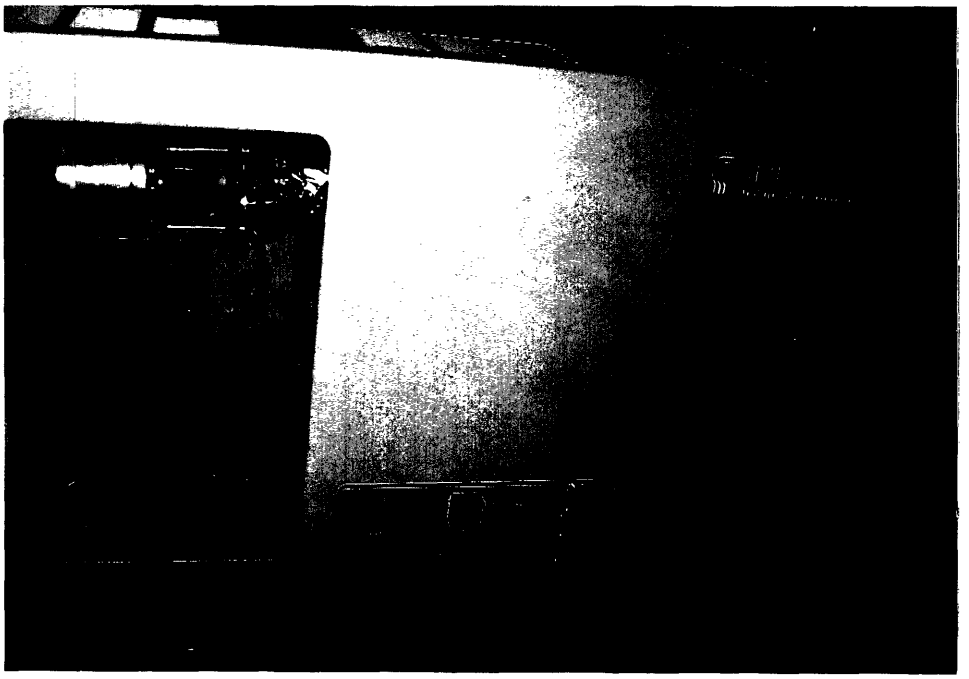

(b)

Fig 3-5. Cross flow nebulizer (a), Ultrasonic nebulizer (b).

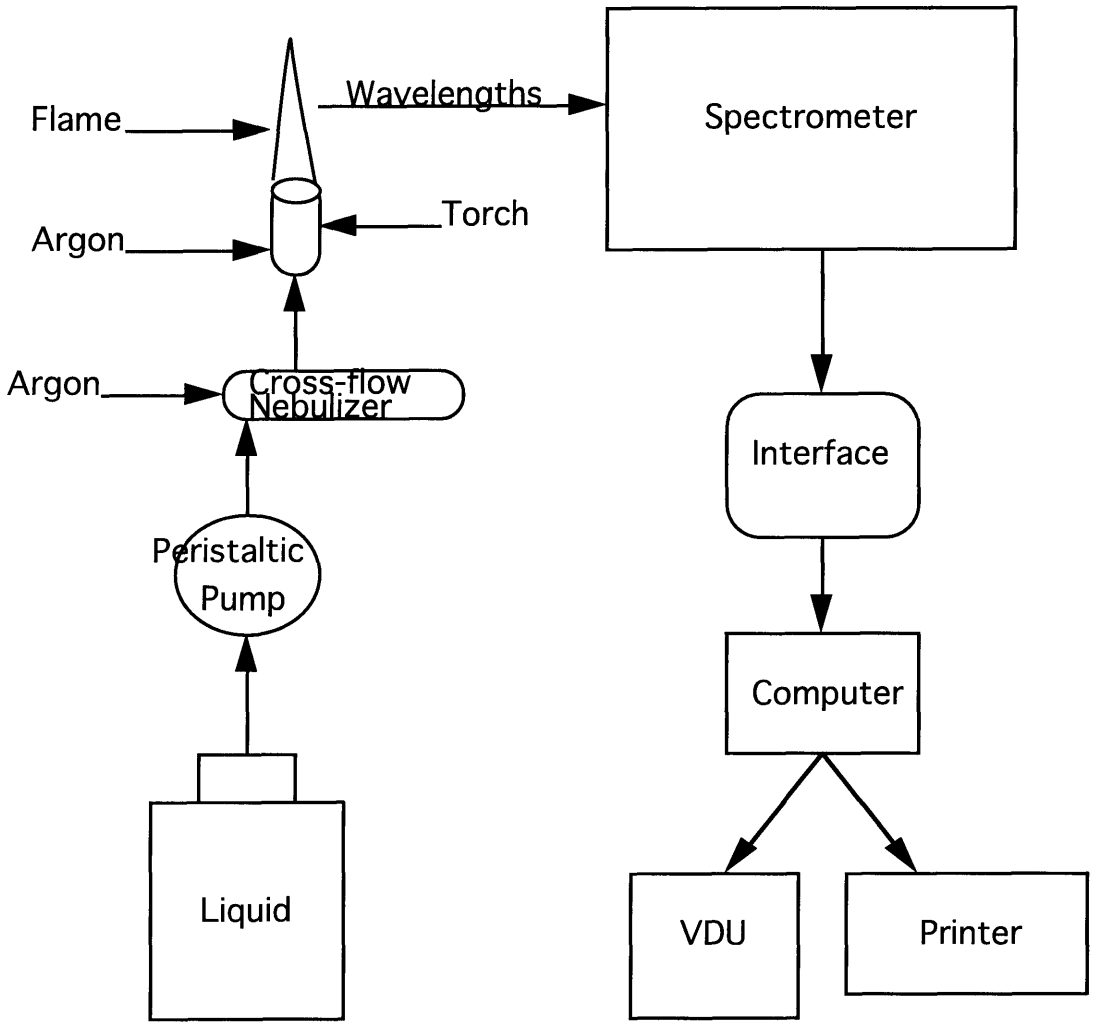

Fig 3-6. ICP Flow Chart

3. A second stage condenser lens
4. A high resolution, high field objective lens for the top stage, and
5. A miniaturized objective lens for the large bottom stage.

The SEM magnification ranged from 10X to 600,000X magnification. The top stage resolution was 30 nm (30Å) and the bottom stage resolution was 4 nm (40Å). The EDAX consisted of a voyager X-RAY quantitative microanalysis system with digital imaging made by Noran Instruments, INC., model 537B-3SSS. Gold coating of samples was done with a Polaron sputtercoater instrument. A carbon power supply, model PS100, and SEM coating unit E5100 made up the bulk of the sputtercoater.

Glass which broke naturally from the mold during cooling or broken on purpose for the SEM was used so that a picture of the unaltered surface could be seen. Glass samples were coated with either gold or carbon. Because gold adheres itself better to glass

than carbon, gold was used to coat the glass. The glass was held down on an aluminum dish with electrical conductive tape or a strip of dried liquid carbon. If necessary, a liquid strip of silver which dried quickly was used to connect the plate to the aluminum dish. The plate was then placed into the SEM and the glass analyzed after tweaking many of the controls. Once an image was found, photographs were taken and EDAX analysis of the surface composition of the glass were made.

Once the sample was placed into the chamber of the SEM, it took approximately ten minutes for the image to come up on the screen. When focusing on the sample, it was best to increase the magnification, focus on the sample, then reduce the magnification in order to attain a more focused picture. A photograph could be taken at this point or a section of the screen could be localized. This localization would be used to identify which elements composed the surface of this area using the EDAX. The Voyager system was very user friendly and only a small amount of time, about one minute, was needed to measure the elements on the surface.

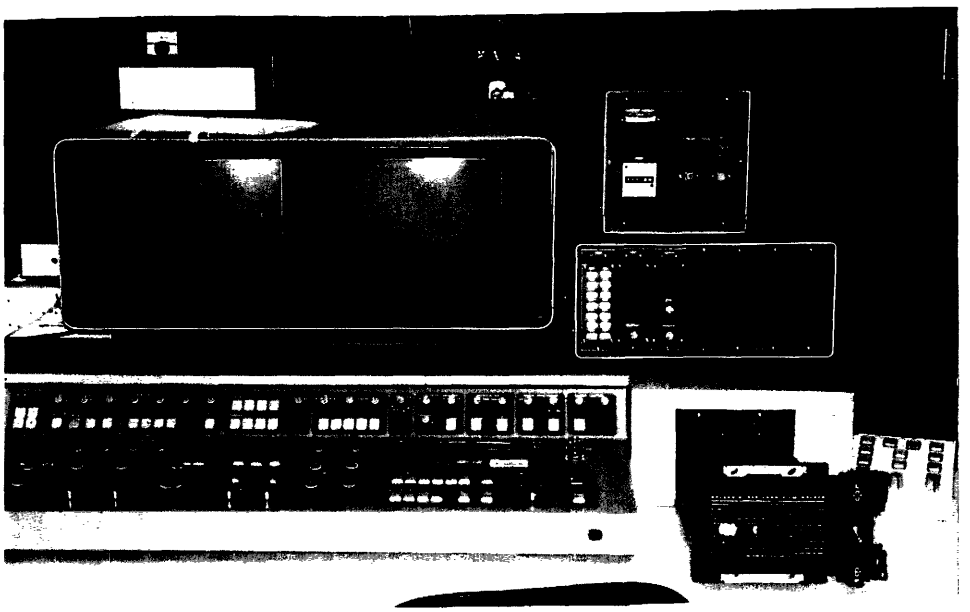

(a)

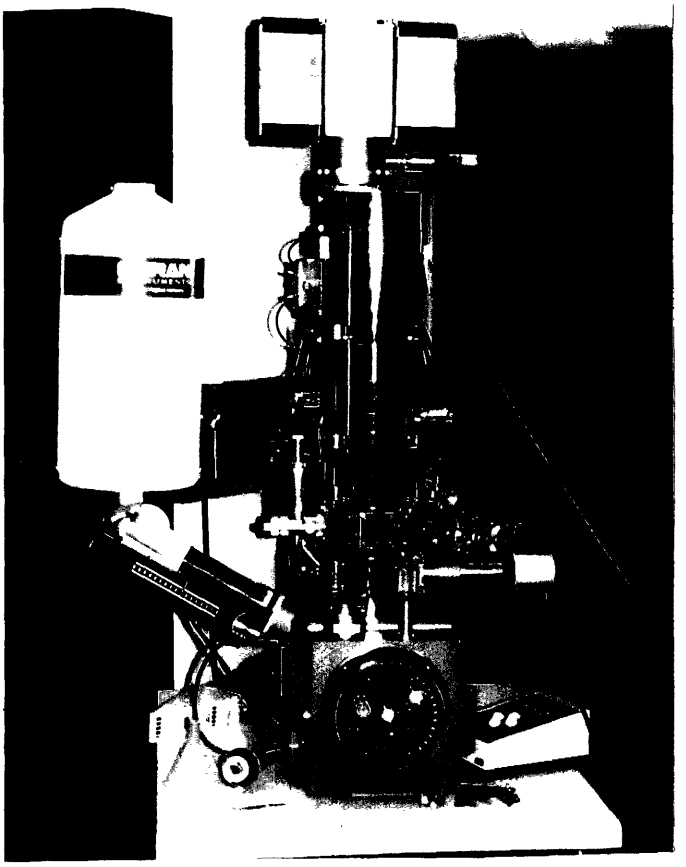

(b)

Fig. 3-7. (a) Scanning Electron Microscope (SEM) control panel in center. (b) Vacuumed LN_2 cooled tungsten unit and EDAX machine.

Chapter 4

DISCUSSION AND RESULTS

4.1 Chapter Summary

This chapter presents the results from the MCC-1 static leach tests, hot fusion tests, SEM-EDAX, and multivariate analysis. Out of the two glass types, only the Rocky Flats glass underwent leach tests. Non-radioactive glass samples were leach tested at room temperature for 3, 7, 14, and 28 days. Th-doped glass samples were tested at room temperature for 14, 28, and 90 days, and at 90°C for up to 180 days. The static leach test data are presented in two formats: g/cm^2 and gram of element in solution per gram of element in glass according to fusion results. SEM-EDAX analysis shows what elements are on the surface of the glass after leaching and if there is any crystallization on the glass before leaching. A multivariate statistical analysis was applied to interpret the results presented.

4.2 Glass Production Summary

Table 4-1 shows the composition of glasses in wt% that underwent leach tests. In total, 80 batches of glass of various compositions were produced, but only those that exhibited reasonable production qualities were subject to additional testing. Two numbers appear for the elements in the various glass compositions in Table 4-1, the first number represents the pre-furnace batch calculations, the second indicates the post-furnace analysis. The differences for silicon and aluminum, result from the leaching of these elements into the melt from the DFC fused silica crucibles, thus increasing the SiO_2 and Al_2O_3 wt% of the glass and lowering the wt% of all other oxides. The temperature at which the compositions were poured is given in Celsius along with the total amount of time the glass was in the furnace. The waste loading amount is based on elemental additions to modify the 100% waste loading sample. The pour quality was a qualitative measure of the viscosity of the glass when pouring at the final temperature and is important for production applications. If the glass poured with a high viscosity like molasses, then the melting temperature would be increased for production. If the pour was like motor oil, then the melting temperature would be lowered somewhat.

Because the method for analyzing the glass composition (a hot fusion) used KOH as the flux, K could not be analyzed for the samples. Elements such as S, P and Th could not be detected by the ICP spectrometer because of the low concentrations present after the dilution of the fusion products.

Two problems existed with the elemental analysis of the glass:

1) If an alumina mortar and pestle was used to crush up glass samples there would be an excess of alumina present in the results.

2) If a tool steel mortar and pestle was used, there was more iron present in the results.

An alumina mortar and pestle was used for batches 29, 31, 32, 35, and 37. The results for Al_2O_3 were not adjusted because the DFC fused silica crucibles had alumina present in them which most likely leached into the glass. However, the tool steel mortar and pestle was used for batches 52, 56, 59, and 61. The results showed that Fe_2O_3 averaged near 13 wt% for all compositions. These results needed modification, because there was no iron coming from the DFC crucible, which meant that it was all coming from the tool steel set. Thus the initial iron content in the mix was artificially adjusted using the method described in section 3.3.

For every batch, the amount of SiO_2 increased because the inside wall of the crucible became part of the glass. Some glasses were more reactive with the crucible than others. The higher the waste loading (i.e., the lower the wt% of the SiO_2), the more severe the reaction with the crucible. It seemed that SiO_2 had an equilibrium point in the molten glass with respect to the other oxides near 60 wt% SiO_2. The batches with the largest relative increase in silica were the ones melted above 1250°C and starting with less than 30 wt%. SiO_2. Notice that batch 59, which initially had the highest amount of SiO_2, had almost no increase in Silica.

The higher waste loadings produced optically darker glasses (light to dark green). Waste loading could be calculated in two different ways. Oak Ridge waste loading divided the total wt% of non-network formers by the total network former wt%. With Rocky Flats, the waste comes as 100% waste loading and has network formers already present. An addition of any element lowers the waste loading (see Appendix D). The composition of the glass is important in analyzing the leach rates which are discussed next.

4.3 Normalized Release Results

Fig.'s 4-1 to 4-12 show various graphs for normalized leach rates of the elements Na, Si, and Ca. Na was the best indicator of glass leaching because its solubility limit in DI water is extremely high. Si was analyzed because it was the network former of the glass. Calcium was shown for two reasons:

1) It was a major constituent in the glass which helped to retard devitrification.

2) The leach rate slope was negative at 90°C which may be related to crystalline phases or colloids forming on the glass surface or in the solution.

Normalized releases were fitted with empirical equations to deduce diffusion or saturation behavior. Goodness-of-fit statistics were compiled and the best fit to the data is shown in the graphs described below. When analyzing the curve fits, a T value, F value, and R^2 value were generated by the RS/1 program. The T value represented how much confidence there was in the individual data points which were fitted. The F value represented how much confidence there was in the curve. The R^2 value was the sum of the squares of the regression coefficient. The higher the T or F value the higher the confidence of the curve fit. For T and F, values generally ranged from 1 to 50, and 5 to 1000, respectively. The closer the R^2 value to 1, the better the curve. The solubility limit equation should follow $C = C_S(1-\exp(-bt))$ and diffusion should follow $C = at^{0.5}$. These mechanisms have been explained in the background chapter, and all of the fitting results can be found in Appendix F.

As a general statement on the effect of the test temperature, approximately an order of magnitude greater leach rates were observed when comparing 90°C tests to room temperature tests. In some cases, the room temperature tests show the curves increasing then topping off. However, in the 90°C tests, the concentration of some elements increased for a couple of weeks then decreased exponentially. This was probably due to precipitates forming in the leachate or on the glass surface which SEM-EDAX analysis can help to show. Other elements were not shown in this chapter because they were either at the limit of detection on the ICP machine or were not as indicative as Si, Na, and Ca. Graphs of other elements can be found in Appendix C.

4.3.1 Melts poured at 1250°C

According to sodium normalized leach results of Fig. 4-1, the glass with the highest leach rate at room temperature is batch 29 which was melted at a temperature of 1250°C and had a waste loading of 93%. The ternary diagram of Fig. 2-11 does not fall within the percentage range of batch 29. Assuming the dark equilibrium lines of Fig. 2-11 can be extended somewhat, the liquidus temperature for batch 29 would appear to fall well above 1250°C which may explain why the glass leached so poorly. This glass was the most difficult to keep from cracking in the mold and usually one of every three tries would be a success. The graph of Si and Ca at room temperature, Fig.'s 4-2 and 4-3, follow the same trend as Na. The pH results were also the highest of all the batches as it jumped up to values near 10 as shown in Fig. 4-17. This glass had the lowest percentage of SiO_2 and thus had the highest number of non-bridging oxygens. According to the network hydrolysis theory, this glass should have the highest dissolution rates of all the glasses due

to the number of nbo's. The statistical curve fits of Fig.'s 4-7 and 4-8 show that batch 29 follows diffusion relatively close with a good R^2 fit for elements Na, and Si.

There were two other glass compositions melted at 1250°C, batches 35 and 56. The effects on batch 35 will be discussed first. As can be seen from Fig.'s 4-1 to 4-3, the leach rates for Na, Si, and Ca, were just below those for batch 29. Batch 35 had a lower waste loading percentage than batch 29 and had a higher wt% of SiO_2. According to the multivariate analysis of Appendix B, Fig. B-1, an increase in Fe_2O_3 content would have helped the chemical durability of the glass. The wt% of Fe_2O_3 in the glass was found to be 4.36%. This is a mid-value relative to the other compositions. The ternary diagram of Fig. 2-11 shows that the liquidus temperature of batch 35 is somewhere near or above 1250°C. If that were the case then the glass should have had a high pour viscosity which it did not. The pour was similar to that of motor oil. The pH of this composition portrays the same trend of the leach rates: it starts with a slow rate and increases quickly to reach rates near batch 29. The data appears to reach solubility limits at the end of 28 days similar to where the saturation limit of silicon in water is (Fig. 4-11), which is near 12 ppm at room temperature. Batch 35 did not follow any particular curve fit and also had poor fitting coefficients.

The last glass of the 1250°C group was batch 56. This composition was almost exactly similar to that of batch 61 (melted at 1350°C) which had some of the lowest leach results. The difference in composition between these two batches was the addition of 7.59 wt% B_2O_3 and a smaller amount of Al_2O_3. Boron acts as a network former and flux as shown in Fig.'s 2-3 and 2-4, which lowers the melting temperature and thus the pouring temperature. Consequently, the melt could be poured at a lower temperature. The liquidus temperature for this melt was theoretically near 1300°C for Fig. 2-3 and the same for Fig. 2-11. Despite a pouring temperature which was theoretically lower than the liquidus temperature, there were no visible secondary phases. If the glass had been melted at 1350°C then it would be possible to determine if the addition of boron to this glass composition was detrimental. Because of the effects of melting temperature, it can not be assumed that boron was a factor in creating higher leach rates than encountered in batch 61. The results of the multivariate analysis are conflicting as one set displays a positive number and the other shows a negative number. However, relative to other numbers, the boron coefficient is small. Boron has an uncertain effect on the glass.

The statistical analysis for batch 56 (Fig.'s 4-7 to 4-10) shows that at room temperature, the glass dissolves according to saturation limits for sodium and silicon. However, when the temperature was increased to 90°C, the glass dissolved according to diffusion ($\sim t^{.5}$). At room temperature, the solubility limit of elements is low enough, so

that if the glass dissolves quickly it will reach the saturation limit quickly in a closed environment. When the leaching temperature is increased to 90°C, the solubility limit of the elements increases and the glass dissolves initially by diffusion. It would be expected as larger pores formed on the reaction layer that the dissolution of the glass would eventually follow t^{1} and then level off when it reached the solubility limit of a particular element.

4.3.2 Melts poured at 1300°C

The remainder of the compositions were poured at 1350°C except for batches 31, and 32 which were poured at 1300°C. Batch 31 and 32 had similar compositions but different melting times. Batch 31 was poured before batch 32 by a difference of 28 minutes. Batch 31 had the higher leach rates among the two. There are two obvious reasons why this would happen:

1) the slight change in waste loading was a crucial factor and/or

2) the longer melt time in the oven created a more homogeneous, stable glass in batch 32.

The leach rates of batches 31, and 32 are between the 1250°C and 1350°C pours. Thus indicating that pouring temperature is important in glass durability. Batch 32 shows consistent results of saturation limit controlled leaching for sodium and silicon as shown in Fig.'s 4-7 and 4-8. Statistical results for batch 31 were poor and no conclusions can be drawn from its data points.

4.3.3 Melts poured at 1350°C

For the four glass compositions which were poured at 1350°C, i.e. batches 37, 52, 59, and 61, all leach rates at room temperature were the lowest. Batch 37 and 61 were similar in composition and leach rates. These two batches had a thorium concentration of approximately 16 ppm. If batches 52 and 59 were also poured at 1350°C, why were their leach rates higher? Batch 59 had a much higher percentage of SiO_2 in it and a lower Na/Si ratio. This means a lower number of nbo's. However the concentration of Fe_2O_3 was an important difference. According to sources discussed in the background chapter and supported by the multivariate analysis, the increase in iron content increases the chemical durability of the glass. For sodium at 90°C, and silicon at room temperature and 90°C, batch 61 showed saturation limit controlled leaching. Batch 37 showed saturation limit leaching but had poor statistical values.

Batch 59 showed the highest leach rates for 90°C MCC-1 leach tests. In the room temperature tests, it had lower leach rates than batch 52 and 56. Batch 59 had a Si/Na ratio of 2.87, lower than that of batch 56, and 61, and the lowest amount of Fe_2O_3 and CaO

than all other Th-doped batches. It also had the lowest waste loading of these batches. In Fig. 4-6, the calcium leach rate decreases with the other batches also but started its descent last, which means that colloids took longer to form. Chick and Pederson's tests showed that reaction layers had no effect on glass leaching. This may have been true for their glass because it had poor chemical durability. Batch 59 displayed diffusion controlled leaching in all statistical analysis. Intuitively, it would be expected that saturation limit controlled leaching would be higher than diffusion because saturation occurs at the maximum value of elemental concentration in solution. However, all of the glasses which display saturation limit controlled leaching have the lowest leach rates. Batch 59 which showed diffusion controlled leaching at room temperature for sodium, continued to do such at 90°C for Na, and Si.

Batch 52, showed excellent chemical durability at 90°C compared to batch 56, and 59. It also had a higher Fe_2O_3 content than batch 59. Batch 52 was also melted in the furnace for a longer period of time. The difference in temperature for batch 52 shows that it leaches quickly at room temperature and perhaps if the tests were done longer it would have reached a saturation limit. The final data points for the graphs of batch 52 and 61 at 90°C are no higher than one order of magnitude than that of the room temperature tests for Si. For Na, however, the difference is even smaller. This would suggest that these two compositions will continue to leach at a slow rate. When the temperature was 90°C, the glass quickly reached a saturation limit as the equation shows for both Na, and Si in Fig.'s 4-9, and 4-10.

An experiment developed by Chick et al. (1984) to test for the dissolution mechanism was performed on batch 58, a duplicate of batch 52. It was found that for room temperature leaching, the glass displayed diffusion controlled leaching (Fig. 4-12). However, the statistical analysis shows that at 90°C, the saturation limit controls the glass degradation. Thus batch 52 starts out by diffusion and as the temperature is increased, switches to solubility controlled leaching.

According to saturation limit controlled leach theory, even thought the glass will not leach into the solution anymore, the glass will continue to interact with the water. The strange part of this is that sodium and silicon are well below their solubility limits in water for the 90°C tests. The fact that calcium is decreasing in the solution concentration may suggest that in fact the glass has stopped dissolving and a calcium rich precipitate has formed on the glass and created a protective layer for the bulk of the glass.

4.4 Elemental Analysis of Leach Test Results

A singular batch can be analyzed by comparing the leach rates of every element which is shown in Fig.'s 4-13 to 4-16. Two graphs representing both ends of the leach rate spectrum are shown for room temperature and 90°C tests. The y-axis units are gram of element in solution per gram of element in the glass. The general trend in each of the room temperature graphs is the following order of concentration:

$$Na, K > Ca > Mg > Si.$$

Batch 29 was chosen because it displayed the highest leach rates. Batch 61 was chosen because it displayed the lowest leach rates for Th-doped glass. The slope of the curves in batch 29 show that the elements are probably reaching their saturation limits which agrees with the results of previous figures. Batch 61, however, seems to increase exponentially. These results mean that the glass has probably passed the diffusion stage and is on the t^1 controlled leaching rate until it reaches saturation (see section 2.3.1). There is the possibility that the glass is at a stage before diffusion which explains the low leach rates. The order in which these elements have leached is because silica is the hardest bond to break according to the free energy of hydration, whereas Na and K are very soluble in water and have a higher free energy.

The best glass at 90°C was either batch 52 or 61. The only other two batches were 56, and 59 in which batch 59 had the highest leach rates. The trends in Fig.'s 4-15 and 4-16 show the following results:

$$Na > Si, B > Ca.$$

A change in this order occurs at 90°C with calcium because it shows a negative slope after a few days in both the 90°C graphs. In Fig. 4-11, boron and silicon leach at the same rates. Sodium has an extremely high solubility in water at 90°C and is expected to leach out the quickest. All other elements were not shown because they were at the limit of detection for the ICP spectrometer.

4.5 pH Results

The pH of each test was measured after the containers were removed from the environmental chambers and cooled to room temperature. Results in Fig. 4-17 show pH starting near the equilibrium point of air saturated DI water, 5.7, and increasing with time. In Fig. 4-18, the data points start at 14 days because the 5.7 pH at t=0, bunched up the remaining results.

pH results show similar trends to that of the leach tests. The higher the pH value, the more likely the glass composition is to display higher leach rates. The only discrepancy was the pH of batch 59 at room temperature which should have been higher than batch 61.

There may have been an error when the pH was measured but the samples were measured at the same time. The pH of the 90°C tests shows the values decreasing over time. This could be related to the amounts of calcium precipitating out of the solution which changes the pH. The highest pH values for the room temperature test reached ten for batch 29. The slope was still increasing at this point albeit it was a small gradient. The thorium batches all decreased in pH value after 28 days for the room temperature tests except for batch 52.

4.6 Multivariate Analysis Results

Data from many types of engineering projects have been used in multivariate analysis in order to discover any factors which shape, influence, or otherwise affect the data. This type of analysis is used in glass leach tests to determine which factors most influence the chemical durability. Examples of factors that may be considered are melt temperature, elemental percentages in the composition (mainly Si, Na, and Fe), melt time, waste loading, and some elemental ratios, i.e. Si/Na, Si/Ca, etc....

Two mathematical models can be used to perform this analysis, standard linear regression techniques, and least squares fitting [19, 20, 21]. The linear regression technique can only be used when the factors can be represented by equations such as:

$$Y_i = aX_i \qquad Y_i = a + bX_i$$

The least squares fit must be used when factors are represented by non-linear equations, e.g.:

$$Yi = a + bX_i^c \qquad Log\ Yi = a + b\log(X_i + c)$$

$$Yi = a + be^{cX_i} \qquad Log\ Yi = a + bX_i^c$$

Although the parameters may not be linear, the corrections to the data during the fit is a linear correction [20].

Once the program has been run, the items with the largest positive coefficients are assumed to influence the chemical durability of the glass as beneficial changes whereas large negative coefficients indicate detrimental changes with increases in the parameter.

In this particular analysis, all parameters have been normalized to the mean number in that particular parameter (Fig.'s B-1 to B-3). For example, in the matrix T (melting temperature) of Fig. B-1 , all temperatures are normalized with respect to 1325°C. It has been assumed that all parameters are linearly related to the leach rate. Although this may be a poor assumption, it simplifies the analysis and will still allow general trends to be shown. Furthermore, it should be noted that parameters were manipulated in different ways until the best results were found and that some values in the b matrix switched from positive to negative and vice-versa.

If the b matrix value was positive, it meant that an increase in that parameter increased the leach rate. A negative value meant that the parameter added chemical durability to the glass. As discussed in the background chapter, the factors used in this analysis were sodium leach rates, melting temperature, and certain oxide wt%'s. Fig. B-1 analyzed the data from 28 day room temperature leach tests involving thorium doped and non-radioactive glass. Fig. B-2 looked at the 90 day results at room temperature for the radioactive glass (<16 ppm) and Fig. B-3 represents the 180 day results at 90°C for radioactive glass.

The strongest indicators for improved durability are an increase in melting temperature and an increase in Fe_2O_3 content. This is consistent with the fact that melts above the liquidus temperature are more stable than melts near or below that temperature according to Fig. 2-11. Also, a higher iron content is supposed to improve chemical durability as this analysis agrees with. Each matrix was normalized to the mean value of that particular matrix. This was the most consistent way to analyze the data because some of the outlying data points may have distorted the other remaining data points less than say using the minimum or maximum matrix values. The oxide percentages examined were SiO_2, B_2O_3, CaO, MgO, Na_2O, and Fe_2O_3.

MgO, Cao, and Na_2O all showed that increases in these compositions also increased leach rates. The strongest of the three oxides was the percentage of MgO. Apparently, MgO induces more leaching than CaO and Na_2O. The amount of SiO_2 content has different implications depending on the data used. For room temperature tests at 28 days, the analysis states that the more SiO_2 there is, the higher the leach rates. However, in Fig. B-2, and B-3, the data states that an increase in SiO_2 lowers the leach rates. It is known that the higher the content of silica present, the lower the leach rates because there are fewer nbo's. Therefore, Fig. B-1 does not have as much reliability to it as do Fig.'s B-2 and B-3.

If the glass is to be analyzed for long term leach rates, then it would be best to look at the longest day test at the highest leaching temperature. Fig. B-3 is exactly that. It states that the following factors improve chemical durability in the following order:

$$\text{Temperature} > SiO_2\ \text{wt\%} > Fe_2O_3\ \text{wt\%}.$$

The following factors decrease chemical durability in the following order:

$$CaO\ \text{wt\%} > MgO\ \text{wt\%}, Na_2O\ \text{wt\%} > B_2O_3\ \text{wt\%}.$$

The magnitude of the numbers is very important in this analysis. For example, temperature has a magnitude of 4, whereas Fe_2O_3 has a magnitude of 0.5. This means that temperature is 8 times more effective than Fe_2O_3 in increasing chemical durability.

4.7 SEM-EDAX Analysis

In order to determine if any crystalline phases were present on the surface of the glass, a SEM-EDAX analysis was performed on two of the best glass compositions, batch 37 and 61. The results can be found in Appendix G. Figure G-1 shows a graph of the elements present on the surface of batch 61 and below that, the micrograph of the glass surface. The EDAX results show that the elements which constitute the bulk of the glass also constitute the surface on a point analysis. At 500X magnification there are no crystal formations present on the glass surface. This was typical of both batches. Micrographs were taken of the smooth surface of the glass and not at natural breaks because the glass could not be mounted in that manner.

The micrograph of Fig. G-2, also of batch 61, shows what was initially thought to be a crystal but turned out to be chunk of bulk glass which was verified by the EDAX. If it had been a crystal it would have been expected to have only a few elements present and not all of them. The final graph, Fig. G-3, shows surface roughness and micro-holes on the otherwise smooth surface of batch 37. The sharp figures were thought to be crystals at first but the EDAX confirmed that it was part of the glass which must have cracked when dropped or cooled.

The fact that there are few crystals present on the surfaces of batch 37 and 61, at least none that could be found, supports the fact that the most chemically durable glasses do not have crystalline structures present. Batch 37 and 61 represented the best non-radioactive and Th-doped glass compositions, respectively.

Table 4-1. Rocky Flats Glass Composition Summary

Oxide	Batch 29	Batch 31	Batch 32	Batch 35	Batch 37	Batch 52	Batch 56	Batch 59	Batch 61	100 % Waste Loading
SiO2	22.73\28.51	22.81\52.62	15.96\51.55	22.61\44.17	22.73\47.46	22.8\45.3	37.69\41.53	61.12\62.01	22.79\43.78	22.8
Na2O	19.57\17.07	49.34\25.82	49.36\25.71	34.59\23.36	19.55\11.97	34.08\22.35	14.01\11.27	22.57\21.64	19.58\11.64	19.6
Al2O3	1.08\2.16	2.77\5.40	9.60\8.31	3.03\3.74	1.12\3.40	3.07\3.21	0.80\0.86	1.24\1.11	1.10\2.08	1.1
B2O3	0\0	0\0	0\0	0\0	0\0	0\0	7.02\7.65	0\0	0\0	0
CaO	23.03\21.2	10.21\5.61	10.20\4.93	16.14\10.84	23.04\13.74	16.27\10.78	16.46\14.79	6.13\6.21	23.02\16.20	23.1
ZnO	0\0	0\0	0\0	0\0	0\0	0\0	0\0	0\0	0\0	0
MgO	13.00\10.71	5.76\3.21	5.74\2.82	9.11\6.11	12.96\7.44	9.18\6.29	9.29\9.08	3.44\3.58	12.99\9.36	13
Fe2O3	9.48\8.28	4.17\2.28	4.15\2.13	6.64\4.36	9.40\5.34	6.66\5.62	6.70\6.43	2.52\2.29	9.36\7.85	9.4
La2O3	0\0	0\0	0\0	0\0	0\0	0\0	0\0	0\0	0\0	0
K2O	6.01\6.54	2.69\2.74	2.70\2.46	4.28\4.03	6.08\5.79	4.31\3.64	4.31\4.65	1.62\1.48	6.07\5.12	6.1
SO3	0.41\0.44	0.19\0.19	0.18\.017	0.29\0.27	0.42\0.40	0.28\0.24	0.31\0.33	0.11\0.1	0.41\0.34	0.4
P2O5	4.69\5.10	2.07\2.13	2.10\1.92	3.31\3.12	4.70\4.47	3.34\2.58	3.41\3.42	1.26\1.59	4.69\3.63	4.7
PbO	0\0	0\0	0\0	0\0	0\0	0\0	0\0	0\0	0\0	0
Cr2O3	0\0	0\0	0\0	0\0	0\0	0\0	0\0	0\0	0\0	0
NiO	0\0	0\0	0\0	0\0	0\0	0\0	0\0	0\0	0\0	0
BaO	0\0	0\0	0\0	0\0	0\0	0\0	0\0	0\0	0\0	0
CdO	0\0	0\0	0\0	0\0	0\0	0\0	0\0	0\0	0\0	0
NaF	0\0	0\0	0\0	0\0	0\0	0\0	0\0	0\0	0\0	0
ThO2	0\0	0\0	0\0	0\0	0\0	0.0014\0.0	0.00123\0.0	0.00051\0.0	0.00193\0.0	16 ppm
UO2	0\0	0\0	0\0	0\0	0\0	0\0	0\0	0\0	0\0	0
Temp C	1250	1300	1300	1250	1350	1350	1250	1350	1350	
Time (min)	155	190	218	155	135	221	201	175	220	
Si/Na ratio	1.67	2.04	2.01	1.89	3.97	2.03	3.68	2.87	3.76	
Waste Loading %	99.61	37.12	23.46	66.28	99.72	66.99	60.92	17.09	99.77	
Color	BLACK	BLACK	BLACK	DARK BROWN	BROWN	BROWN\BROWN		GREEN	DARK BROWN	
Pour Quality	MOTOR OIL	MOLASSES	MOTOR OIL	MOTOR OIL	MOTOR OIL	MOTOR OIL	MOTOR OIL	MOLASSES	MOLASSES	
Leach Resistance	WORST	FAIR	FAIR	POOR	BEST	GOOD	GOOD	GOOD	GOOD	

Fig. 4-1. Room Temperature, DI Water
MCC-1, Normalized Leach Results

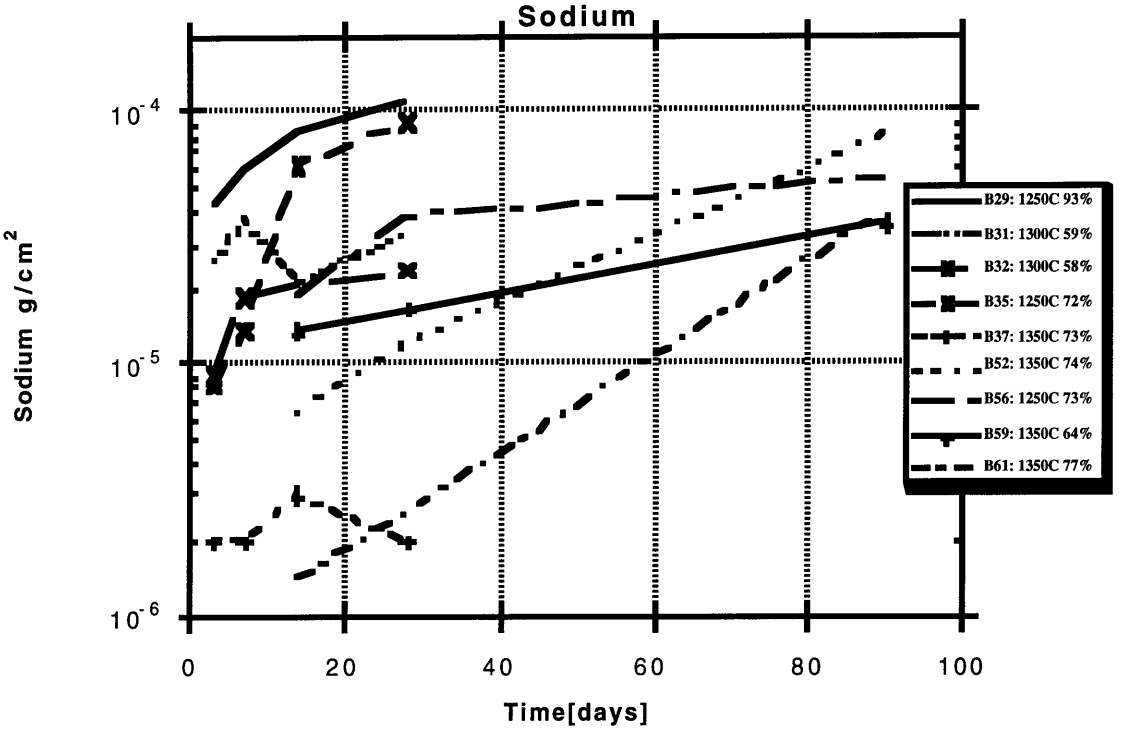

Fig. 4-2. Room Temperature, DI Water
MCC-1, Normalized Leach Results

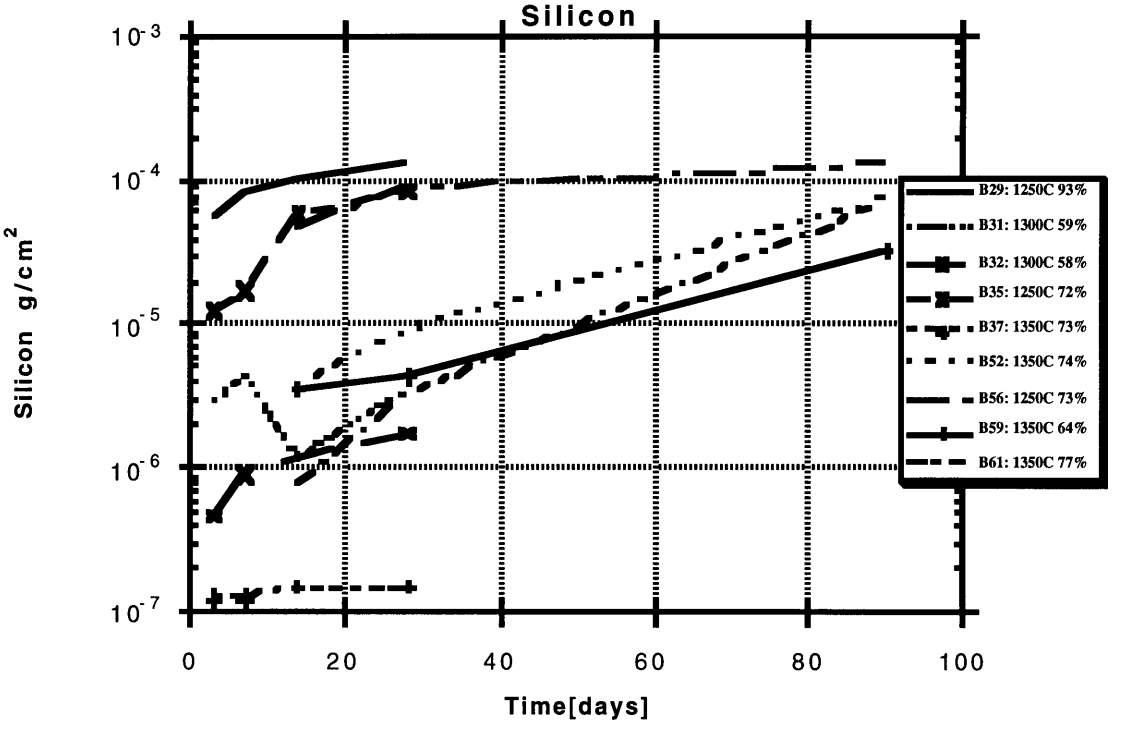

Fig. 4-3. Room Temperature, DI Water
MCC-1, Normalized Leach Results

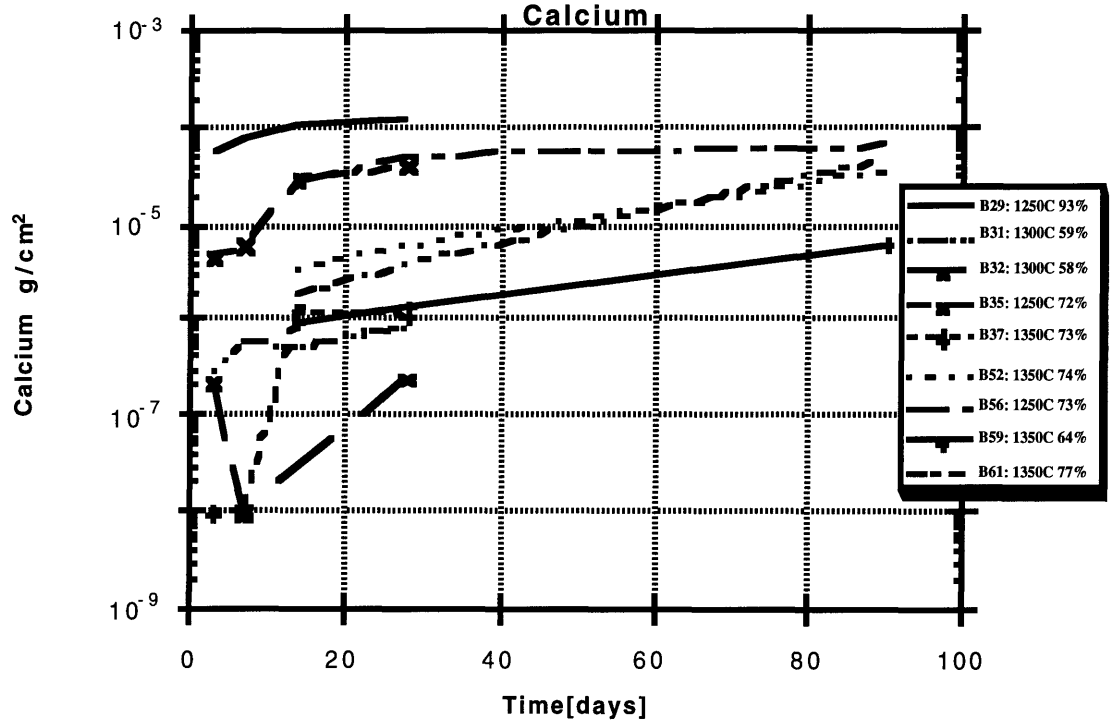

Fig. 4-4. 90°C, DI Water
MCC-1, Normalized Leach Results

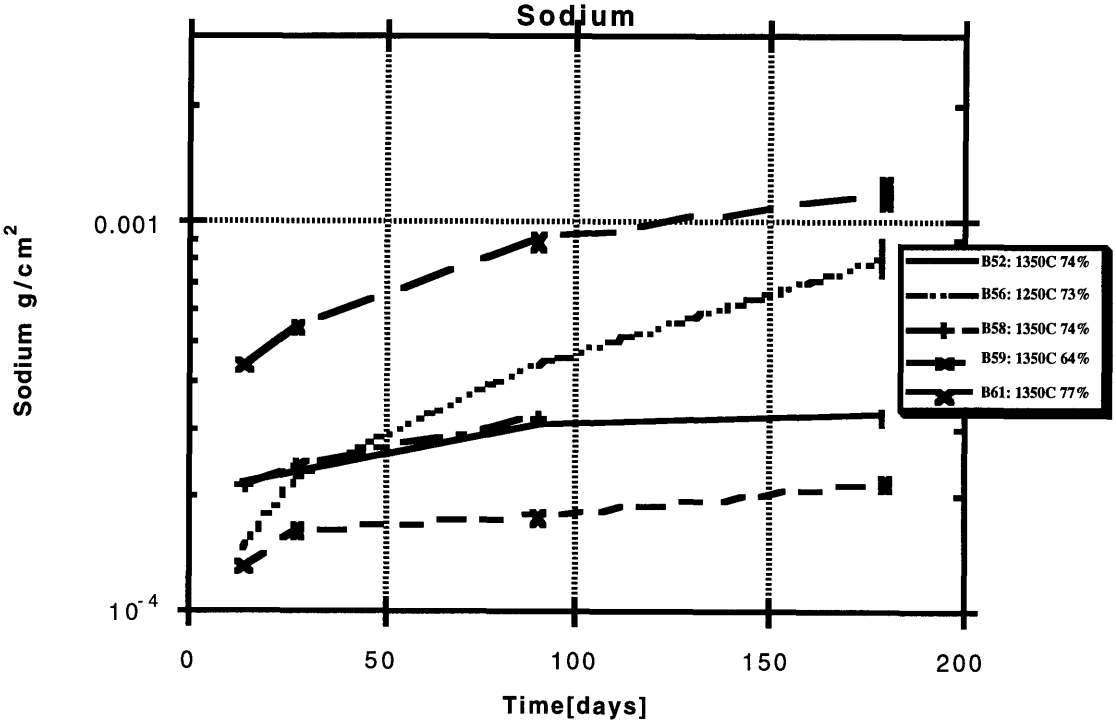

Fig. 4-5. 90°C, DI Water
MCC-1, Normalized Leach Results
Silicon

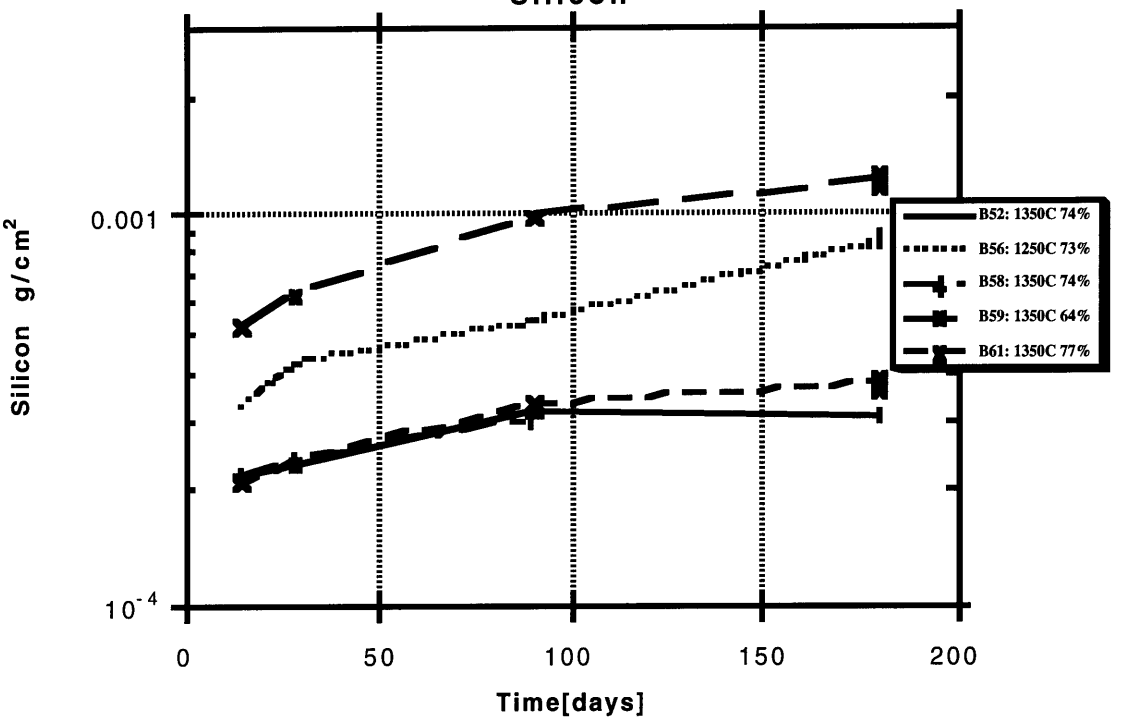

Fig. 4-6. 90°C, DI Water
MCC-1, Normalized Leach Results
Calcium

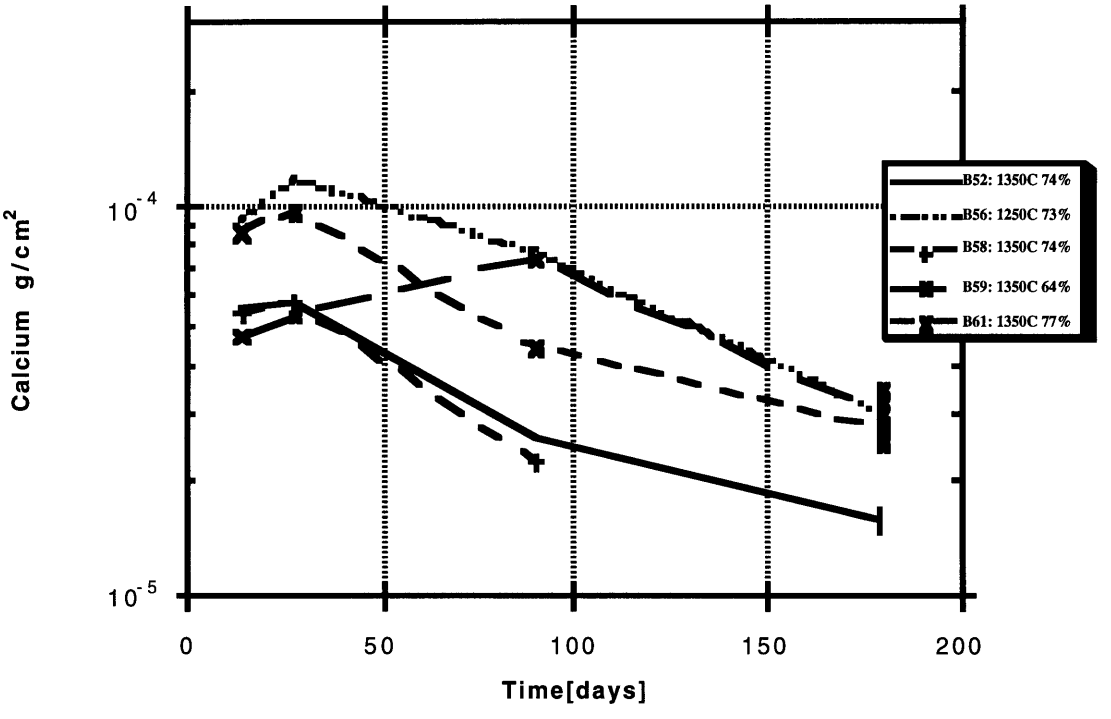

Fig. 4-7. Room Temperature, DI Water
MCC-1, Normalized Leach Results
Sodium

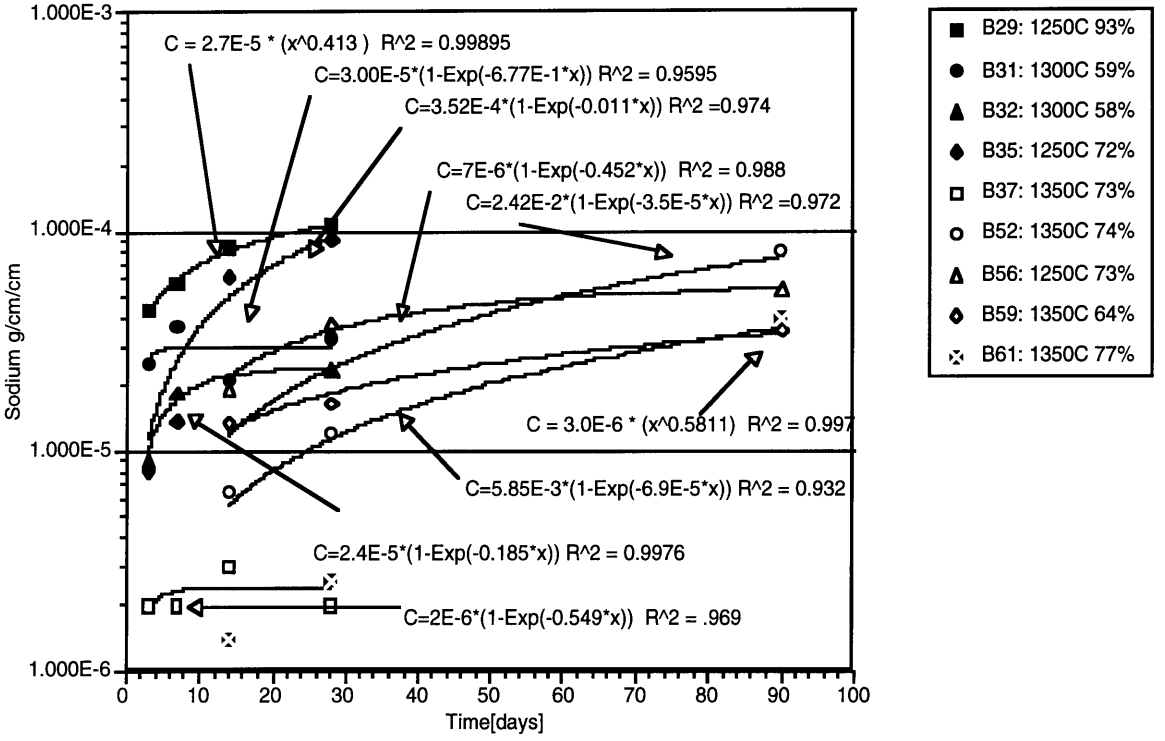

Fig. 4-8. Room Temperature, DI Water
MCC-1, Normalized Leach Results
Silicon

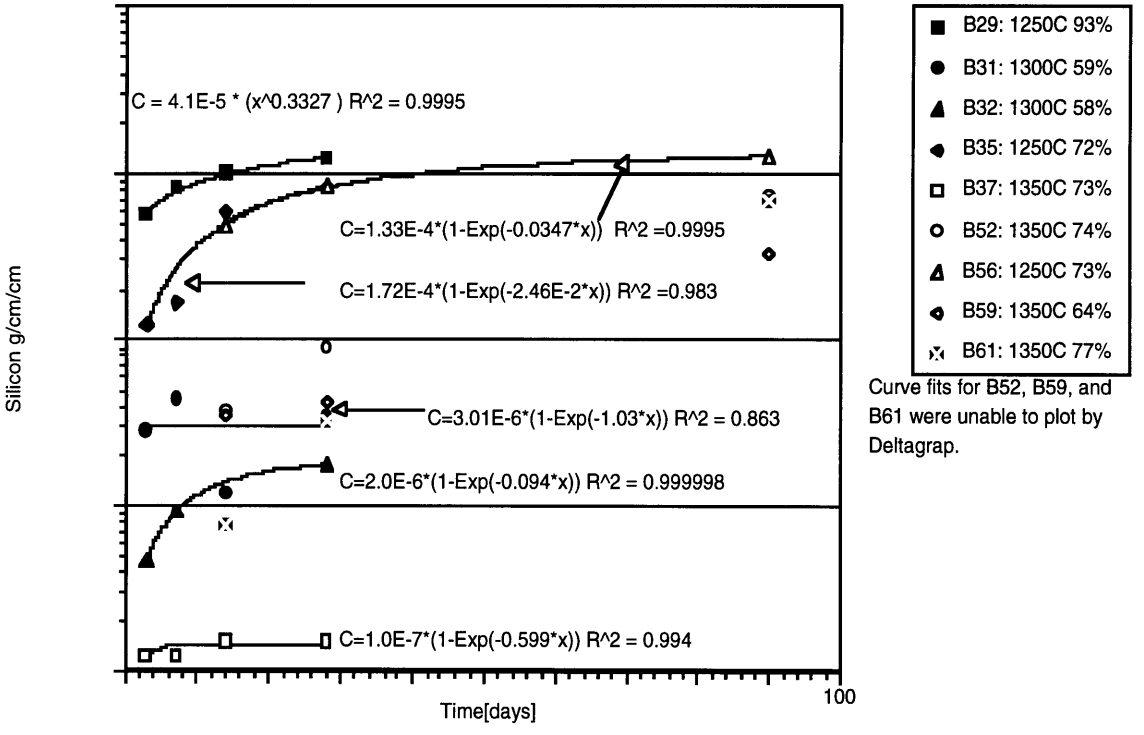

Curve fits for B52, B59, and B61 were unable to plot by Deltagrap.

Fig. 4-9. 90°C, DI Water
MCC-1, Normalized Leach Results
Sodium

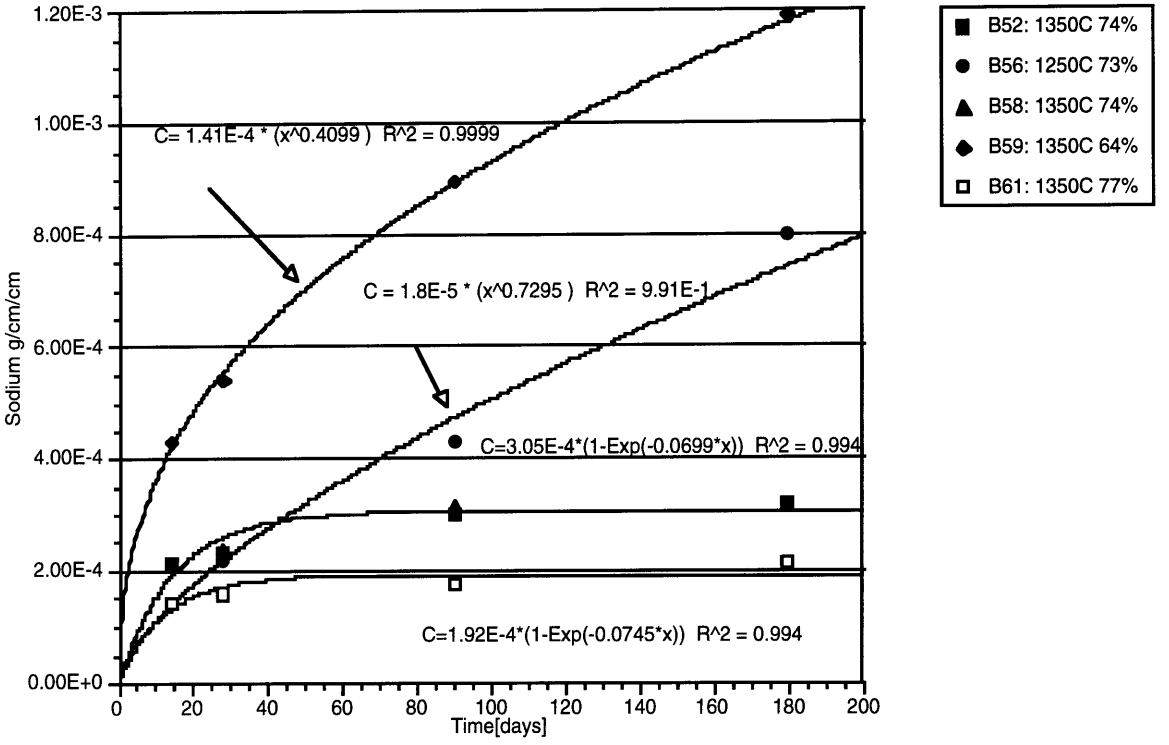

Fig. 4-10. 90°C, DI Water
MCC-1, Normalized Leach Results
Silicon

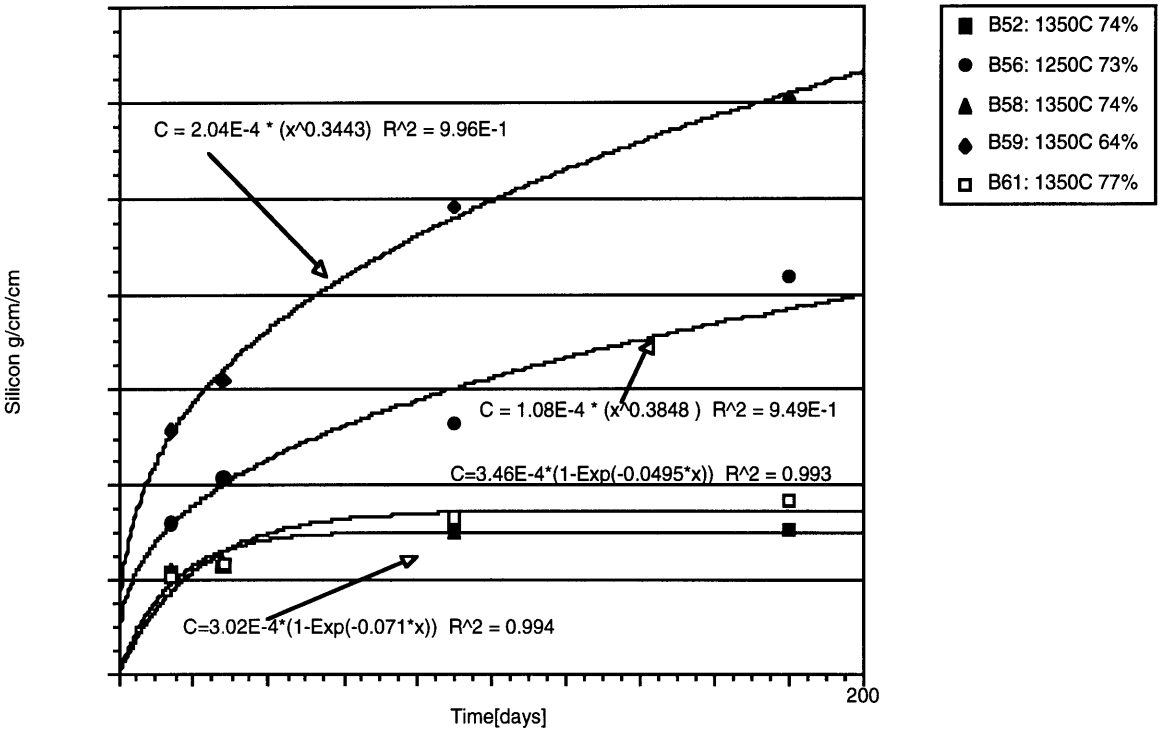

Fig. 4-11. Room Temperature, DI Water, MCC-1 Solubility limit of Silicon vs. Normalized Leach Results

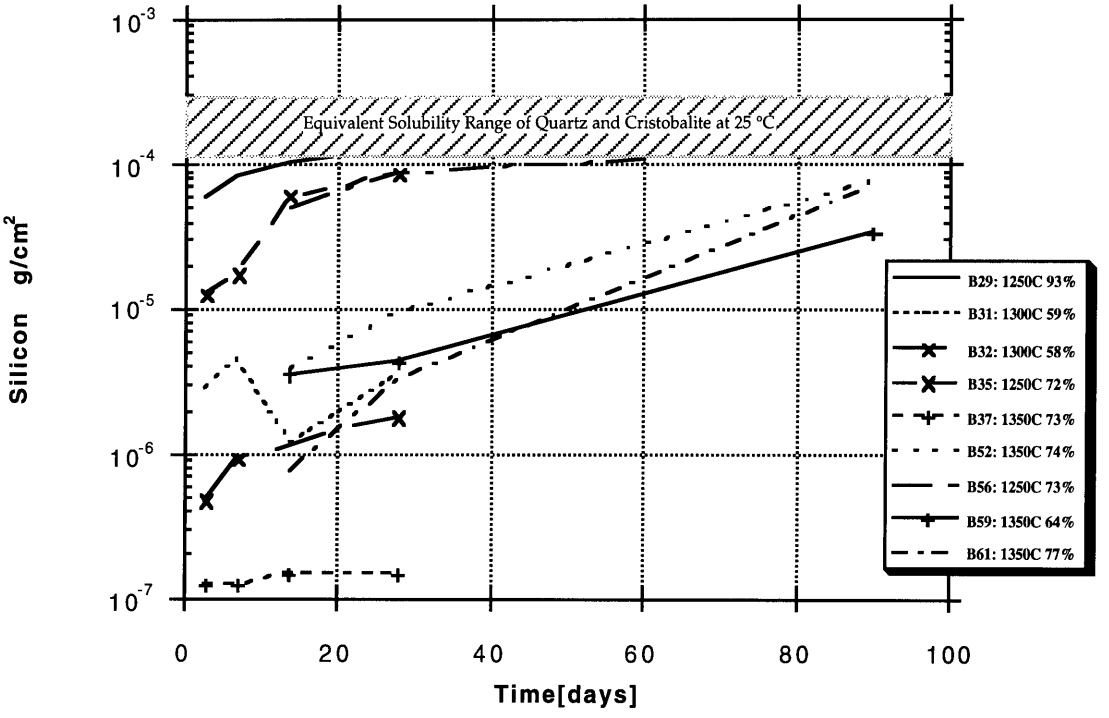

Figure 4-12. Investigation of Mechanism of Dissolution of Rocky Flats Sludge Glass (73% waste loading) Batch 58

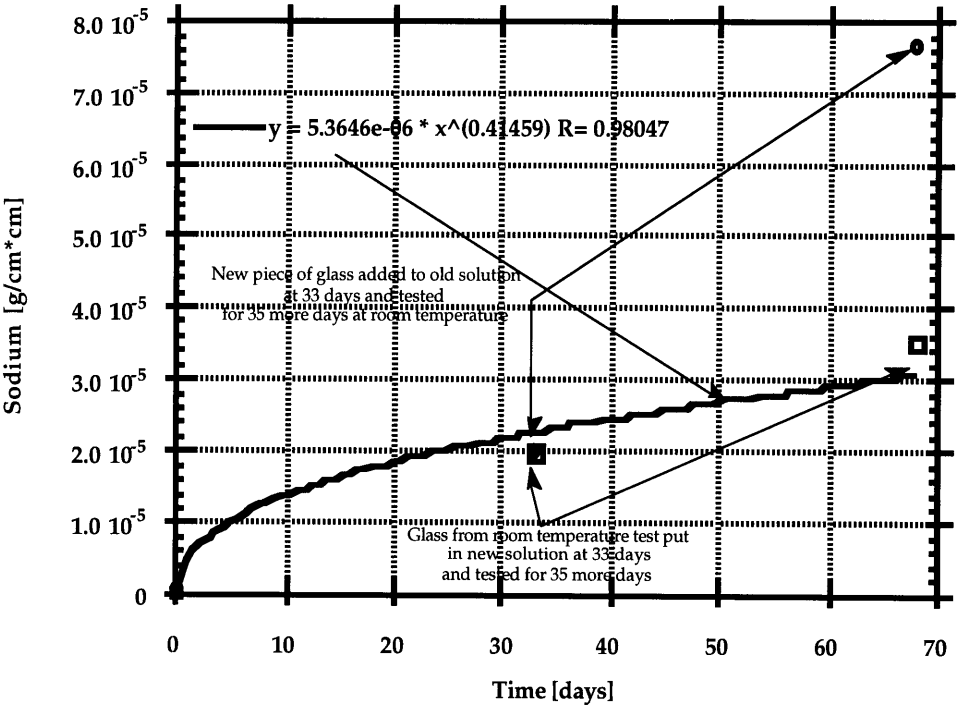

Fig. 4-13. Room Temperature, DI Water
MCC-1, Elemental Analysis
Batch 29

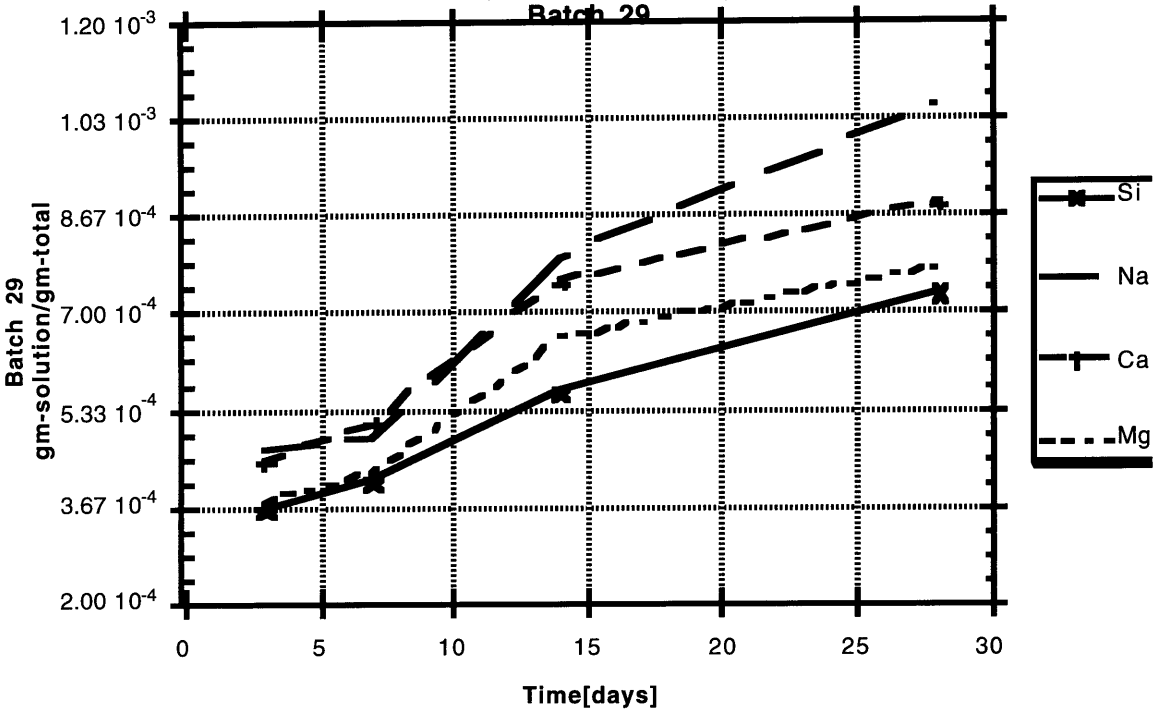

Fig. 4-14. Room Temperature, DI Water
MCC-1, Elemental Analysis
Batch 61

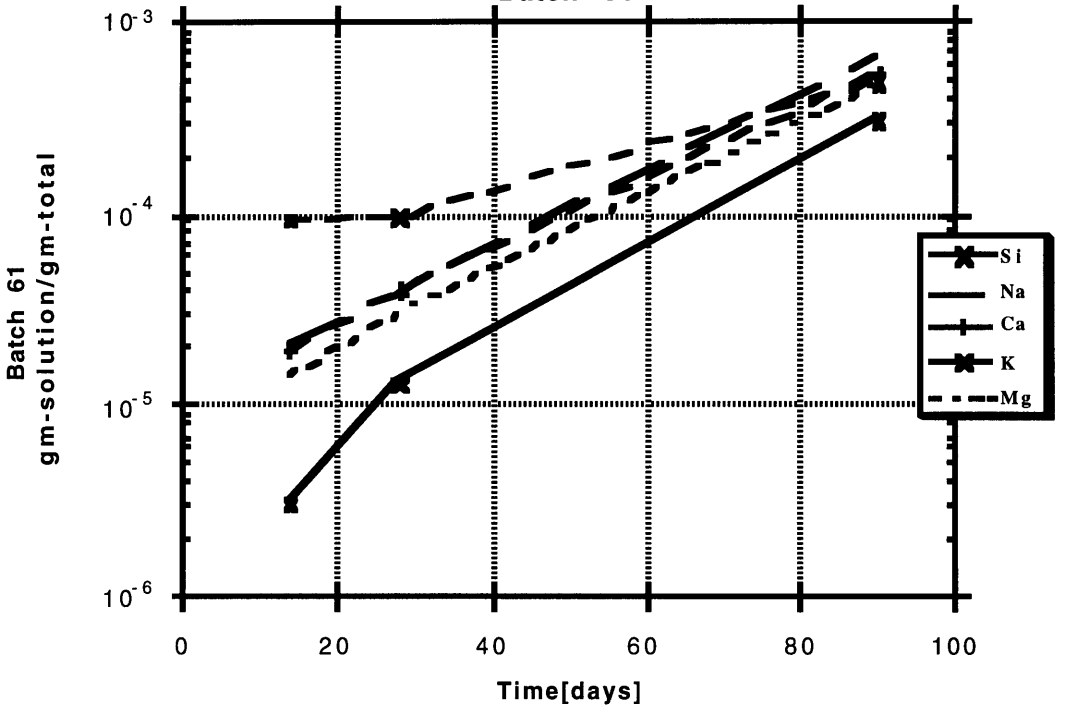

Fig. 4-15. 90°C, DI Water
MCC-1, Elemental Analysis
Batch 52

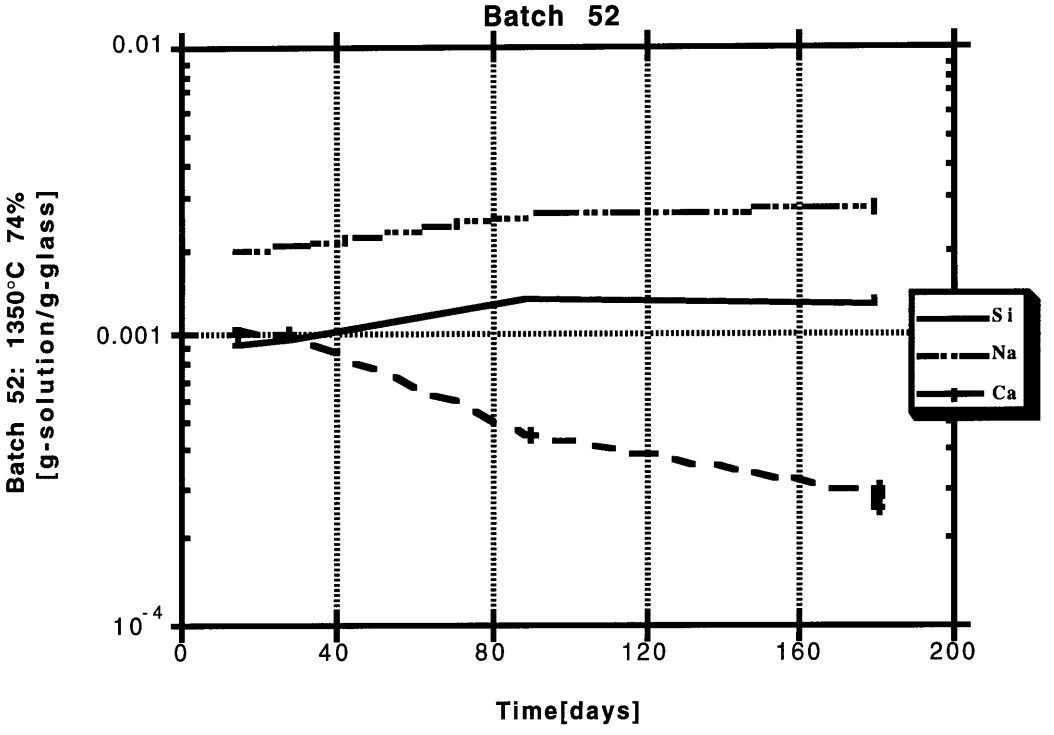

Fig. 4-16. 90°C, DI Water
MCC-1, Elemental Analysis
Batch 56

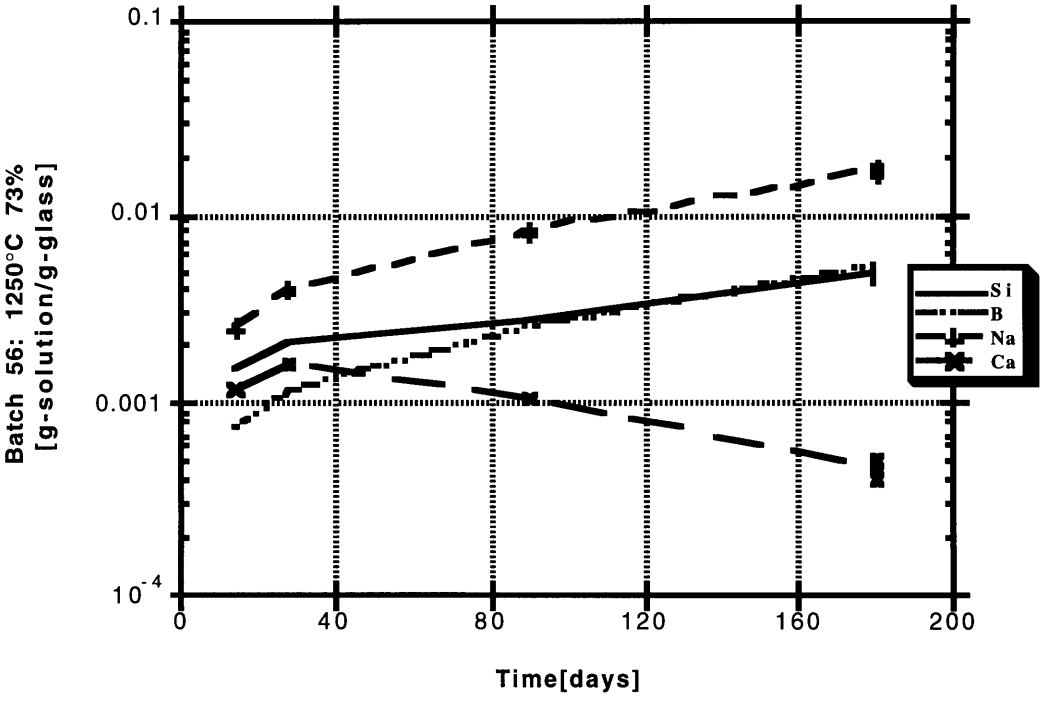

Fig. 4-17. Room Temperature, DI Water MCC-1, Normalized Leach Results pH

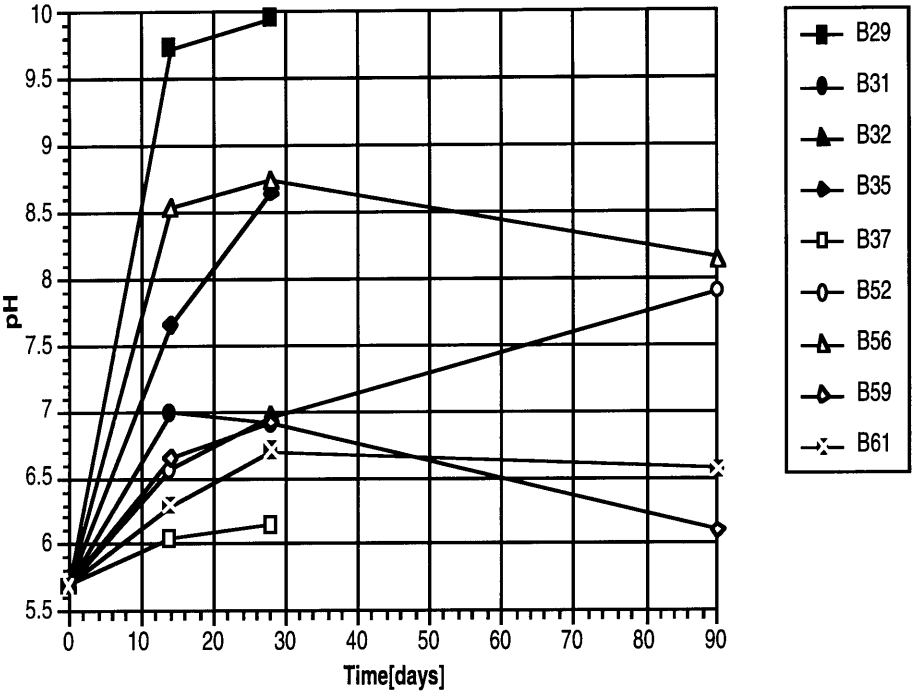

Fig. 4-18. 90°C, DI Water MCC-1, Normalized Leach Results pH

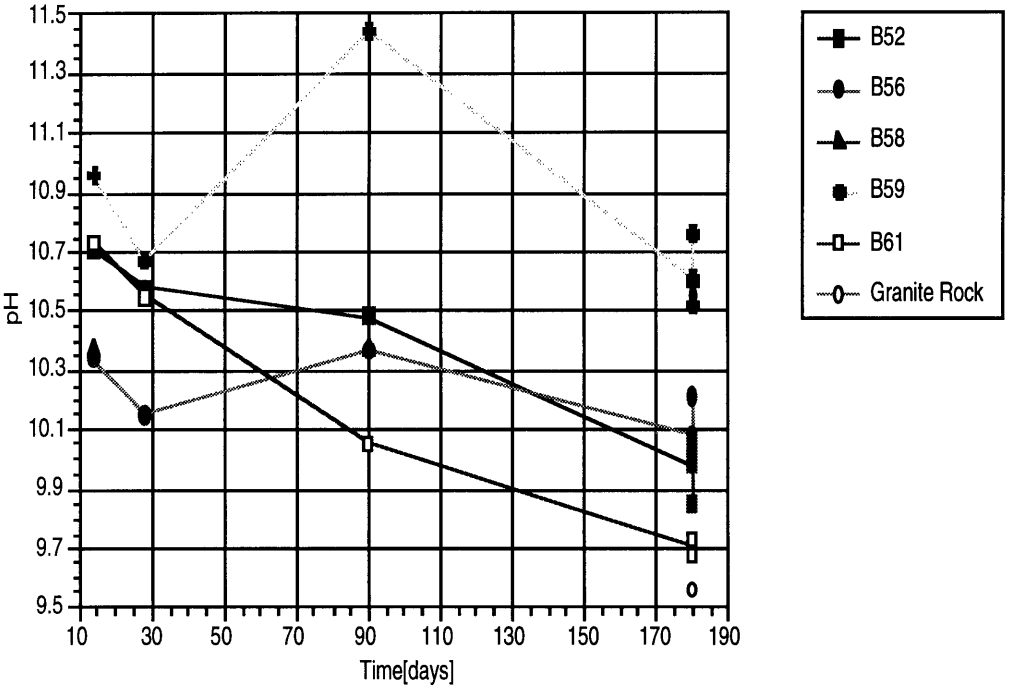

Chapter 5

CONCLUSIONS AND FUTURE WORK

5.1 Chapter Summary

The main points of the discussion and results chapter are concluded in this section. After this, the importance of continuing work on the Rocky Flats glass is discussed along with a series of experiments which will help define the characteristics of the glass and its relationship to all other glass forms.

5.2 Conclusions

The overall effects of melting temperature, leach test temperature, glass composition, time in furnace, waste loading, and other factors, were presented in chapter 4. Of these factors, the most important variables in improving chemical durability were melting temperature and glass composition. In general, it was found that the higher the melting temperature of the furnace, the more chemically durable the glass. Despite the broad range of chemical compositions for Rocky Flats glass, the optimum melting temperature was 1350°C. The optimum glass composition was found to be near 74% waste loading with a SiO_2/Na_2O ratio between 3.5 and 4.0. The addition of Fe_2O_3 to the glass improved chemical durability also.

5.2.1 Melting temperature

Any glass melted at 1250°C turned out to have poor chemical durability relative to the other glasses. One exception to the glasses melted at 1350°C was batch 59, which had the overall highest leach rate for the 90°C leach tests.

It is hard to say which glass would be the worst since that all depends on the underground repository results. Obviously, the glasses melted at 1250°C with leach rates approximately one order of magnitude or higher than 1350°C melts would not be desirable whether they leached via diffusion or saturation limits. Also, all glasses leached at 90°C showed leaching approximately one order of magnitude higher than room temperature tests. The best glass for the Th-doped batches was batch 61. It had a melting temperature of 1350°C, a Si/Na ratio of 3.76, and a waste loading of 77%.

The worst glass was batch 29. This glass had the lowest wt% of SiO_2, the lowest ratio of Si/Na at 1.67, and the highest waste loading of the batches. If the glass was melted at 1350°C, perhaps this would have been a better glass. In fact this was attempted with batches 37, and 61. Due to the corrosiveness of the melt at that temperature, more silicon

from the crucible seeped into the molten glass. In general batch 37 showed better results than 61 even though they started out with the same compositions. Batch 37 spent less time in the furnace but ended up with more silicon than batch 61. This has not been explained.

5.2.2 Oxide influence on chemical durability

According to information in the background chapter, and supporting data from the multivariate analysis, an increase in Fe_2O_3 content increased the chemical durability of the glass. Al_2O_3 has the same structure in glass as Fe_2O_3 and has shown to increase the chemical durability of the glass. The best glass for the Th-doped batches was batch 61. It had a high percentage of Fe_2O_3, a long melting time, and a low percentage of Na_2O. Another contributor to the leach rate may have been the high CaO wt%. which retards devitrification. In all cases, a SiO_2/Na_2O ratio near 4 seems to be the optimum glass composition. In summary the following factors improved chemical durability according to the MCC-1 leach test results and multivariate analysis:

Melting Temperature > Fe_2O_3 wt% > SiO_2 wt%

Because the coefficient for B_2O_3 was small, it is not sure whether or not the contribution has any effect on the glass durability. The following factors helped to decrease the chemical durability:

MgO wt%. > Na_2O wt%. > CaO wt%.

The gram per gram analysis was in good agreement with expected results as far as which elements leach the fastest. According to the results the following order applies to room temperature and 90°C tests, respectively:

Na > Ca > Mg > Si,

Na > B, Si > Ca

Other elements were not analyzed due to the fact that they were at the limit of detection on the ICP machine.

5.2.3 pH significance

The consistency of the pH results show that by looking for the lowest pH's in the MCC-1, the best glass could be found. pH varied from 6.0 to 8 and 9.5 to 11 for room temperature and 90°C tests, respectively. Those glasses with the lowest pH showed in general two orders of magnitude lower leach rates than those glasses with the highest pH. It is expected that one pH point is equivalent to one order of magnitude in leach rate according to the following dissociation of Na_2O in glass:

$$Na_2O + H_2O \rightarrow 2Na^+ + 2OH^-.$$

The correlation between pH difference and leach magnitude is significant in that good assumptions could be made about the leach rate of all other batches once one all pH values were known and only one data point from leach tests were found.

5.2.4 Comparison to lead-iron-phosphate and borosilicate glass

In conclusion, the glass made for Rocky Flats plant sludge showed normal characteristics for glass dissolution. Some glasses showed diffusion and others leached via saturation limit controls. When compared to other glass produced for different projects (Fig. 5-1), i.e. Savannah River borosilicate glass, the leach rates were two orders of magnitude lower except for lead-iron-phosphate (LIP) glass which has extremely low leaching rates [2]. The best glass from Rocky Flats was within one order of magnitude of the leach rate of LIP glass. The glass leached via network hydrolysis mechanisms for an initial time and would develop pores large enough to begin the transition from $t^{.5}$ to t^{1} leaching. This eventually lead to saturation limit controlled leaching where no more oxides in the glass could dissolve in the leachate but could still react with the glass. If new water was placed into the environment, leaching would be extremely rapid.

Fig. 5-1. 30 Day Corrosion Rate, 90°C DIW, Leach Test

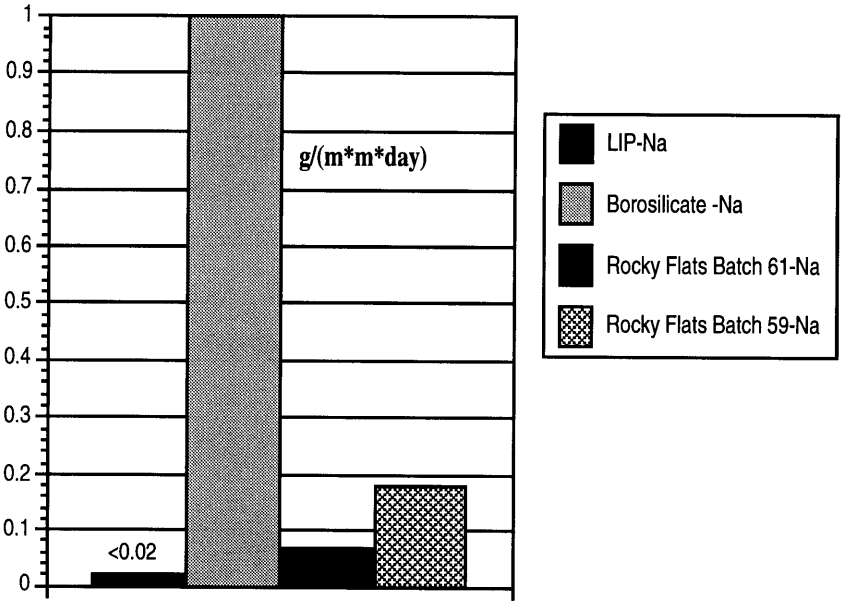

5.3 Future Experimental Work

Future work is important because it allows the results from this thesis to be incorporated into a large picture of glass degradation. Many contributions from this study can still be made. The leach tests undergone in this thesis only scratched the surface of possible experiments. In order for this work to be more valid, there should be some results duplicated in order to make sure that the tests are reproducible and precise. Beyond those lines, the Rocky Flats glass can be used for a wide variety of experiments such as radiolysis tests in the MITR-3 reactor, 40°C leach tests, phase separation tests, and others described in the following paragraphs.

5.3.1 Duplication of results

Several aspects of this work could be re-verified such as leach tests, and fusion results. Even though batch 58, a duplicate of batch 52, leached with similar results, some of the best glasses should now be re-tested such as batches 37 and 61. Tests were completed in room temperature and 90°C environments but not in the 40°C environment. Once a student completes tests for that temperature, they can be correlated to the other two temperatures which will increase the accuracy on long term predictions of this glass.

5.3.2 Radiolysis tests

There has been some literature which shows that a low level radiation field can cause the glass to decompose rapidly versus no radiation or strong radiation. Rocky Flats glass contained the TRU limit for low level waste of plutonium. That amount of radiation may be in the high decomposition range according to the study.

5.3.3 Oak Ridge leach tests

Unfortunately, Oak Ridge vitrified waste was not leach tested. The amount of time required to prep the samples and leaching containers could only be dedicated to Rocky Flats glass samples. However, three compositions of Oak Ridge glass were made and are ready for leach testing. The same analysis could be completed on this glass to determine if the same variables affect the chemical durability of the glass.

5.3.4 Chemicals used to produce oxides

The effects of using different chemicals which ultimately produce the same oxide when melted should be studied to determine how much of a reaction they create in the crucible when decomposing. For example, Na_2O could be made with $NaHCO_3$ or NaOH or $NaNO_3$ and one of these chemicals reacts more with the crucible than the other.

5.3.5 Diffusion vs. saturation limit tests

Tests attempting to determine whether the glass leached via diffusion or some other mechanism were completed on batch 58 which was a duplicate of batch 52 via Chick and Pederson's fluid/glass switching procedures. Room temperature results showed diffusion. However, the curve fitting program of Deltagraph Pro version 3.1 showed a dependence of $t^{1.6}$ which means the leach rate was increasing exponentially. The test created by Chick and Pederson does not have enough data points to determine what curve fit the data should belong to. However, it is an excellent indicator of determining if the glass leach rate is controlled by the surface layer or solution elemental concentration. Tests of this nature should be completed on the best glass compositions from Rocky Flats and Oak Ridge glasses.

5.3.6 Phase separation tests

Tests where the glass sits in the furnace for over 24 hours near the melting temperature are necessary to determine if the glass will phase separate. Also, rather than cooling the glass off within thirty minutes of pouring, the glass should be cooled slowly. This would simulate the large amount of time required when pouring glass into large canisters which sometimes propagates devitrification. Glass can also be tested in the SEM after sitting at a furnace temperature of 1000°C which would promote secondary phase growth and hence show glass stability.

Chapter 6

REFERENCES AND BIBLIOGRAPHY

References

1 Scholes, S. R. 1975. Modern Glass Practice. CBI Publishing, Company, Inc.,Boston.

2 Lutze, W., and R. C. Ewing, ed. 1988. Radioactive Waste Forms for the Future. North-Holland, Amsterdam.

3 Ebert W. L., and J. K. Bates. 1991. The Importance of Secondary Phases in Glass Corrosion. Scientific Basis for Nuclear Waste Management XIV **212**:89-97.

4 Bunker, B. C. 1987. Waste Glass Leaching: Chemistry and Kinetics. Scientific Basis for Nuclear Waste Management X **84**:493-507.

5 Carroll, S. A., W. L. Bourcier, and B. L. Phillips. 1993. Surface Chemistry and Durability of Borosilicate Glass. Scientific Basis for Nuclear Waste Management XVI.

6 Fax from Kathy Wittington, PNL, Hanford WA. March 1994.

7 of Van Isegham, P., W. Timmermans, and R. DeBatist. 1984. Corrosion Behavior TRUW Base and Reference Glasses. Scientific Basis for Nuclear Waste Management VII **26**:527-534.

8 Chick, L. A. and Pederson L. R. 1984. Relationship Between Reaction Layer Thickness and Leach Rate for Nuclear Waste Glasses. Scientific Basis for Nuclear Waste Management X **26**:635-642.

9 Grambow, B., and D. M. Strachman. 1984. Leach Testing of Waste Glasses under Near-Saturation Conditions. Scientific Basis for Nuclear Waste Management X **26**:623-634.

10 Kingery, W. D., H. K. Bowen, and D. R. Uhlmann. 1976. Introduction to Ceramics. New York, John Wiley & Sons, Inc., NY, New York

11 Mozzi, R. L. 1967. Sc.D. thesis MIT.

12 Flint, and Wells. 1933. The System Lime-Boric Oxide-Silica. *J. National Bureau of Standards* **17**:727-752.

13 Morey, G. W., 1954. The Properties of Glass. Reinhold, New York.

14 Morey, G. W., *J. Am. Ceram. Soc.*, **15**, 457 (1932).

15 Morey and Bowen. 1924. Professional Paper 440-L, Geological Survey, U.S. Department of the Interior, Reston, Virginia.

16 Rankin and Wright. 1915. Professional Paper 440-L, Geological Survey, U.S. Department of the Interior, Reston, Virginia.

17 Wyckoff, W. G., and G. W. Morey. 1925. The Melting Relations of the Soda-Lime-Silica Glasses. *J. Soc. Glass Technology* **9**:226-264.

18 Shahid, K. A., and F. P. Glasser: Phase Equilibria in the system Na-Ca-Mg-Si. *Physics and Chemistry of Glasses* **13**:27-42.

19 Conway, G. R., N. R. Glass, and J. C. Wilcox. 1970. Fitting Nonlinear Models to Biological Data by Marquardt's Algorithm. *Ecology* **51**:503-07.

20 Glass, N. R. 1967. A Technique for Fitting Nonlinear Models to Biological Data. *Ecology* **48**:1010-13.

21 Watson, C. R., M. I. Cochran, J. W. Thomas, and L. L. Eberhardt. 1977. Comp - A Basic Non-linear Least Squares Curve Fitting Package. Proceedings of the Digital Equipment Computer Users Society: 515-19.

Bibliography

Abrajano, T. A. Jr., J. K. Bates, and C. D. Byers. 1986. Aqueous Corrosion of Natural and Nuclear Waste Glasses. *Journal of Non-Crystalline Solids* **84**:251-57.

Bergeron, C. G. 19 . General Aspects of the Crystallization of Glass:173-96.

Berkhout, F., A. Diakov, H. Feiveson, H. Hunt, E. Lyman, M. Miller, and F. von Hippel. 1992. Disposition of Separated Plutonium. Science & Global Security **3**: 1-53.

Coles, D. G., S. A. Simonson, L. E. Thomas, J. A. Schramke, and S. G. McKinley. 1984. Investigation of the Hydrothermal Interaction of ^{99}Tc-Doped Glass with Basalt Repository Nuclear Waste Package Components. Scientific Basis for Nuclear Waste Management VII **26**:323-332.

De Villiers, N., and D. Glasser. 1981. A continuation Method for Nonlinear Regression. *SIAM J. of Numer. Anal.* **18**:1139-54.

Doremus, R. H. 1973. Glass Science. John Wiley & Sons, Inc., New York.

Ebert and Bates. 1990. The Reaction of Synthetic Nuclear Waste Glass in Steam and Hydrothermal Solution. Scientific Basis for Nuclear Waste Management XIII **176**:339-346.

Jones, G. O. 1971. Glass. London: Chapman and Hall LTD., London, England.

Jantzen, C. M. 1986. Systems Approach to Nuclear Waste Glass Development. DP-MS-85-72.

Mark, J. C. 1993. Explosive Properties of Reactor-Grade Plutonium. Science & Global Security **4**:111-128.

Marquardt, D. W. 1963. An Algorithm for Least-squares Estimation of Nonlinear Parameters. *J. Soc. Indust. Appl. Math.* **11**:431-41.

Morey, G. W. 1954. The Properties of Glass. Reinhold Publishing, New York.

Osborn, M. R. Some Aspects of Non-linear Least Squares Calculations:171-89.

Uhlmann, D. R. 1971. A Kinetic Treatment of Glass Formation. *Journal of Non-Crystalline Solids* **7**:337-48.

Uhlmann, D. R., and N. J. Kreidl, ed. 1986. Glass: Science and Technology Volume 3 Viscosity and Relaxation. Academic Press, Inc., Orlando, Fl.

Weyl, W. A., and E. C. Marboe. 1964. The Constitution of Glasses. John Wiley & Sons, Inc., New York.

Appendix A

VITRIFICATION TECHNOLOGY

A.1 Chapter Summary

Many types of glass production exist and a long history of commercial glass production has contributed greatly to the cost effectiveness of vitrification. The only existing technology which turns high level liquid waste into a solid form is vitrification. Glass is poured into steel vessels and can be monitored in above ground storage or buried underground. Three large vitrification plants have been vitrifying liquid wastes with the first being the AVM starting in the late 1970's at Marcoule, France. The other two are PAMELA in Mol, Belgium, and WIP in Tarapur, India. The first conversion of liquid wastes took place in 1963 in Idaho with liquid wastes being calcined [2].

A.2 Vitrification Basics in Production

There are four processes for vitrification of glass: the discontinuous/one stage process; the discontinuous two stage process; the continuous/ one stage process; and the continuous/two stage process. There are also three phases for each of the above process: evaporation of the mixed waste at 100°C; calcination, i.e. denitration of the waste into oxide form which takes place between 500 and 900°C; and vitrification, i.e. melting the glass formers and waste together at temperatures above 1100°C [2]. In the discontinuous/one stage process, all three phases are done inside a "pot". The waste and frit are both placed into the pot at the same time. Once the melt has formed, the pot is cooled and serves as the storage container or the pot may have a draining device to pour glass into another storage container. The heat is increased slowly and the chemical feeding process and heating may be altered without changing the type of process. An example of this type of process would be the WIP in Tarapur, India. [2].

The discontinuous/two stage process calcines the glass separately from the vitrification process. The evaporation may take place in a drum dryer or microwave furnace. The calcination process can be added to the drying process by using a fluidized bed, rotary furnace, or spray calciner. The vitrification of the mix can take place in a resistance furnace, induction furnace with/without susceptors, microwave furnace, or a direct induction heating furnace [2].

When the frit and waste are continuously fed into a ceramic melter which incorporates all three phases and can pour the glass discontinuously, then that is known as a continuous/one stage process. Individual systems are defined by several qualities: the

position of the electrodes and material (i.e. SnO_2, Inconel 690, Mo, Mo +ZrO_2); the refractory material; the size of the melting chamber and number of melt refining chambers; the type of primary materials, either solid or liquid; current density at electrode level; type of drain such as overflow or bottom; and the starting system in which surface heaters or immersed heaters exist. Several countries use this process such as: WVDP in West Valley (DOE), USA; PAMELA in Mol, Belgium; DWPF at SRP, USA; and PNC in Japan [2].

When chemicals are evaporated and calcined before entering the vitrification furnace, the process is known as a continuous/two stage process. The pouring of the glass may be discontinuous. Three types of calciners may be used: a fluidized bed calciner; a spray calciner; and a rotating furnace. The vitrification furnace can be the following: a ceramic furnace with electrodes; a metallic induction furnace; a ceramic furnace with direct induction heating; and a resistance furnace. An example of this process exists in Marcoule, France with the AVM [2].

Three of these processes have been developed to the industrial level with the discontinuous/two stage process not being one of those. The continuous/one stage and two stage process is heavily used today.

A.3 Industrial Size Vitrification Plants

Atelier de Vitrification de Marcoule (AVM), is a continuous/two stage process. A schematic of this vitrification facility is shown in Fig. 2-14. Radioactive waste acidified in nitric acid and in liquid phase pours into a rotary calciner. The nitrates decompose at temperatures between 600 to 900°C. The pot is made of Inconel 600 with an average lifetime from 2000 to 3000 hours. The glass is melted using induction heating at 1100°C, which has extended the lifetime to 6000 hours because local overheating has been reduced by bringing the furnace up to temperature slowly with the mix inside the furnace. The furnace melts 15 kg of glass per hour so that every eight hours, 120 kg of glass can be poured into a steel canister. Each canister can hold 360 kg of glass. Thus one day is required to fill up one container. Approximately 205 containers in 205 days can be filled before the Inconel 600 is no longer capable of handling molten glass [2].

The first industrial scale plant used in the USA was the Defense Waste Processing Facility (DWPF), which is a continuous/one stage process. It vitrifies waste from the Savannah River Plant. Fig. 2-15 shows the flowsheet for this project. The waste is in the form of a low-level salt stream which is pre-separated with tetraphenyl-borate/sodium titanate treatment. The furnace is a joule-heated ceramic-lined furnace with four Inconel electrodes and a glass forming temperature of 1150°C. It produces 100 kg/h and is poured into a large canister which holds 1700 kg of glass via an overflow system[2]. With a larger

canister, the center of the canister will take longer to cool thus the possibility of devitrification problems exist. Fig. 2-16 shows streaks in a cross-sectioned canister (Matzke et al. 1984) [2].

The second high-level waste vitrification plant in the USA was the West Valley Demonstration Project (WVDP). West Valley was a commercial reprocessing plant that was shut down and now contains tanks which hold high-level wastes. Fig. 2-17 shows the continuous/one stage process (Leclaire et al. 1985) [2]. The unique part of this plant is the design of the melter. The ceramic melter is a triangular shape which reduces the melter volume, waste hold-up, and uses three electrodes rather than the four encountered at DWPF. Also a zeolite based prep stage is used instead of the tetraphenyl-borate step with DWPF. There is also a Thorex waste stream which can be vitrified [2].

WIP in Tarapur, India, is a modified version of the pot process. The melting pot is not the final container but is used to pour molten glass into canisters at a rate of 4 kg/h. The pot is made of Inconel 690, and is held at 600°C for drying and calcining, then raised to 1100 to 1200°C to form the glass. This last temperature is held for five hours and the glass is poured into the canister which is cooled slowly and annealed. Fig. 2-18 shows the WIP flowsheet (Grover 1977) [2].

The Windscale Vitrification Plant (WVP) is a takeoff of the AVM plant where two vitrification lines are put in parallel shown in Fig. 2-19 (Smith 1985) [2]. A Japanese plant operates off a Joule-heated ceramic melter which produces 9 kg/hr of borosilicate glass. It will produce 140 canisters of glass per year with each canister holding 300 kg of glass. The glass itself will contain 25% waste loading which includes 10% fission products [2].

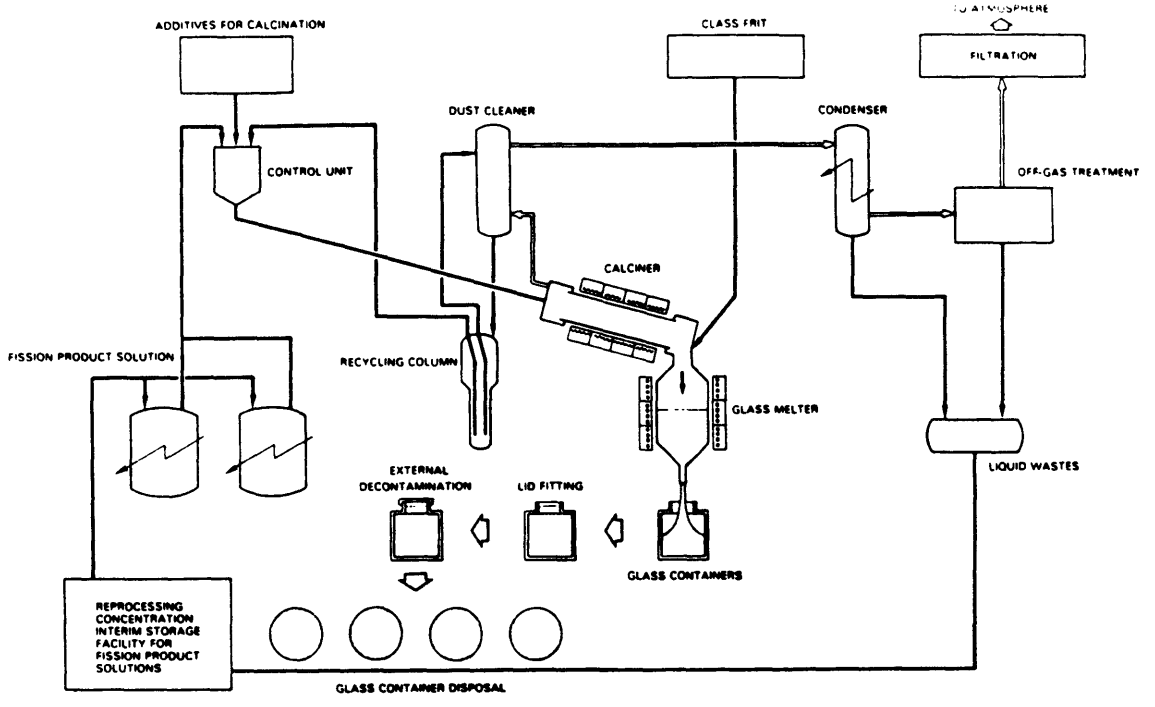

Fig. A-1. AVM continuous/two stage process (Bastien Thiry et al. 1984) [2].

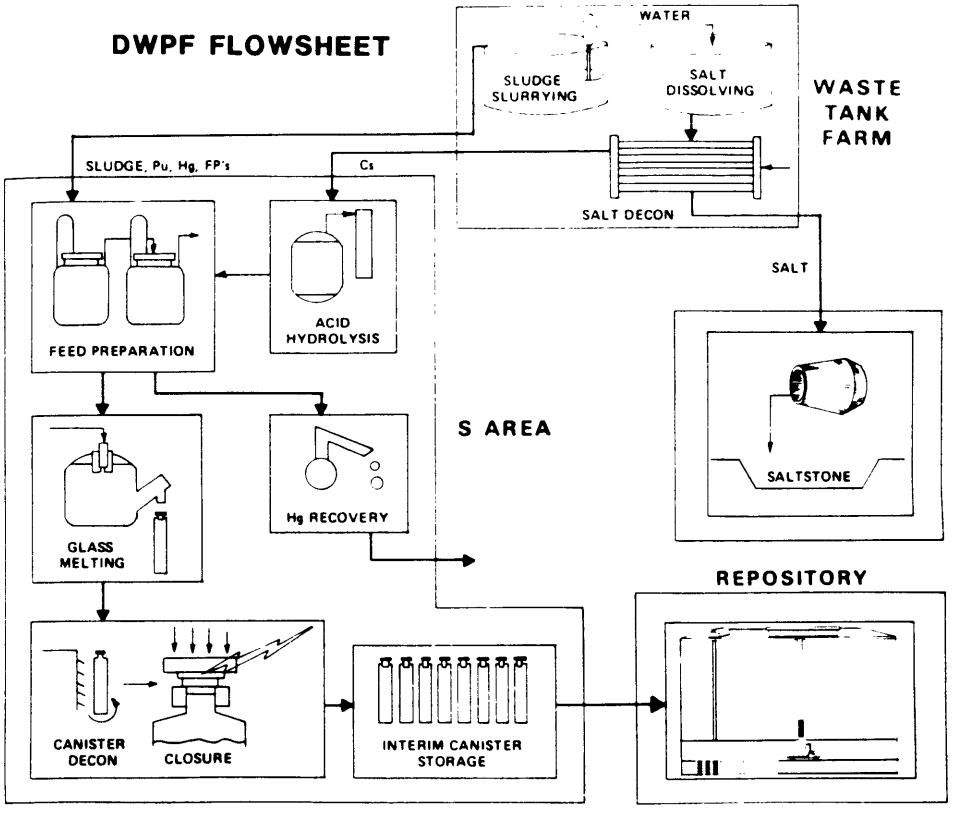

Fig. A-2. Savannah River Defense Waste Processing Facility [2].

Fig. A-3. Full-size canister cross-section of glass product SM58LW11 with streaks [2].

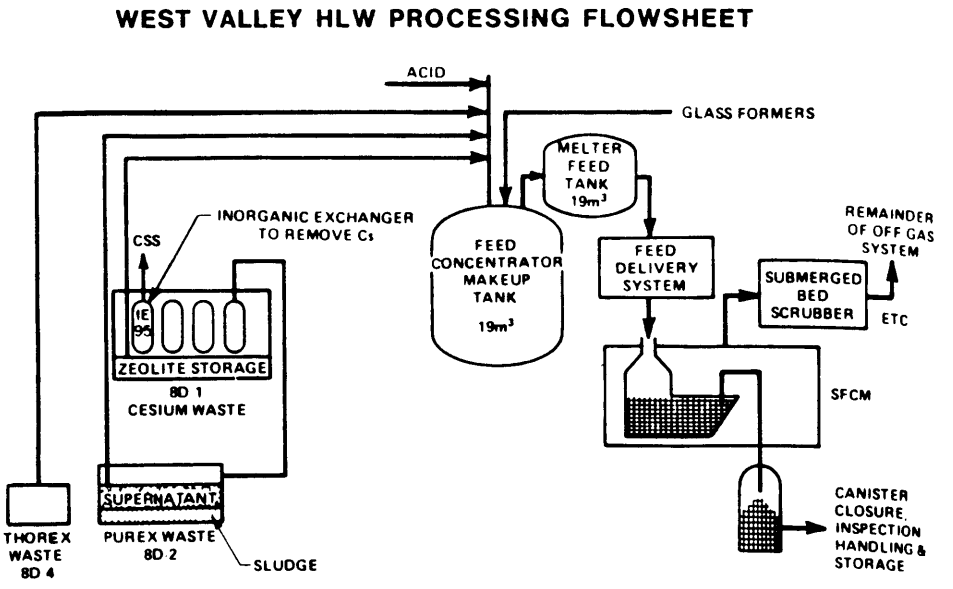

Fig. A-4. West Valley HLW vitrification plant schematic [2].

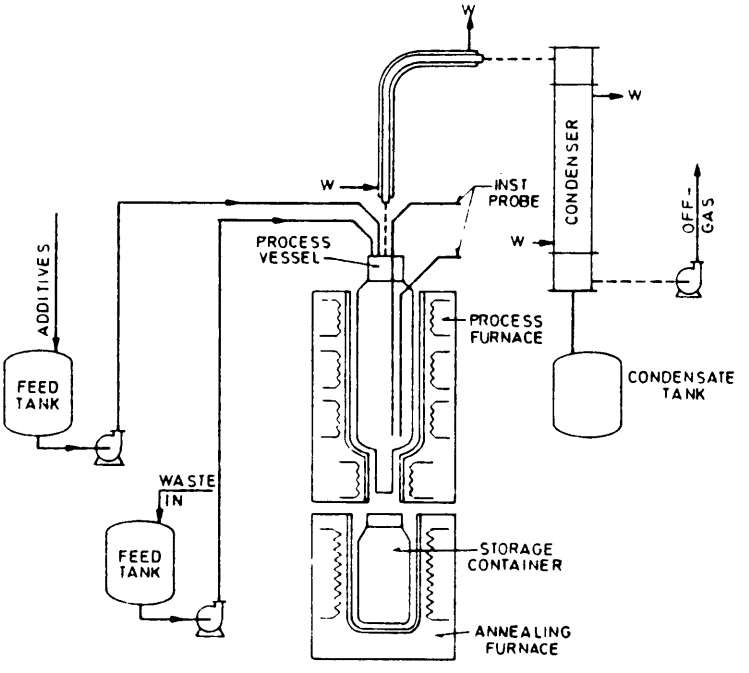

Fig. A-5. WIP pot process flowsheet [2].

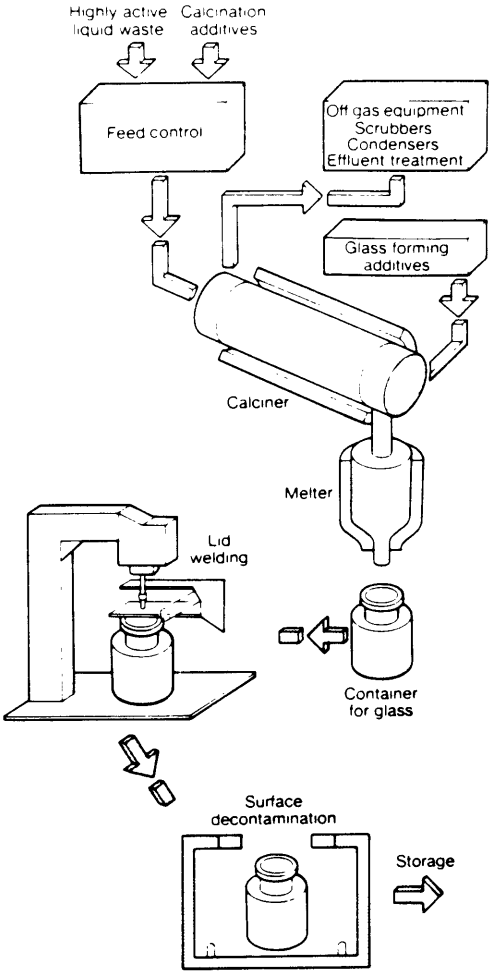

Fig. A-6. WVP continuous vitrification process [2].

APPENDIX B

MULTIVARIATE ANALYSIS RESULTS

$n := 9 \qquad i := 0, 1 .. 8$

$$y := \begin{bmatrix} 1.07 \cdot 10^{-4} \\ 3.26 \cdot 10^{-5} \\ .234 \cdot 10^{-4} \\ .912 \cdot 10^{-4} \\ .0197 \cdot 10^{-4} \\ .12 \cdot 10^{-4} \\ .38 \cdot 10^{-4} \\ .164 \cdot 10^{-4} \\ .0253 \cdot 10^{-4} \end{bmatrix} \quad T := \begin{bmatrix} 1250 \\ 1300 \\ 1300 \\ 1250 \\ 1350 \\ 1350 \\ 1250 \\ 1350 \\ 1350 \end{bmatrix} \quad W := \begin{bmatrix} 1 \cdot 10^{-8} \\ 1 \cdot 10^{-8} \\ 1 \cdot 10^{-8} \\ 1 \cdot 10^{-8} \\ 1 \cdot 10^{-8} \\ 1 \cdot 10^{-8} \\ .0759 \\ 1 \cdot 10^{-8} \\ 1 \cdot 10^{-8} \end{bmatrix} \quad S := \begin{bmatrix} .285 \\ .5262 \\ .5155 \\ .4417 \\ .475 \\ .453 \\ .4119 \\ .6201 \\ .438 \end{bmatrix}$$

T=temp
y=leach rate at 28 days for sodium
W=B wt%
S=Si wt%
C=Ca wt%
N=Mg wt%
F=Fe wt%
SN=Na wt%

$$SN := \begin{bmatrix} .1707 \\ .2582 \\ .2571 \\ .2336 \\ .1197 \\ .2235 \\ .1118 \\ .2164 \\ .1164 \end{bmatrix} \quad F := \begin{bmatrix} .0828 \\ .0228 \\ .0213 \\ .0436 \\ .0534 \\ .0562 \\ .0718 \\ .0229 \\ .0785 \end{bmatrix} \quad N := \begin{bmatrix} .1071 \\ .0321 \\ .0282 \\ .0611 \\ .0744 \\ .0629 \\ .0901 \\ .0358 \\ .0936 \end{bmatrix} \quad C := \begin{bmatrix} .212 \\ .0561 \\ .0493 \\ .1084 \\ .1374 \\ .1078 \\ .1467 \\ .0621 \\ .1620 \end{bmatrix}$$

$$T := \frac{T}{mean(T)} \qquad F := \frac{F}{mean(F)} \qquad W := \frac{W}{mean(W)}$$

$$y := \frac{y}{mean(y)} \qquad SN := \frac{SN}{mean(SN)} \qquad N := \frac{N}{mean(N)}$$

$$S := \frac{S}{mean(S)} \qquad C := \frac{C}{mean(C)}$$

$$M := \begin{bmatrix} n & \sum T & \sum W & \sum SN & \sum C & \sum S & \sum N & \sum F \\ \sum T & \sum_i T_i \cdot T_i & \sum_i T_i \cdot W_i & \sum_i T_i \cdot SN_i & \sum_i T_i \cdot C_i & \sum_i T_i \cdot S_i & \sum_i T_i \cdot N_i & \sum_i T_i \cdot F_i \\ \sum W & \sum_i W_i \cdot T_i & \sum_i W_i \cdot W_i & \sum_i W_i \cdot SN_i & \sum_i W_i \cdot C_i & \sum_i W_i \cdot S_i & \sum_i W_i \cdot N_i & \sum_i W_i \cdot F_i \\ \sum SN & \sum_i SN_i \cdot T_i & \sum_i SN_i \cdot W_i & \sum_i SN_i \cdot SN_i & \sum_i SN_i \cdot C_i & \sum_i SN_i \cdot S_i & \sum_i SN_i \cdot N_i & \sum_i SN_i \cdot F_i \\ \sum C & \sum_i C_i \cdot T_i & \sum_i C_i \cdot W_i & \sum_i C_i \cdot SN_i & \sum_i C_i \cdot C_i & \sum_i C_i \cdot S_i & \sum_i C_i \cdot N_i & \sum_i C_i \cdot F_i \\ \sum S & \sum_i S_i \cdot T_i & \sum_i S_i \cdot W_i & \sum_i S_i \cdot SN_i & \sum_i S_i \cdot C_i & \sum_i S_i \cdot S_i & \sum_i S_i \cdot N_i & \sum_i S_i \cdot F_i \\ \sum N & \sum_i N_i \cdot T_i & \sum_i N_i \cdot W_i & \sum_i N_i \cdot SN_i & \sum_i N_i \cdot C_i & \sum_i N_i \cdot S_i & \sum_i N_i \cdot N_i & \sum_i N_i \cdot F_i \\ \sum F & \sum_i F_i \cdot T_i & \sum_i F_i \cdot W_i & \sum_i F_i \cdot SN_i & \sum_i F_i \cdot C_i & \sum_i F_i \cdot S_i & \sum_i F_i \cdot N_i & \sum_i F_i \cdot F_i \end{bmatrix}$$

$$h := \begin{bmatrix} \sum y \\ \sum_i y_i \cdot T_i \\ \sum_i y_i \cdot W_i \\ \sum_i y_i \cdot SN_i \\ \sum_i y_i \cdot C_i \\ \sum_i y_i \cdot S_i \\ \sum_i y_i \cdot N_i \\ \sum_i y_i \cdot F_i \end{bmatrix} \qquad b := M^{-1} \cdot h \qquad b = \begin{bmatrix} 9.056 \\ -17.437 \\ -0.021 \\ 3.469 \\ 0.64 \\ 2.346 \\ 6.54 \\ -3.593 \end{bmatrix}$$

Temperature
Boron Wt%
Sodium Wt%
Calcium Wt%
Silicon Wt%
Magnesium Wt%
Iron Wt%

$$z_i := b_0 + b_1 \cdot T_i + b_2 \cdot W_i + b_3 \cdot SN_i + b_4 \cdot C_i + b_5 \cdot S_i + b_6 \cdot N_i + b_7 \cdot F_i$$

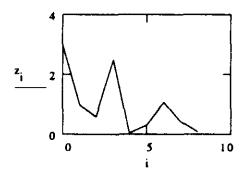

Fig. B-1. Multivariate analysis of 28 day, room temperature, non-radioactive and Th-doped glass, sodium leach test results.

$n := 9 \qquad i := 0, 1 .. 3$

$$y := \begin{bmatrix} 8\cdot10^{-5} \\ 5.37\cdot10^{-5} \\ 3.56\cdot10^{-5} \\ 3.97\cdot10^{-5} \end{bmatrix} \quad T := \begin{bmatrix} 1350 \\ 1250 \\ 1350 \\ 1350 \end{bmatrix} \quad W := \begin{bmatrix} 1\cdot10^{-8} \\ .0759 \\ 1\cdot10^{-8} \\ 1\cdot10^{-8} \end{bmatrix} \quad S := \begin{bmatrix} .453 \\ .4119 \\ .6201 \\ .4378 \end{bmatrix}$$

T=temp
y=leach rate at 28 days for sodium
W=B wt%
S=Si wt%
C=Ca wt%
N=Mg wt%
F=Fe wt%
SN=Na wt%

$$SN := \begin{bmatrix} .2253 \\ .1118 \\ .2164 \\ .1164 \end{bmatrix} \quad F := \begin{bmatrix} .0562 \\ .0718 \\ .0229 \\ .0785 \end{bmatrix} \quad N := \begin{bmatrix} .0629 \\ .0901 \\ .0358 \\ .0936 \end{bmatrix} \quad C := \begin{bmatrix} .1078 \\ .1467 \\ .0621 \\ .1620 \end{bmatrix}$$

$$T := \frac{T}{mean(T)} \qquad F := \frac{F}{mean(F)} \qquad W := \frac{W}{mean(W)}$$

$$y := \frac{y}{mean(y)} \qquad SN := \frac{SN}{mean(SN)} \qquad N := \frac{N}{mean(N)}$$

$$S := \frac{S}{mean(S)} \qquad C := \frac{C}{mean(C)}$$

$$M := \begin{bmatrix} n & \sum T & \sum W & \sum SN & \sum C & \sum S & \sum N & \sum F \\ \sum T & \sum_i T_i \cdot T_i & \sum_i T_i \cdot W_i & \sum_i T_i \cdot SN_i & \sum_i T_i \cdot C_i & \sum_i T_i \cdot S_i & \sum_i T_i \cdot N_i & \sum_i T_i \cdot F_i \\ \sum W & \sum_i W_i \cdot T_i & \sum_i W_i \cdot W_i & \sum_i W_i \cdot SN_i & \sum_i W_i \cdot C_i & \sum_i W_i \cdot S_i & \sum_i W_i \cdot N_i & \sum_i W_i \cdot F_i \\ \sum SN & \sum_i SN_i \cdot T_i & \sum_i SN_i \cdot W_i & \sum_i SN_i \cdot SN_i & \sum_i SN_i \cdot C_i & \sum_i SN_i \cdot S_i & \sum_i SN_i \cdot N_i & \sum_i SN_i \cdot F_i \\ \sum C & \sum_i C_i \cdot T_i & \sum_i C_i \cdot W_i & \sum_i C_i \cdot SN_i & \sum_i C_i \cdot C_i & \sum_i C_i \cdot S_i & \sum_i C_i \cdot N_i & \sum_i C_i \cdot F_i \\ \sum S & \sum_i S_i \cdot T_i & \sum_i S_i \cdot W_i & \sum_i S_i \cdot SN_i & \sum_i S_i \cdot C_i & \sum_i S_i \cdot S_i & \sum_i S_i \cdot N_i & \sum_i S_i \cdot F_i \\ \sum N & \sum_i N_i \cdot T_i & \sum_i N_i \cdot W_i & \sum_i N_i \cdot SN_i & \sum_i N_i \cdot C_i & \sum_i N_i \cdot S_i & \sum_i N_i \cdot N_i & \sum_i N_i \cdot F_i \\ \sum F & \sum_i F_i \cdot T_i & \sum_i F_i \cdot W_i & \sum_i F_i \cdot SN_i & \sum_i F_i \cdot C_i & \sum_i F_i \cdot S_i & \sum_i F_i \cdot N_i & \sum_i F_i \cdot F_i \end{bmatrix}$$

$$h := \begin{bmatrix} \sum y \\ \sum_i y_i \cdot T_i \\ \sum_i y_i \cdot W_i \\ \sum_i y_i \cdot SN_i \\ \sum_i y_i \cdot C_i \\ \sum_i y_i \cdot S_i \\ \sum_i y_i \cdot N_i \\ \sum_i y_i \cdot F_i \end{bmatrix} \qquad b := M^{-1} \cdot h \qquad b = \begin{bmatrix} 2.586 \\ -9 \\ -0.016 \\ 3.25 \\ 1.25 \\ -0.75 \\ 7 \\ -3 \end{bmatrix}$$

Temperature
Boron Wt%
Sodium Wt%
Calcium Wt%
Silicon Wt%
Magnesium Wt%
Iron Wt%

$$z_i := b_0 + b_1 \cdot T_i + b_2 \cdot W_i + b_3 \cdot SN_i + b_4 \cdot C_i + b_5 \cdot S_i + b_6 \cdot N_i + b_7 \cdot F_i$$

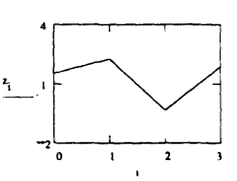

Fig. B-2. Multivariate analysis of 90 day, Th-doped glass, room temperature, sodium leach test results.

$n := 9 \qquad i := 0, 1 .. 3$

$$y := \begin{bmatrix} \begin{bmatrix} 3.19 \cdot 10^{-4} \\ 7.99 \cdot 10^{-4} \\ 1.19 \cdot 10^{-4} \\ 2.11 \cdot 10^{-4} \end{bmatrix} \end{bmatrix} \quad T := \begin{bmatrix} 1350 \\ 1250 \\ 1350 \\ 1350 \end{bmatrix} \quad W := \begin{bmatrix} 1 \cdot 10^{-8} \\ .0759 \\ 1 \cdot 10^{-8} \\ 1 \cdot 10^{-8} \end{bmatrix} \quad S := \begin{bmatrix} .453 \\ .4119 \\ .6201 \\ .4378 \end{bmatrix}$$

T=temp
y=leach rate at 28 days for sodium
W=B wt%
S=Si wt%
C=Ca wt%
N=Mg wt%
F=Fe wt%
SN=Na wt%

$$SN := \begin{bmatrix} .2253 \\ .1118 \\ .2164 \\ .1164 \end{bmatrix} \quad F := \begin{bmatrix} .0562 \\ .0718 \\ .0229 \\ .0785 \end{bmatrix} \quad N := \begin{bmatrix} .0629 \\ .0901 \\ .0358 \\ .0936 \end{bmatrix} \quad C := \begin{bmatrix} .1078 \\ .1467 \\ .0621 \\ .1620 \end{bmatrix}$$

$$T := \frac{T}{mean(T)} \quad F := \frac{F}{mean(F)} \quad W := \frac{W}{mean(W)}$$

$$y := \frac{y}{mean(y)} \quad SN := \frac{SN}{mean(SN)} \quad N := \frac{N}{mean(N)}$$

$$S := \frac{S}{mean(S)} \quad C := \frac{C}{mean(C)}$$

$$M := \begin{bmatrix} n & \sum T & \sum W & \sum SN & \sum C & \sum S & \sum N & \sum F \\ \sum T & \sum_i T_i \cdot T_i & \sum_i T_i \cdot W_i & \sum_i T_i \cdot SN_i & \sum_i T_i \cdot C_i & \sum_i T_i \cdot S_i & \sum_i T_i \cdot N_i & \sum_i T_i \cdot F_i \\ \sum W & \sum_i W_i \cdot T_i & \sum_i W_i \cdot W_i & \sum_i W_i \cdot SN_i & \sum_i W_i \cdot C_i & \sum_i W_i \cdot S_i & \sum_i W_i \cdot N_i & \sum_i W_i \cdot F_i \\ \sum SN & \sum_i SN_i \cdot T_i & \sum_i SN_i \cdot W_i & \sum_i SN_i \cdot SN_i & \sum_i SN_i \cdot C_i & \sum_i SN_i \cdot S_i & \sum_i SN_i \cdot N_i & \sum_i SN_i \cdot F_i \\ \sum C & \sum_i C_i \cdot T_i & \sum_i C_i \cdot W_i & \sum_i C_i \cdot SN_i & \sum_i C_i \cdot C_i & \sum_i C_i \cdot S_i & \sum_i C_i \cdot N_i & \sum_i C_i \cdot F_i \\ \sum S & \sum_i S_i \cdot T_i & \sum_i S_i \cdot W_i & \sum_i S_i \cdot SN_i & \sum_i S_i \cdot C_i & \sum_i S_i \cdot S_i & \sum_i S_i \cdot N_i & \sum_i S_i \cdot F_i \\ \sum N & \sum_i N_i \cdot T_i & \sum_i N_i \cdot W_i & \sum_i N_i \cdot SN_i & \sum_i N_i \cdot C_i & \sum_i N_i \cdot S_i & \sum_i N_i \cdot N_i & \sum_i N_i \cdot F_i \\ \sum F & \sum_i F_i \cdot T_i & \sum_i F_i \cdot W_i & \sum_i F_i \cdot SN_i & \sum_i F_i \cdot C_i & \sum_i F_i \cdot S_i & \sum_i F_i \cdot N_i & \sum_i F_i \cdot F_i \end{bmatrix}$$

$$h := \begin{bmatrix} \sum y \\ \sum_i y_i \cdot T_i \\ \sum_i y_i \cdot W_i \\ \sum_i y_i \cdot SN_i \\ \sum_i y_i \cdot C_i \\ \sum_i y_i \cdot S_i \\ \sum_i y_i \cdot N_i \\ \sum_i y_i \cdot F_i \end{bmatrix} \quad b := M^{-1} \cdot h \quad b = \begin{bmatrix} 2.743 \\ -4 \\ 0.414 \\ 0.5 \\ 2.75 \\ -0.562 \\ 0.5 \\ -0.5 \end{bmatrix}$$

Temperature
Boron Wt%
Sodium Wt%
Calcium Wt%
Silicon Wt%
Magnesium Wt%
Iron Wt%

$$z_i := b_0 + b_1 \cdot T_i + b_2 \cdot W_i + b_3 \cdot SN_i + b_4 \cdot C_i + b_5 \cdot S_i + b_6 \cdot N_i + b_7 \cdot F_i$$

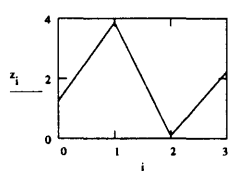

Fig. B-3. Multivariate analysis of 180 day, 90°C, Th-doped glass, sodium leach test results.

Appendix C

SUPPORTING GRAPHS FOR THE MCC-1 LEACH TEST RESULTS

C.1 Appendix Summary

The normalized leach results and elemental analysis graphs presented in chapter 4 showed the general trends of Rocky Flats glass degradation. The graphs of other elements and glass compositions in this appendix show similar trends with those presented in chapter four.

Fig. C-1. Room Temperature, DI Water MCC-1, Normalized Leach Results Magnesium

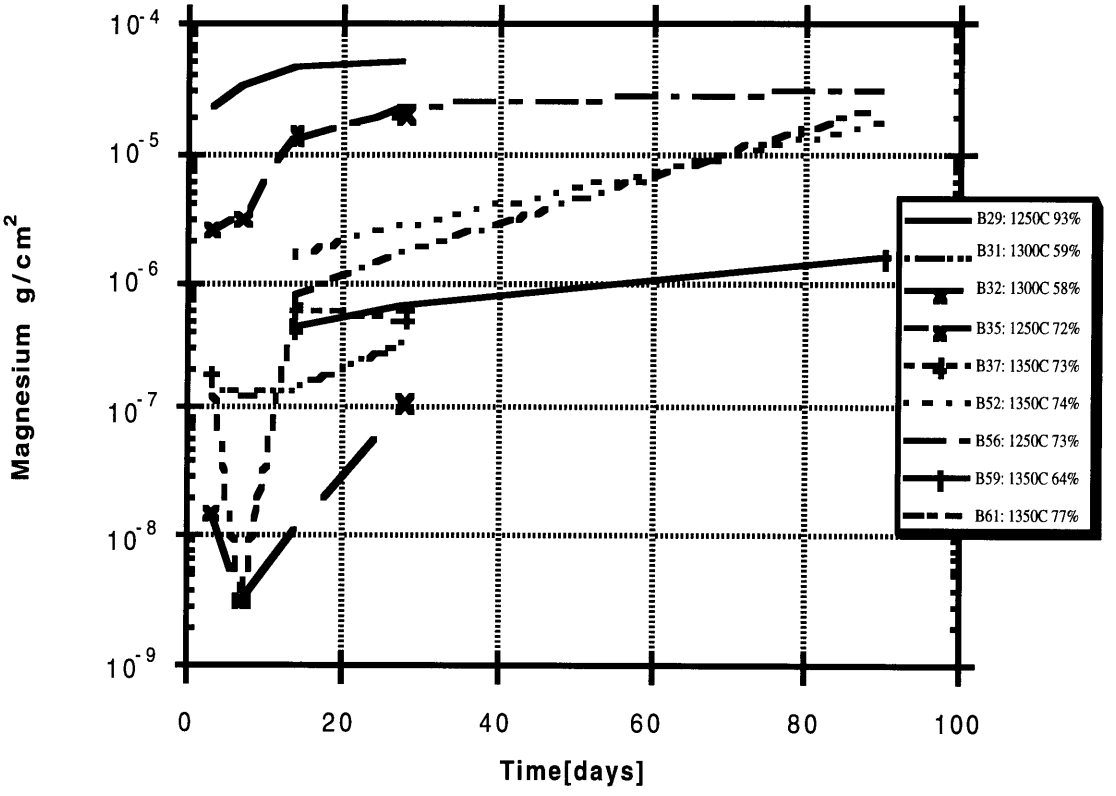

Fig. C-2. Room Temperature, DI Water
MCC-1, Normalized Leach Results
Potassium

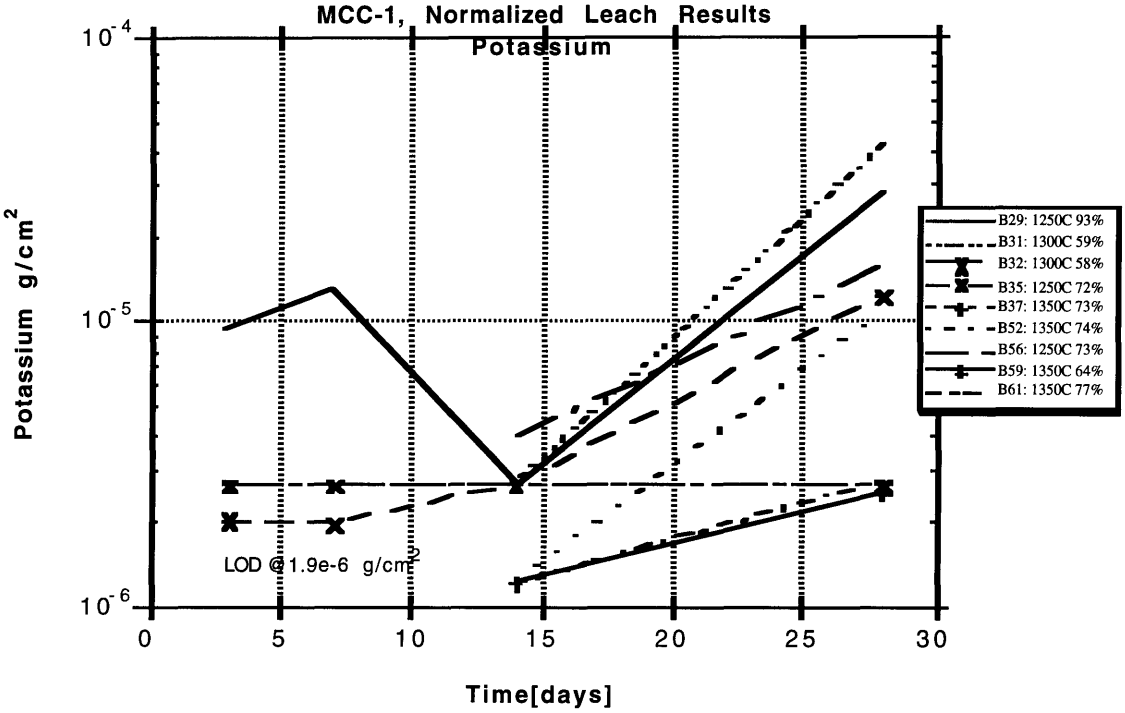

Fig. C-3. 90°C, DI Water
MCC-1, Normalized Leach Results
Potassium

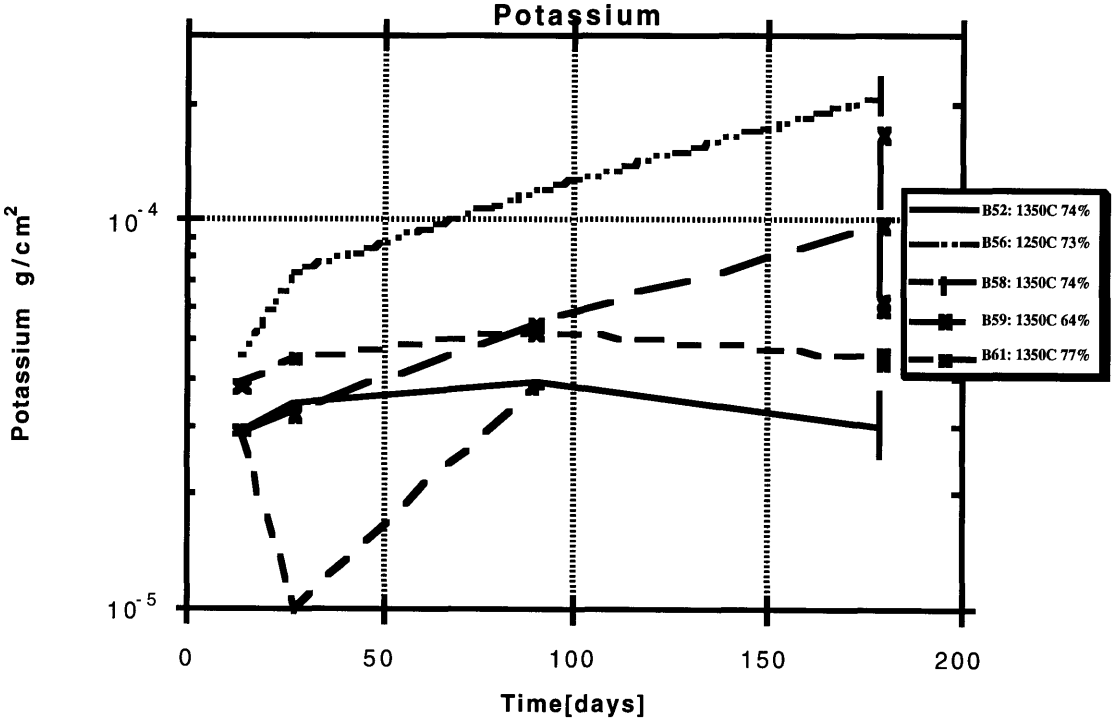

Fig. C-4. Room Temperature, DI Water
MCC-1, Elemental Analysis
Batch 31: 1300°C 59%

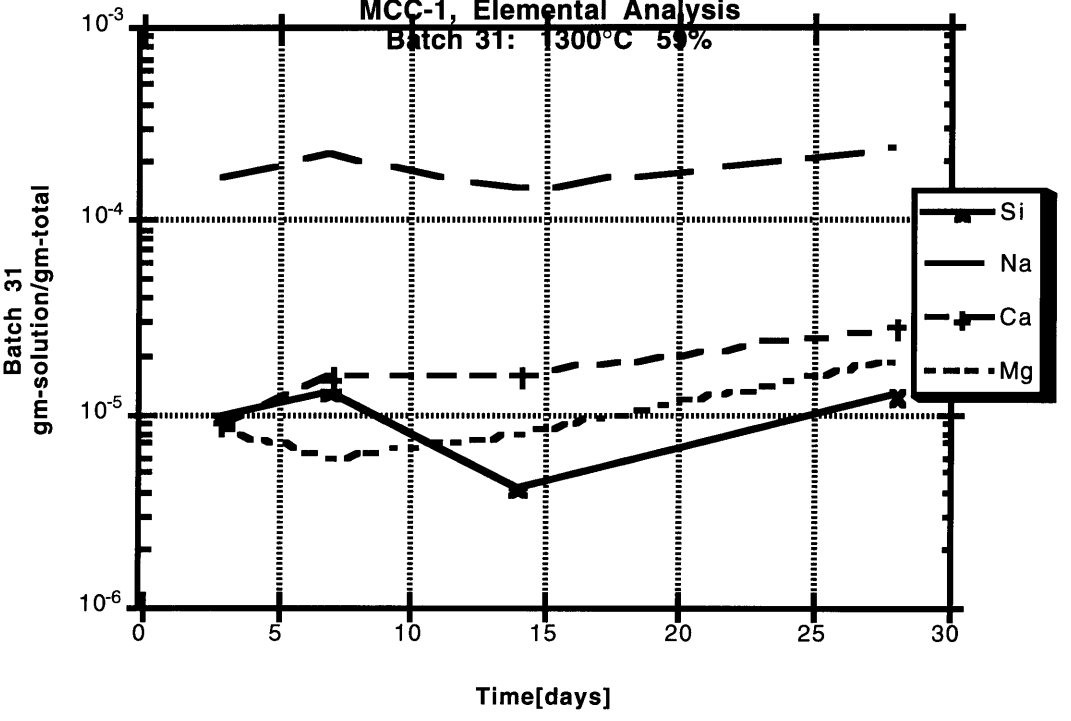

Fig. C-5. Room Temperature, DI Water
MCC-1, Elemental Analysis
Batch 32: 1300°C 58%

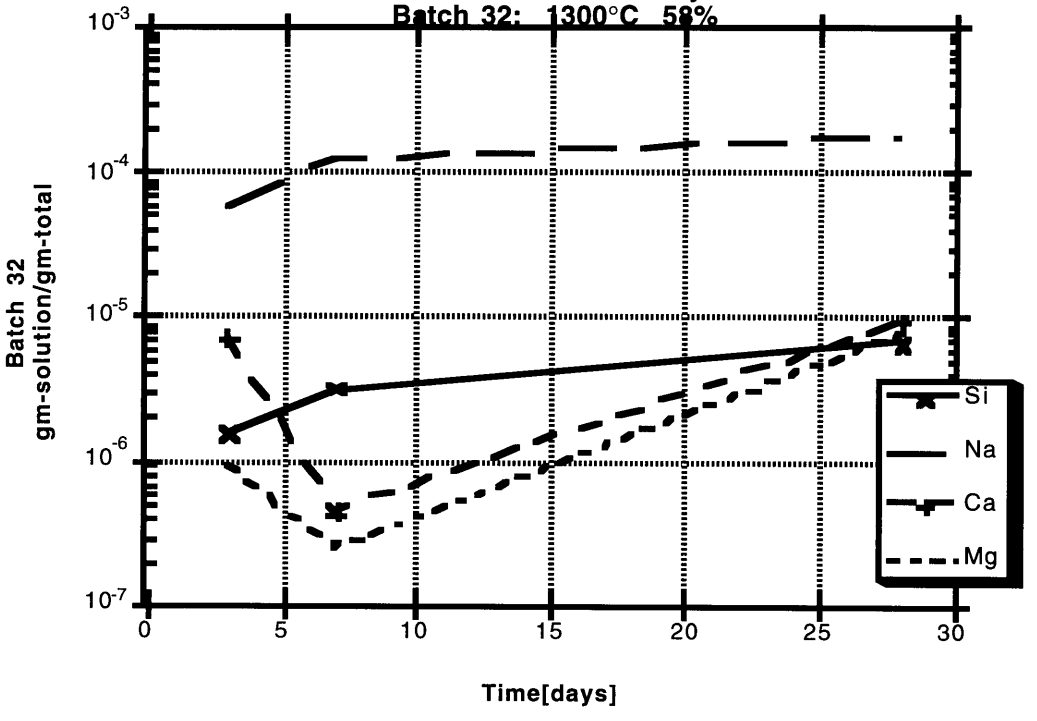

Fig. C-6. Room Temperature, DI Water
MCC-1, Elemental Analysis
Batch 35: 1250°C 72%

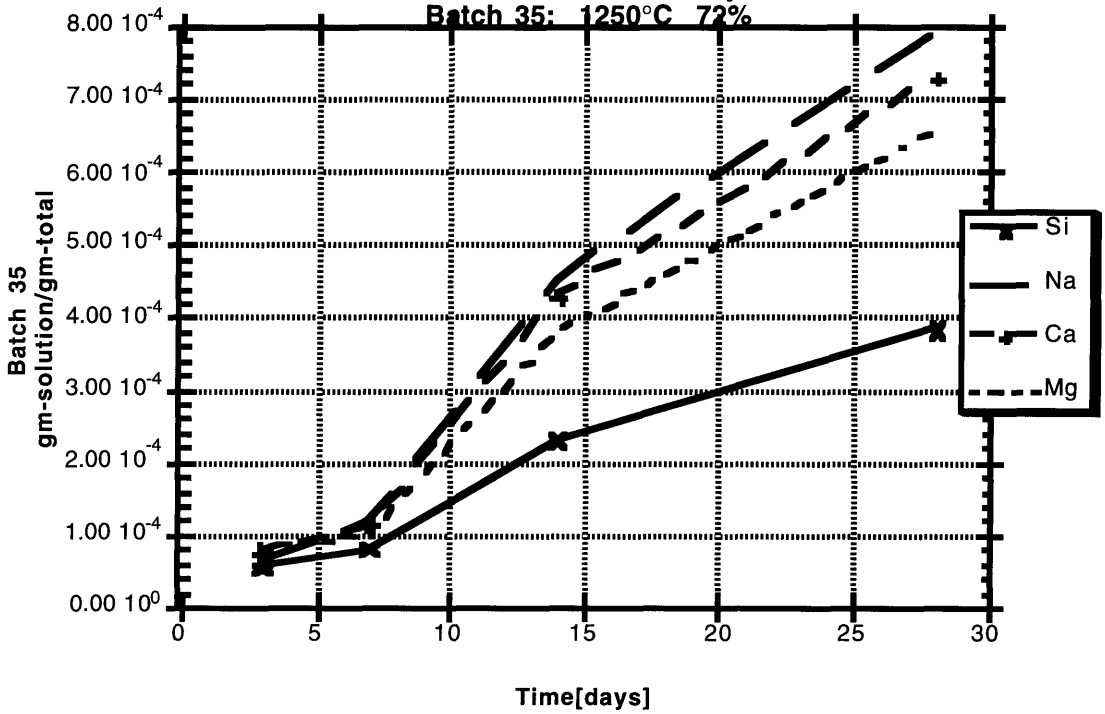

Fig. C-7. Room Temperature, DI Water
MCC-1, Elemental Analysis
Batch 37: 1350°C 73%

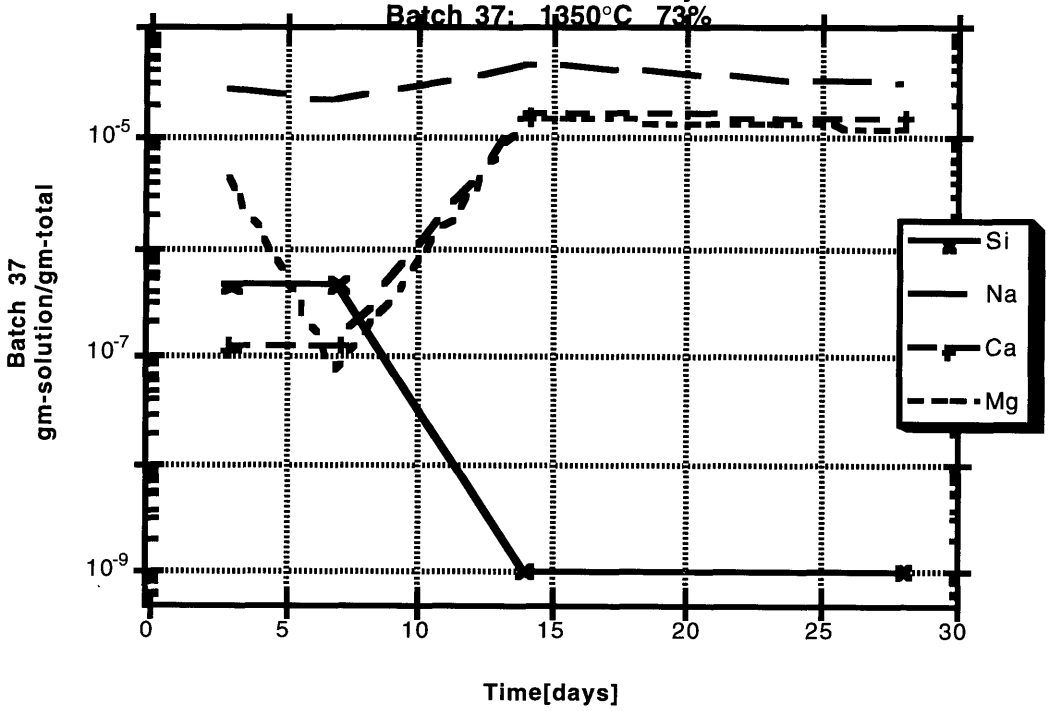

Fig. C-8. Room Temperature, DI Water
MCC-1, Elemental Analysis
Batch 52: 1350°C 74%

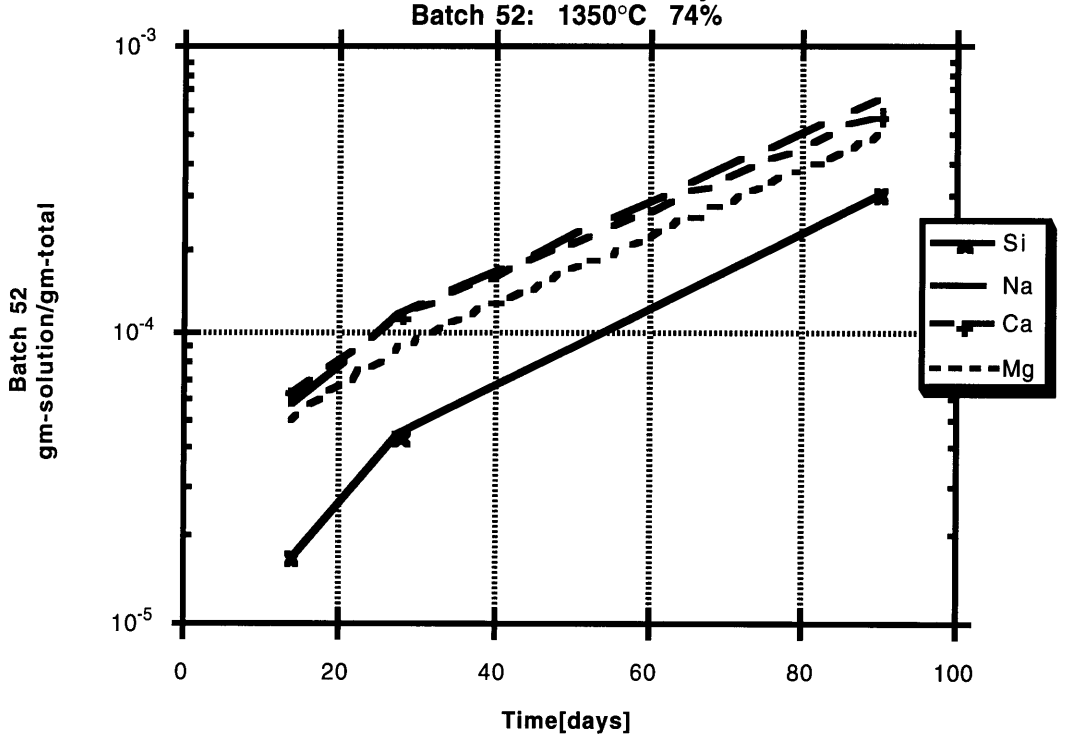

Fig. C-9. Room Temperature, DI Water
MCC-1, Elemental Analysis
Batch 56: 1250°C 73%

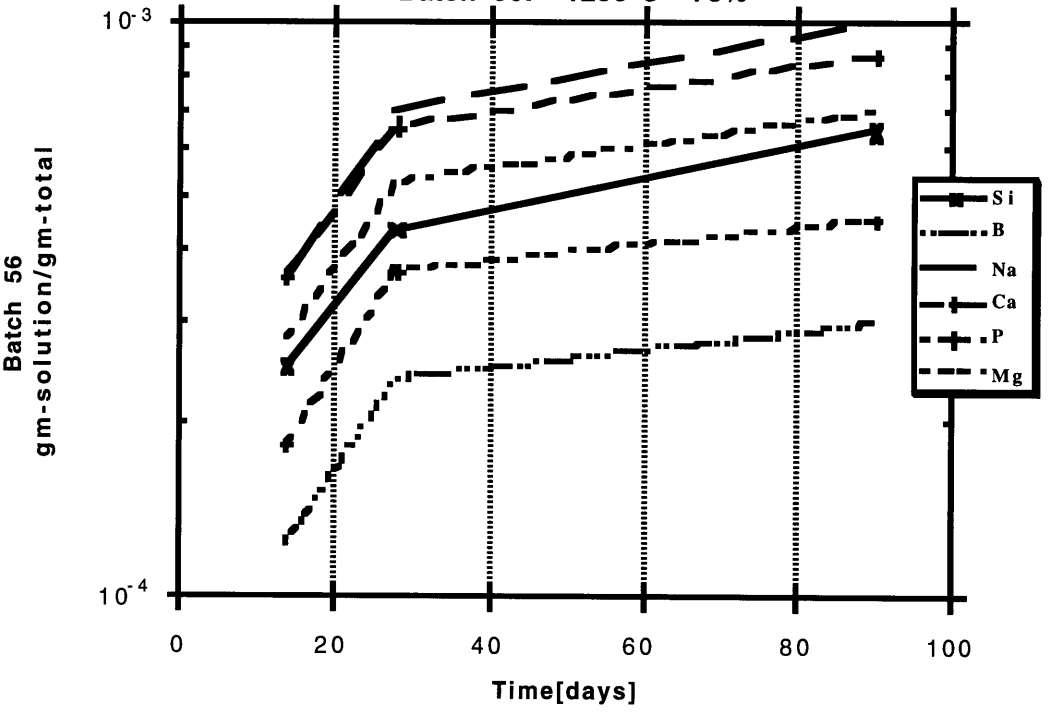

Fig. C-10. Room Temperature, DI Water
MCC-1, Elemental Analysis
Batch 59: 1350°C 64%

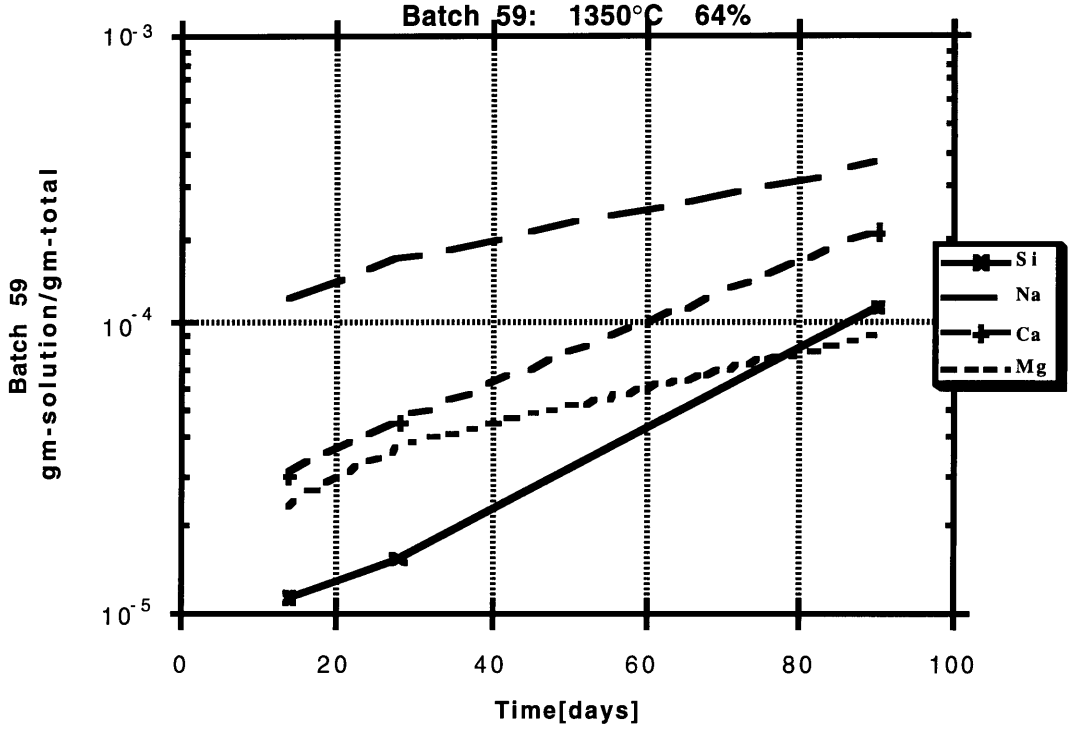

Fig. C-11. 90°C, DI Water
MCC-1, Elemental Analysis
Batch 58: 1350°C 74%

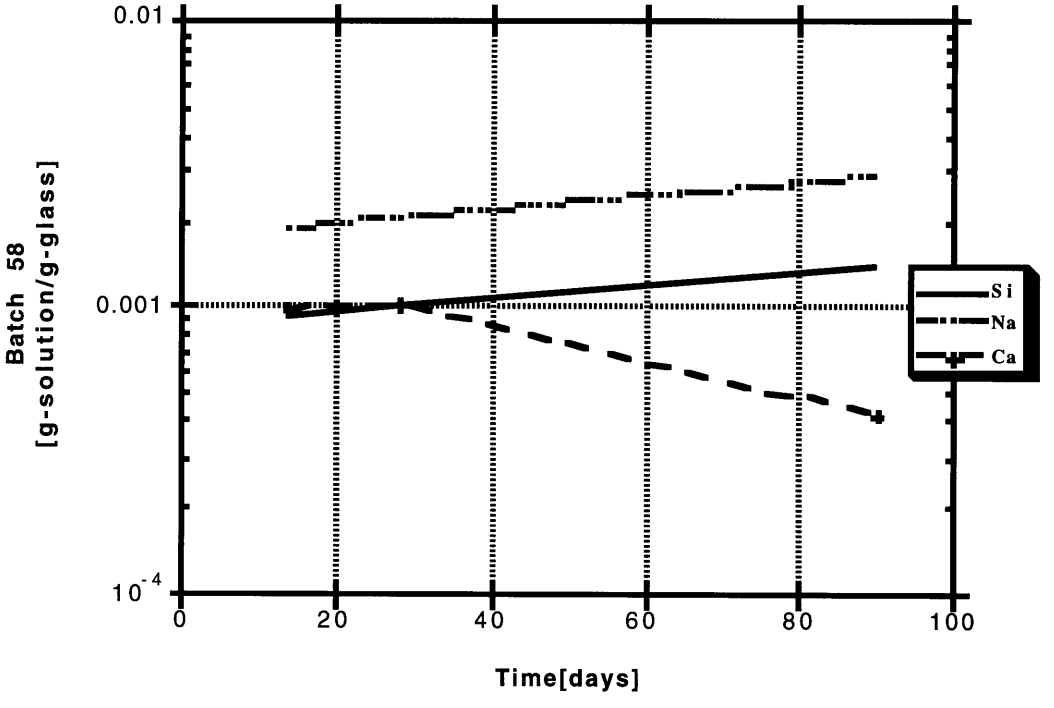

Fig. C-12. 90°C, DI Water
MCC-1, Elemental Analysis
Batch 59: 1350°C 64%

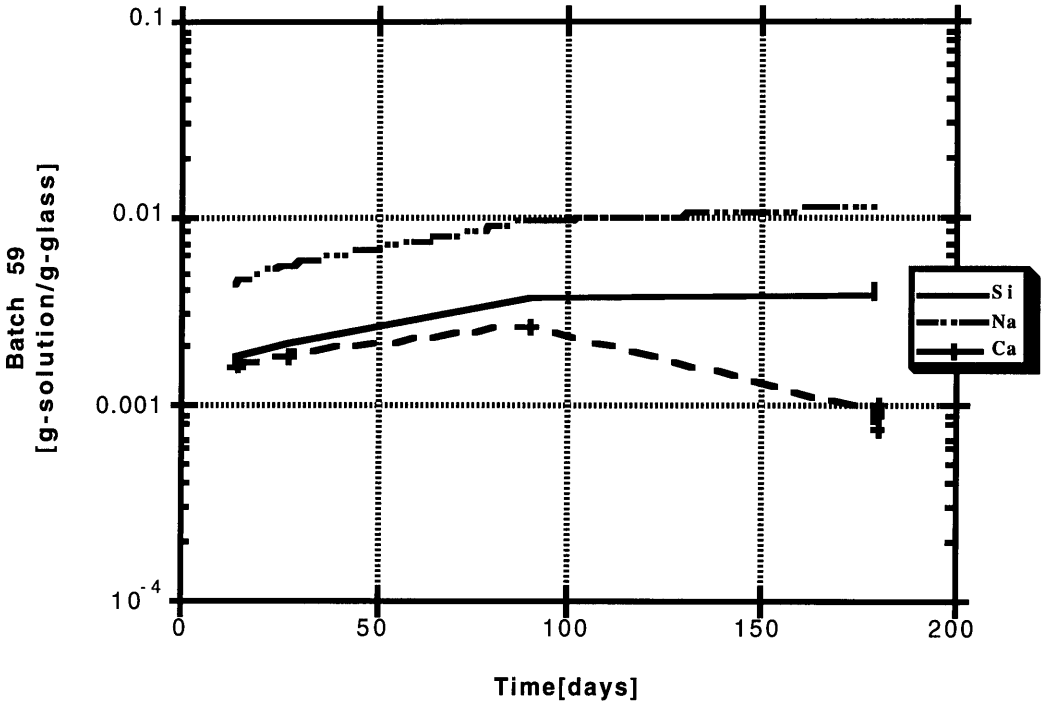

Fig. C-13. 90°C, DI Water
MCC-1, Elemental Analysis
Batch 61: 1350°C 77%

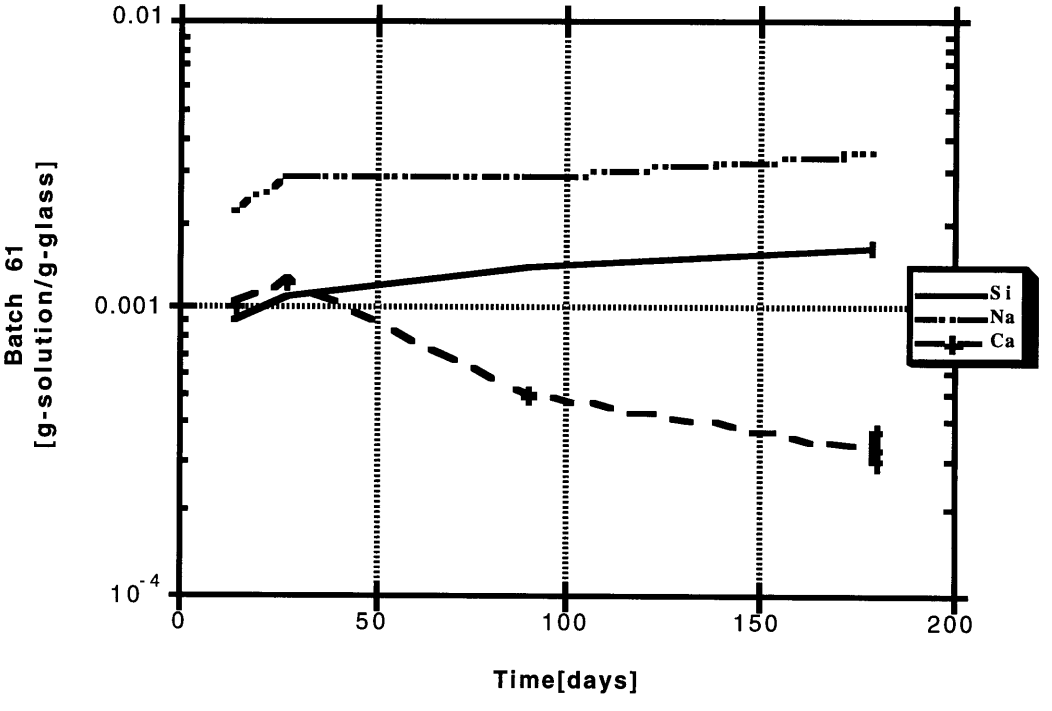

Appendix D

DATA COMPILATION

D.1 Appendix Summary

This appendix presents the worksheets from Excel which were used to convert raw data into meaningful results. Excel was used to convert ppm quantities from the fusion results into oxide wt%'s. It was also used to create the two types of leach graphs, normalized leach results and elemental analysis, from the leach test ppm quantities obtained from the ICP analysis.

Table D-1. Non-Radioactive Rocky Flats Glass Fusion Data Conversion

b29	ppm	X dilut.	oxide conv	wt%	Si/Na
Si	2.48	125488	268392	28.51%	1.67
Na	2.356	119214	160676	17.07%	Time
Al	10.62	10747	20300	2.16%	155
Ca	2.819	142641	199555	21.20%	Temp
Mg	1.202	60821	100866	10.71%	1250
Fe	1.077	54496	77930	8.28%	
K *	1.01	51106	61562	6.54%	
S *	0.033	1670	4175	0.44%	
P *	0.414	20948	47978	5.10%	
			941434	100.00%	
b32	ppm	X dilut.	oxide conv	wt%	Si/Na
Si	5.355	298274	637944	51.55%	2.01
Na	4.238	236057	318157	25.71%	Time
Al	0.977	54419	102786	8.31%	190
Ca	0.783	43613	61015	4.93%	Temp
Mg	0.378	21055	34917	2.82%	1300
Fe	0.331	18437	26364	2.13%	
K *	0.454	25288	30462	2.46%	
S *	0.015	836	2089	0.17%	
P *	0.186	10360	23728	1.92%	
			1237462	100.00%	
b31	ppm	X dilut.	oxide conv	wt%	Si/Na
Si	4.917	247325	528976	52.62%	2.04
Na	3.829	192599	259585	25.82%	Time
Al	0.571	28721	54249	5.40%	218
Ca	0.802	40341	56436	5.61%	Temp
Mg	0.387	19466	32283	3.21%	1300
Fe	0.319	16046	22945	2.28%	
K *	0.454	22836	27508	2.74%	
S *	0.015	755	1886	0.19%	
P *	0.186	9356	21428	2.13%	
			1005297	100.00%	
b35	ppm	X dilut.	oxide conv	wt%	Si/Na
Si	4.441	234041	500564	44.17%	1.89
Na	3.727	196413	264725	23.36%	Time
Al	7.09	22419	42344	3.74%	155
Ca	1.666	87798	122830	10.84%	Temp
Mg	0.792	41738	69219	6.11%	1250
Fe	0.656	34571	49437	4.36%	
K *	0.719	37891	45644	4.03%	
S *	0.023	1212	3030	0.27%	
P *	0.293	15441	35365	3.12%	
			1133158	100.00%	
b37	ppm	X dilut.	oxide conv	wt%	Si/Na
Si	4.721	240299	513949	47.46%	3.97
Na	1.889	96150	129591	11.97%	Time
Al	6.39	19515	36860	3.40%	135
Ca	2.089	106330	148756	13.74%	Temp
Mg	0.955	48610	80614	7.44%	1350
Fe	0.795	40466	57866	5.34%	
K *	1.022	52020	62663	5.79%	
S *	0.034	1731	4327	0.40%	
P *	0.415	21124	48379	4.47%	
			1083004	100.00%	
*K, S, and P were not analyzed.					

Table D-2. Th-doped Rocky Flats Glass Fusion Data Conversion

Blank						
Si	Na	Al	Ca	Mg	Fe	K
0.1263	0	0	0.0293	0.0045	0	0
S	P	Th	B			
3.839	0	0	0			
b52	10.96 ppm					
	ppm	corrected	X dilut.	oxide conv	wt%	Si/Na
Si	2.418	2.2917	251170	537201	45.30%	2.03
Na	1.794	1.794	196622	265008	22.35%	Time
Al	0.184	0.184	20166	38090	3.21%	261
Ca	0.863	0.8337	91374	127832	10.78%	Temp
Mg	0.4149	0.4104	44980	74595	6.29%	1350
Fe*	N/A	N/A	N/A	66600	5.62%	
K*	N/A	N/A	N/A	43200	3.64%	
S*	N/A	N/A	N/A	2800	0.24%	
P	0.1218	0.1218	13349	30574	2.58%	
Th*	N/A	N/A	N/A	12	0.00%	
				1185911	100.00%	
b56	10.60 ppm					
	ppm	corrected	X dilut.	oxide conv	wt%	Si/Na
Si	1.972	1.8457	202289	432653	41.53%	3.68
Na	0.795	0.795	87132	117437	11.27%	Time
Al	N/A	N/A	N/A	9000	0.86%	201
Ca	1.034	1.0047	110115	154051	14.79%	Temp
B	0.2258	0.2258	24748	79688	7.65%	1250
Mg	0.525	0.5205	57047	94606	9.08%	
Fe*	N/A	N/A	N/A	67000	6.43%	
K*	N/A	N/A	N/A	48442	4.65%	
S*	N/A	N/A	N/A	3411	0.33%	
P	0.1418	0.1418	15541	35594	3.42%	
Th*	N/A	N/A	N/A	12	0.00%	
				1041894	100.00%	
b59	11.03 ppm					
	ppm	corrected	X dilut.	oxide conv	wt%	Si/Na
Si	3.036	2.9097	318903	682067	62.01%	2.87
Na	1.611	1.611	176566	237975	21.64%	Time
Al	N/A	N/A	N/A	12200	1.11%	175
Ca	0.4745	0.4452	48794	68263	6.21%	Temp
Mg	0.2212	0.2167	23750	39388	3.58%	1350
Fe*	N/A	N/A	N/A	25200	2.29%	
K*	N/A	N/A	N/A	16270	1.48%	
S*	N/A	N/A	N/A	1058	0.10%	
P	0.0695	0.0695	7617	17446	1.59%	
Th*	N/A	N/A	N/A	5	0.00%	
				1099870	100.00%	
b61	11.86 ppm					
	ppm	corrected	X dilut.	oxide conv	wt%	Si/Na
Si	2.352	2.2257	243937	521729	43.78%	3.76
Na	0.939	0.939	102914	138708	11.64%	Time
Al	0.1197	0.1197	13119	24769	2.08%	220
Ca	1.288	1.2587	137954	192997	16.20%	Temp
Mg	0.618	0.6135	67240	111510	9.36%	1350
Fe*	N/A	N/A	N/A	93600	7.85%	
K*	N/A	N/A	N/A	61000	5.12%	
S*	N/A	N/A	N/A	4000	0.34%	
P	0.1724	0.1724	18895	43275	3.63%	
Th*	N/A	N/A	N/A	16	0.00%	
				1191605	100.00%	
*K, Fe, Th, and S were not analyzed.						

Table D-3. MCC-1 Leach Test Room Temperature Data Conversion

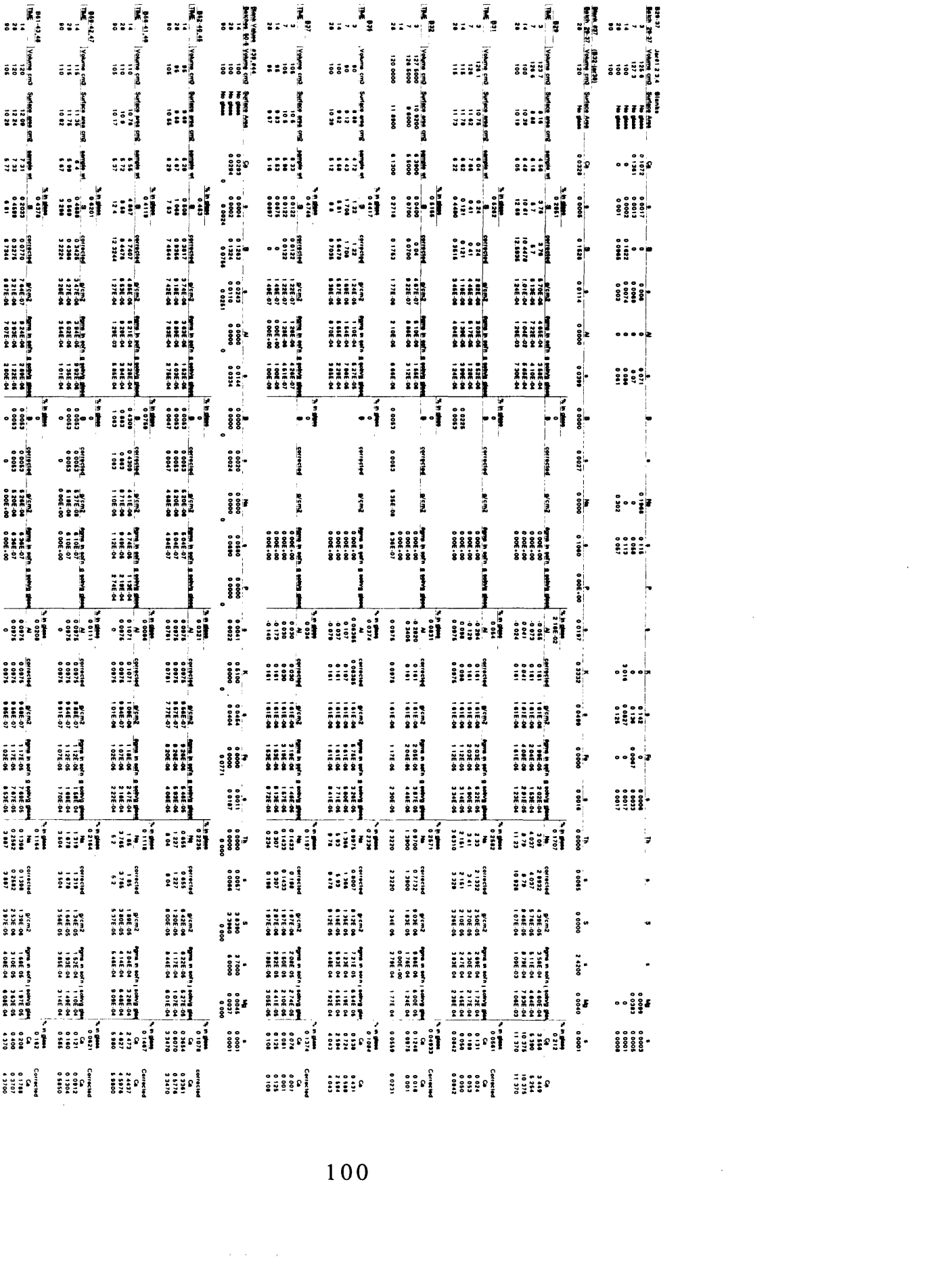

Table D-3. MCC-1 Leach Test Room Temperature Data Conversion (Cont.)

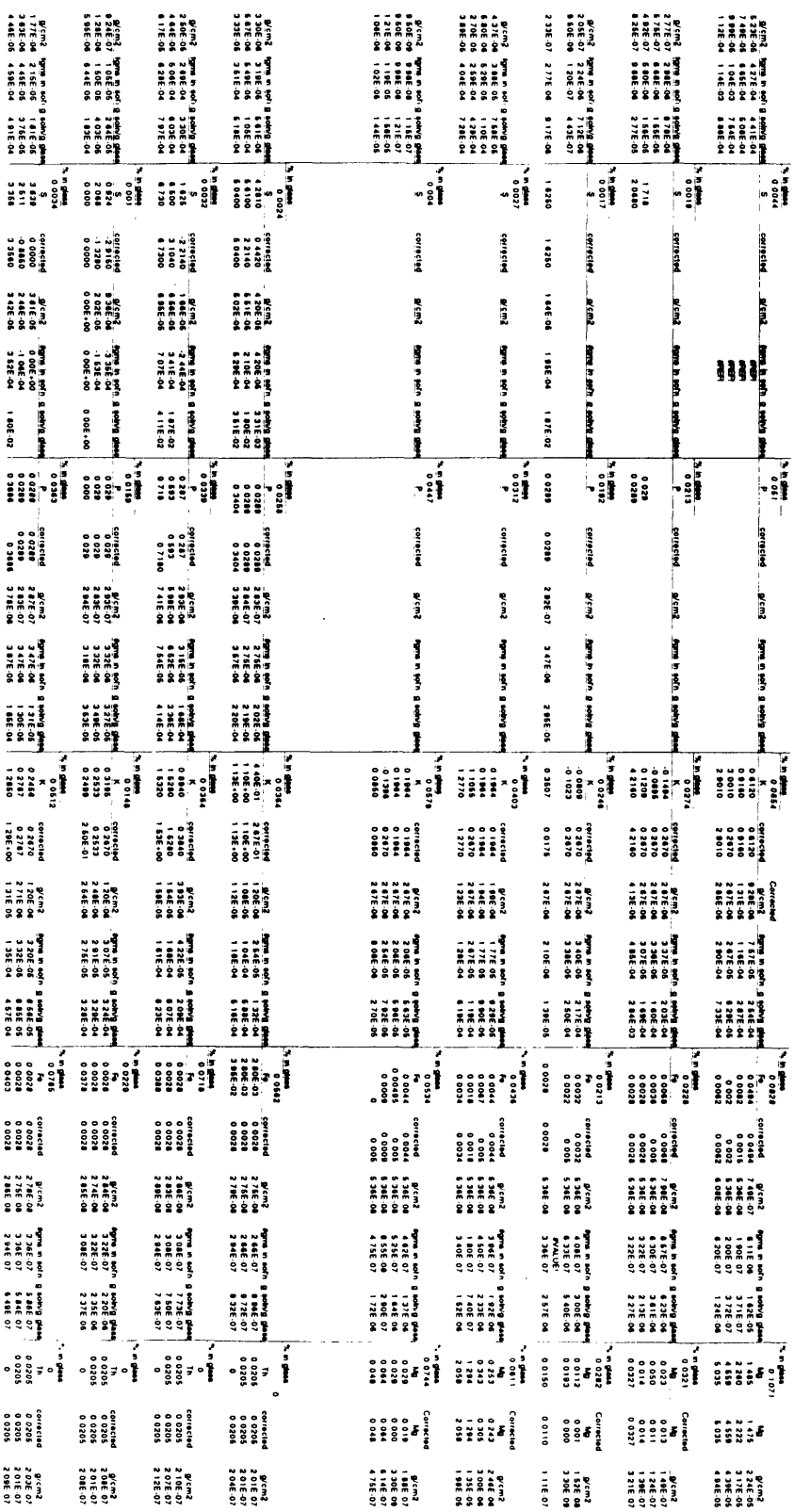

Table D-3. MCC-1 Leach Test Room Temperature Data Conversion (Cont.)

Table D-4. MCC-1 Leach Test 90°C Data Conversion

Blanks

Time(days)	Volume cm3	Surface Area	Ca	B	Si	B	Al	B	B	Na	B	P	B	K	B
		No glass	0		0.0199		0		0	0		0		0	
28	100	No glass	0		0		0		0	0		0		1.047	
90	100	No glass	0.0294		0.0214		0		0	0		0		0	
180	110	No glass	0		0.0338		0		0	0		0		1.625	

B52

TIME	Volume cm3	Surface area cm2	sample wt	% in glass 0.453 Si	corrected	g/cm2	#gms in soln g solv/g glass	% in glass 0 B	corrected	g/cm2	#gms in soln g solv/g glass	% in glass 0.0321 Al	corrected	g/cm2
14	105	10.8	5.79	21.84	21.8201	2.14E-04	2.27E-03 8.86E-04	0	0.0053	5.25E-08	5.57E-07 #DIV/0!	0.728	0.728	7.21E-06
28	105	10.66	5.96	23.27	23.2700	2.29E-04	2.44E-03 9.05E-04	0	0.0053	5.22E-08	5.57E-07	0.736	0.736	7.25E-06
90	115	11.77	6.68	31.96	31.9388	3.12E-04	3.67E-03 1.21E-03	0	0.0053			0.776	0.776	7.58E-06
180	1.05E+02	10.55	5.97	30.67	30.6782	3.05E-04	3.22E-03 1.19E-03	0	0.0053			0.712	0.712	7.09E-06
180	1.05E+02	10.7	6.06	32	31.9682	3.14E-04	3.36E-03 1.22E-03	0	0.0053			0.764	0.764	7.50E-06
180	1.05E+02	10.66	6.01	29.9	29.8682	2.94E-04	3.14E-03 1.15E-03	0	0.0053			0.667	0.667	6.57E-06
180	1.05E+02	10.3	5.83	30.23	30.1982	3.08E-04	3.17E-03 1.20E-03	0	0.0053			0.706	0.706	7.20E-06

B56

TIME	Volume cm3	Surface area cm2	sample wt	% in glass 0.4119 Si	corrected	g/cm2	#gms in soln g solv/g glass	% in glass 0.0759 B	corrected	g/cm2	#gms in soln g solv/g glass	% in glass 0.0086 Al	corrected	g/cm2
14	110	10.92	6.13	31.73	31.7101	3.19E-04	3.49E-03 1.38E-03	2.895	2.895	2.92E-05	3.19E-04 6.84E-04	0.0781	0.0781	7.87E-07
28	90	8.87	4.84	41.4	41.4000	4.15E-04	3.73E-03 1.87E-03	4.394	4.394	4.41E-05	3.95E-04 1.08E-03	0.0781	0.0781	7.84E-07
90	110	11.09	5.79	53.5	53.4786	5.30E-04	5.89E-03 2.47E-03	9.29	9.29	9.21E-05	1.02E-03 2.33E-03	0.0781	0.0781	7.75E-07
180	110	10.9	5.17	83.07	83.0362	8.38E-04	9.13E-03 4.20E-03	17.01	17.01	1.72E-04	1.87E-03 4.77E-03	0.0781	0.0781	7.88E-07
180	110	11.08	5	86.2	86.1662	8.55E-04	9.40E-03 4.60E-03	17.44	17.44	1.73E-04	1.92E-03 5.06E-03	0.511	0.511	5.07E-06
180	110	10.76	4.71	78.5	78.4662	8.02E-04	8.63E-03 4.45E-03	15.34	15.34	1.57E-04	1.69E-03 4.72E-03	0.0781	0.0781	7.98E-07
180	110	10.54	5.8	84.5	84.4662	8.62E-04	9.29E-03 3.89E-03	18.24	18.24	1.90E-04	2.01E-03 4.56E-03	0.0781	0.0781	8.15E-07

B58

TIME	Volume cm3	Surface area cm2	sample wt	% in glass 0.453 Si	corrected	g/cm2	#gms in soln g solv/g glass	% in glass 0 B	corrected	g/cm2	#gms in soln g solv/g glass	% in glass 0.0321 Al	corrected	g/cm2
14	100	9.87	5.42	21.38	21.3601	2.16E-04	2.14E-03 8.70E-04	0	0	0.00E+00	0.00E+00 0.00E+00	0.768	0.768	7.78E-06
28	100	9.83	5.58	23.2	23.2000	2.34E-04	2.32E-03 9.18E-04	0	0	0.00E+00	0.00E+00 0.00E+00	0.785	0.785	7.91E-06
90	125	12.65	6.77	30.52	30.4986	3.01E-04	3.81E-03 1.24E-03	0	0	0		0.911	0.911	9.00E-06

B59

TIME	Volume cm3	Surface area cm2	sample wt	% in glass 0.6201 Si	corrected	g/cm2	#gms in soln g solv/g glass	% in glass 0 B	corrected	g/cm2	#gms in soln g solv/g glass	% in glass 0.0111 Al	corrected	g/cm2
14	110	10.95	5.63	51.2	51.1801	5.14E-04	5.83E-03 1.81E-03	0	0	0.00E+00	0.00E+00	0.3676	0.3676	3.69E-06
28	105	10.56	5.52	62.6	62.6000	6.22E-04	6.57E-03 1.92E-03	0	0	0.00E+00	0.00E+00	0.34	0.34	3.38E-06
90	110	10.75	5.54	96.1	96.0786	9.83E-04	1.04E-02 3.08E-03	0	0			0.4368	0.4368	4.47E-06
180	100	10.08	5.78	121.73	121.6962	1.21E-03	1.22E-02 3.40E-03	0	0			0.539	0.539	5.35E-06
180	95	9.86	6.1	127.2	127.1662	1.25E-03	1.21E-02 3.19E-03	0	0			0.583	0.583	5.73E-06
180	95	9.81	5.75	119	118.9662	1.18E-03	1.13E-02 3.17E-03	0	0			0.523	0.523	5.17E-06
180	110	10.98	5.5	119	118.9662	1.19E-03	1.31E-02 3.84E-03	0	0			0.511	0.511	5.12E-06

B61

TIME	Volume cm3	Surface area cm2	sample wt	% in glass 0.4378 Si	corrected	g/cm2	#gms in soln g solv/g glass	% in glass 0 B	corrected	g/cm2	#gms in soln g solv/g glass	% in glass 0.0208 Al	corrected	g/cm2
14	105	10.87	5.91	20.76	20.7401	2.04E-04	2.18E-03 8.42E-04	0	0	0.00E+00	0.00E+00 #DIV/0!	0.0816	0.0816	8.03E-07
28	95	9.5	4.84	23.14	23.1400	2.31E-04	2.20E-03 1.04E-03	0	0	0.00E+00	0.00E+00 #DIV/0!	0.0781	0.0781	7.81E-07
90	110	11.15	6.38	33.34	33.3186	3.29E-04	3.67E-03 1.31E-03	0	0	0.00E+00	0.00E+00 #DIV/0!	0.0932	0.0932	9.19E-07
180	110	10.96	6.14	36.55	36.5182	3.66E-04	4.02E-03 1.49E-03	0.0235	0.0235	2.36E-07	2.59E-06 #DIV/0!	0.0781	0.0781	7.84E-07
180	110	11.01	6.24	35.89	35.8562	3.58E-04	3.94E-03 1.44E-03	0.0611	0.0611	6.10E-07	6.72E-06 #DIV/0!	0.0781	0.0781	7.80E-07
180	110	10.92	6.13	36.73	36.6962	3.70E-04	4.04E-03 1.50E-03	0.0047	0.0047	4.73E-08	5.17E-07 #DIV/0!	0.0781	0.0781	7.87E-07
180	110	10.81	6.06	37.02	36.9962	3.76E-04	4.07E-03 1.53E-03	0.0047	0.0047	4.78E-08	5.17E-07 #DIV/0!	0.0781	0.0781	7.95E-07

Granite Rock	Si	Ca	Al	Na	B	S	P	Th	Mg	K
# days										
180	0.706	6.77	0.0781	0.0928	0.0047	2.41E+00	5.91E-02	5.86E-02	3.60E-03	0.2081
SA										
9.23										
vol										
100										

Table D-4. MCC-1 Leach Test 90°C Data Conversion (Cont.)

Fe	Ti	Si	Mg	K
0.0392	0	0	0	
0.0484	0	0	0	
0.0365	0	4.685	0	
0.0398		8.29	0	

Blank values which equal 0.0 were at the LOD
LOD were not subtracted from the Leach results.

| % in glass | | |

Table D-4. MCC-1 Leach Test 90°C Data Conversion (Cont.)

corrected	g/cm2	#gms in soln	g soln/g glass
0.0591	5.85E-07	6.21E-06	4.15E-05
0.0591	5.77E-07	6.80E-06	3.94E-05

% in glass																							
0.0364																							
K	corrected	g/cm2	#gms in soln	g soln/g glass	K	corrected	g/cm2	#gms in soln	g soln/g glass	K	corrected	g/cm2	#gms in soln	g soln/g glass	K	corrected	g/cm2	#gms in soln	g soln/g glass	K	corrected	g/cm2	#gms in soln
2.84E+00	2.84E+00	2.82E-05	2.98E-04	1.42E-03	4.51E+00	3.47E+00	3.44E-05	3.64E-04	1.68E-03	3.90E+00	3.90E+00	3.81E-05	4.48E-04	1.84E-03	4.81E+00	4.81E+00	4.48E-05	2.98E+00	1.44E-03	5.32E+00	3.70E+00	3.63E-05	3.88E-04
4.4240	4.42E+00	4.46E-05	4.87E-04	2.18E-03	8.2800	7.23E+00	7.26E-05	6.51E-04	3.89E-03	11.7600	1.18E+01	1.17E-04	1.29E-03	6.14E-03	22.1600	2.05E+01	2.07E-04	2.26E-03	1.20E-02	23.2000	2.16E+01	2.14E-04	2.37E-03
3.8090	3.81E+00	3.75E-05	4.00E-04	1.32E-03	5.4400	4.39E+00	4.39E-05	4.17E-04	1.68E-03	5.2200	5.22E+00	5.15E-05	5.74E-04	1.76E-03	6.0200	4.40E+00	4.41E-05	4.83E-04	1.54E-03	5.9800	4.38E+00	4.35E-05	4.79E-04
4.4200	4.42E+00	4.46E-05	4.87E-04	2.18E-03	8.2800	7.23E+00	7.26E-05	6.51E-04	3.89E-03	11.7600	1.18E+01	1.17E-04	1.29E-03	6.14E-03	22.1600	2.05E+01	2.07E-04	2.26E-03	1.20E-02	23.2000	2.16E+01	2.14E-04	2.37E-03
3.8090	3.81E+00	3.75E-05	4.00E-04	1.32E-03	5.4400	4.39E+00	4.39E-05	4.17E-04	1.68E-03	5.2200	5.22E+00	5.15E-05	5.74E-04	1.76E-03	6.0200	4.40E+00	4.41E-05	4.83E-04	1.54E-03	5.9800	4.38E+00	4.35E-05	4.79E-04
3.81E+00	3.75E-05	4.00E-04	1.32E-03	4.39E-05	4.17E-04	1.68E-03	5.15E-05	5.74E-04	1.76E-03	4.41E-05	4.83E-04	1.54E-03	4.35E-05	4.79E-04	1.50E-03	4.57E-05	4.99E-04	1.59E-03	4.37E-05	4.72E-04	1.52E-03		

corrected	g/cm2	#gms in soln	g soln/g glass
0.059	5.95E-07	6.50E-06	3.13E-05
0.059	5.86E-07	6.50E-06	3.31E-05

% in glass																							
0.0364																							
K	corrected	g/cm2	#gms in soln	g soln/g glass	K	corrected	g/cm2	#gms in soln	g soln/g glass	K	corrected	g/cm2	#gms in soln	g soln/g glass	K	corrected	g/cm2	#gms in soln	g soln/g glass	K	corrected	g/cm2	#gms in soln
2.7950	2.80E+00	2.83E-05	0.0003	1.42E-03	2.8520	2.85E+00	2.87E-05	3.14E-04	3.77E-03	4.2320	3.19E+00	3.17E-05	3.34E-04	4.09E-03	5.2700	5.27E+00	5.30E-05	5.80E-04	7.07E-03	11.3300	9.71E+00	9.63E-05	9.71E-04
2.7950	2.80E+00	2.83E-05	0.0003	1.42E-03	2.8520	2.85E+00	2.87E-05	3.14E-04	3.77E-03	4.2320	3.19E+00	3.17E-05	3.34E-04	4.09E-03	5.2700	5.27E+00	5.30E-05	5.80E-04	7.07E-03	11.3300	9.71E+00	9.63E-05	9.71E-04
2.8520	2.85E+00	2.87E-05	3.14E-04	3.77E-03	4.2320	3.19E+00	3.17E-05	3.34E-04	4.09E-03	5.2700	5.27E+00	5.30E-05	5.80E-04	7.07E-03	11.3300	9.71E+00	9.63E-05	9.71E-04	1.13E-02	7.9900	6.37E+00	6.28E-05	6.05E-04
3.7750	3.78E+00	3.73E-05	0.0005	1.91E-03	6.05E-04	6.70E-03	7.9900	6.37E+00	6.28E-05	6.05E-04	6.70E-03												

corrected	g/cm2	#gms in soln	g soln/g glass
0.059	5.94E-07	6.50E-06	7.28E-05
0.059	6.05E-07	6.50E-06	7.38E-05

% in glass																							
0.0148																							
K	corrected	g/cm2	#gms in soln	g soln/g glass	K	corrected	g/cm2	#gms in soln	g soln/g glass	K	corrected	g/cm2	#gms in soln	g soln/g glass	K	corrected	g/cm2	#gms in soln	g soln/g glass	K	corrected	g/cm2	#gms in soln
2.8520	2.85E+00	2.87E-05	3.14E-04	3.77E-03	4.2320	3.19E+00	3.17E-05	3.34E-04	4.09E-03	5.2700	5.27E+00	5.30E-05	5.80E-04	7.07E-03	11.3300	9.71E+00	9.63E-05	9.71E-04	1.13E-02	7.9900	6.37E+00	6.28E-05	6.05E-04
3.7750	3.78E+00	3.73E-05	0.0005	1.91E-03	6.05E-04	6.70E-03	7.9900	6.37E+00	6.28E-05	6.05E-04	6.70E-03	1.07E-04	1.81E-03	1.89E-02	1.69E+01	1.67E-04	1.81E-03	1.89E-02	18.5200	1.69E+01	1.67E-04	1.86E-05	6.43E-04
3.7750	3.78E+00	3.73E-05	0.0005	1.91E-03	6.05E-04	6.70E-03	7.9900	6.37E+00	6.28E-05	6.05E-04	6.70E-03	1.07E-04	1.81E-03	1.89E-02	1.69E+01	1.67E-04	1.81E-03	1.89E-02	18.5200	1.69E+01	1.67E-04	1.86E-05	6.43E-04
7.4700	5.86E+00	5.78E-05	6.43E-04	7.90E-03																			

corrected	g/cm2	#gms in soln	g soln/g glass
0.0591	5.82E-07	6.21E-06	2.89E-05
0.0591	5.83E-07	6.50E-06	2.81E-05

% in glass																							
0.0512																							
K	corrected	g/cm2	#gms in soln	g soln/g glass	K	corrected	g/cm2	#gms in soln	g soln/g glass	K	corrected	g/cm2	#gms in soln	g soln/g glass	K	corrected	g/cm2	#gms in soln	g soln/g glass	K	corrected	g/cm2	#gms in soln
3.8090	3.81E+00	3.75E-05	4.00E-04	1.32E-03	5.4400	4.39E+00	4.39E-05	4.17E-04	1.68E-03	5.2200	5.22E+00	5.15E-05	5.74E-04	1.76E-03	6.0200	4.40E+00	4.41E-05	4.83E-04	1.54E-03	5.9800	4.38E+00	4.35E-05	4.79E-04
5.2200	5.22E+00	5.15E-05	5.74E-04	1.76E-03	6.0200	4.40E+00	4.41E-05	4.83E-04	1.54E-03	5.9800	4.38E+00	4.35E-05	4.79E-04	1.50E-03	6.1600	4.54E+00	4.57E-05	4.99E-04	1.59E-03	5.9200	4.30E+00	4.37E-05	4.72E-04
6.0200	4.40E+00	4.41E-05	4.83E-04	1.54E-03	5.9800	4.38E+00	4.35E-05	4.79E-04	1.50E-03	6.1600	4.54E+00	4.57E-05	4.99E-04	1.59E-03	5.9200	4.30E+00	4.37E-05	4.72E-04	1.52E-03				

corrected	g/cm2	#gms in soln	g soln/g glass
0.059	5.98E-07	5.91E-06	4.23E-05
0.059	5.84E-07	7.39E-06	4.23E-05

% in glass																							
0.0562																							
Fe	corrected	g/cm2	#gms in soln	g soln/g glass	Fe	corrected	g/cm2	#gms in soln	g soln/g glass	Fe	corrected	g/cm2	#gms in soln	g soln/g glass	Fe	corrected	g/cm2	#gms in soln	g soln/g glass	Fe	corrected	g/cm2	#gms in soln
0.0686	0.0294	2.98E-07	2.94E-06	9.65E-06	0.0440	0.0048	4.82E-08	5.28E-07	4.10E-06	0.0389	0.0042	4.12E-08	4.40E-07	9.48E-07	0.0409	0.0042	4.19E-08	3.98E-07	1.05E-06	0.0361	0.0042	4.13E-08	4.61E-07
0.0332	0.0042	4.22E-08	1.19E-07	1.34E-06	0.0444	0.0042	4.17E-08	4.40E-07	3.48E-06	0.0384	0.0042	4.20E-08	4.61E-07	3.63E-06	0.0401	0.0042	4.16E-08	4.19E-07	3.17E-06	0.0407	0.0042	4.12E-08	3.98E-07
0.0332	0.0042	4.14E-08	5.24E-07	1.38E-06	0.0400	0.0042	4.20E-08	4.61E-07	3.66E-06	0.0396	0.0042	4.14E-08	3.98E-07	3.02E-06	0.0383	0.0042	4.21E-08	4.61E-07	9.56E-07	0.0379	0.0042	4.19E-08	4.61E-07
0.0440	0.0048	4.82E-08	5.28E-07	4.10E-06	0.0389	0.0042	4.12E-08	4.40E-07	9.48E-07	0.0409	0.0042	4.19E-08	3.98E-07	1.05E-06	0.0361	0.0042	4.13E-08	4.61E-07	9.20E-07	0.0383	0.0042	4.21E-08	4.61E-07
0.0444	0.0042	4.17E-08	4.40E-07	3.48E-06	0.0384	0.0042	4.20E-08	4.61E-07	3.63E-06	0.0401	0.0042	4.16E-08	4.19E-07	3.17E-06	0.0407	0.0042	4.12E-08	3.98E-07	2.85E-06	0.0396	0.0042	4.14E-08	3.98E-07
0.0400	0.0042	4.20E-08	4.61E-07	3.66E-06																			

corrected	g/cm2	#gms in soln
0.059	5.94E-07	6.45E-06
0.059	5.86E-07	6.45E-06

% in glass																							
0.0229																							
Fe	corrected	g/cm2	#gms in soln	g soln/g glass	Fe	corrected	g/cm2	#gms in soln	g soln/g glass	Fe	corrected	g/cm2	#gms in soln	g soln/g glass	Fe	corrected	g/cm2	#gms in soln	g soln/g glass	Fe	corrected	g/cm2	#gms in soln
0.0440	0.0048	4.82E-08	5.28E-07	4.10E-06	0.0389	0.0042	4.12E-08	4.40E-07	9.48E-07	0.0409	0.0042	4.19E-08	3.98E-07	1.05E-06	0.0361	0.0042	4.13E-08	4.61E-07	9.20E-07	0.0383	0.0042	4.21E-08	4.61E-07
0.0444	0.0042	4.17E-08	4.40E-07	3.48E-06	0.0384	0.0042	4.20E-08	4.61E-07	3.63E-06	0.0401	0.0042	4.16E-08	4.19E-07	3.17E-06	0.0407	0.0042	4.12E-08	3.98E-07	2.85E-06	0.0396	0.0042	4.14E-08	3.98E-07
0.0400	0.0042	4.20E-08	4.61E-07	3.66E-06																			

corrected	g/cm2	#gms in soln
0.059	5.94E-07	5.86E-06
0.059	5.84E-07	7.39E-06

% in glass																							
0.0686																							
Fe	corrected	g/cm2	#gms in soln	g soln/g glass	Fe	corrected	g/cm2	#gms in soln	g soln/g glass	Fe	corrected	g/cm2	#gms in soln	g soln/g glass	Fe	corrected	g/cm2	#gms in soln	g soln/g glass	Fe	corrected	g/cm2	#gms in soln
0.0686	0.0294	2.98E-07	2.94E-06	9.65E-06	0.0440	0.0048	4.82E-08	5.28E-07	4.10E-06	0.0389	0.0042	4.12E-08	4.40E-07	9.48E-07	0.0409	0.0042	4.19E-08	3.98E-07	1.05E-06	0.0361	0.0042	4.13E-08	4.61E-07
0.0332	0.0042	4.22E-08	1.19E-07	1.34E-06	0.0444	0.0042	4.17E-08	4.40E-07	3.48E-06	0.0384	0.0042	4.20E-08	4.61E-07	3.63E-06	0.0401	0.0042	4.16E-08	4.19E-07	3.17E-06	0.0407	0.0042	4.12E-08	3.98E-07
0.0332	0.0042	4.14E-08	5.24E-07	1.38E-06	0.0400	0.0042	4.20E-08	4.61E-07	3.66E-06	0.0396	0.0042	4.14E-08	3.98E-07	3.02E-06	0.0383	0.0042	4.21E-08	4.61E-07	9.56E-07	0.0379	0.0042	4.19E-08	4.61E-07
0.0440	0.0048	4.82E-08	5.28E-07	4.10E-06	0.0389	0.0042	4.12E-08	4.40E-07	9.48E-07	0.0409	0.0042	4.19E-08	3.98E-07	1.05E-06	0.0361	0.0042	4.13E-08	4.61E-07	9.20E-07	0.0383	0.0042	4.21E-08	4.61E-07
0.0444	0.0042	4.17E-08	4.40E-07	3.48E-06	0.0384	0.0042	4.20E-08	4.61E-07	3.63E-06	0.0401	0.0042	4.16E-08	4.19E-07	3.17E-06	0.0407	0.0042	4.12E-08	3.98E-07	2.85E-06	0.0396	0.0042	4.14E-08	3.98E-07
0.0400	0.0042	4.20E-08	4.61E-07	3.66E-06																			

corrected	g/cm2	#gms in soln
0.059	5.98E-07	5.91E-06
0.059	5.86E-07	6.45E-06

% in glass																							
0.0562																							
Fe	corrected	g/cm2	#gms in soln	g soln/g glass	Fe	corrected	g/cm2	#gms in soln	g soln/g glass	Fe	corrected	g/cm2	#gms in soln	g soln/g glass	Fe	corrected	g/cm2	#gms in soln	g soln/g glass	Fe	corrected	g/cm2	#gms in soln
0.0686	0.0294	2.98E-07	2.94E-06	9.65E-06	0.0440	0.0048	4.82E-08	5.28E-07	4.10E-06	0.0389	0.0042	4.12E-08	4.40E-07	9.48E-07	0.0409	0.0042	4.19E-08	3.98E-07	1.05E-06	0.0361	0.0042	4.13E-08	4.61E-07
0.0332	0.0042	4.22E-08	1.19E-07	1.34E-06	0.0444	0.0042	4.17E-08	4.40E-07	3.48E-06	0.0384	0.0042	4.20E-08	4.61E-07	3.63E-06	0.0401	0.0042	4.16E-08	4.19E-07	3.17E-06	0.0407	0.0042	4.12E-08	3.98E-07
0.0332	0.0042	4.14E-08	5.24E-07	1.38E-06	0.0400	0.0042	4.20E-08	4.61E-07	3.66E-06	0.0396	0.0042	4.14E-08	3.98E-07	3.02E-06	0.0383	0.0042	4.21E-08	4.61E-07	9.56E-07	0.0379	0.0042	4.19E-08	4.61E-07
0.0440	0.0048	4.82E-08	5.28E-07	4.10E-06	0.0389	0.0042	4.12E-08	4.40E-07	9.48E-07	0.0409	0.0042	4.19E-08	3.98E-07	1.05E-06	0.0361	0.0042	4.13E-08	4.61E-07	9.20E-07	0.0383	0.0042	4.21E-08	4.61E-07
0.0444	0.0042	4.17E-08	4.40E-07	3.48E-06	0.0384	0.0042	4.20E-08	4.61E-07	3.63E-06	0.0401	0.0042	4.16E-08	4.19E-07	3.17E-06	0.0407	0.0042	4.12E-08	3.98E-07	2.85E-06	0.0396	0.0042	4.14E-08	3.98E-07
0.0400	0.0042	4.20E-08	4.61E-07	3.66E-06																			

corrected	g/cm2	#gms in soln
0.059	5.98E-07	5.94E-06
0.059	5.84E-07	5.86E-06

% in glass																							
0																							
Th	corrected	g/cm2	#gms in soln	g soln/g glass	Th	corrected	g/cm2	#gms in soln	g soln/g glass	Th	corrected	g/cm2	#gms in soln	g soln/g glass	Th	corrected	g/cm2	#gms in soln	g soln/g glass	Th	corrected	g/cm2	#gms in soln
0.0586	0.0586	5.80E-07	6.15E-06	4.61E-05	0.0586	0.0586	5.90E-07	6.45E-06	5.09E-07	0.0586	0.0586	5.94E-07	5.86E-06	4.23E-05	0.0586	0.0586	5.94E-07	5.86E-06	4.23E-05	0.0586	0.0586	5.86E-07	6.15E-06

corrected	g/cm2	#gms in soln
0.0591	5.77E-07	6.15E-06

% in glass																							
0																							
Th	corrected	g/cm2	#gms in soln	g soln/g glass	Th	corrected	g/cm2	#gms in soln	g soln/g glass	Th	corrected	g/cm2	#gms in soln	g soln/g glass	Th	corrected	g/cm2	#gms in soln	g soln/g glass	Th	corrected	g/cm2	#gms in soln
0.0586	0.0586	5.80E-07	6.15E-06	4.61E-05	0.0586	0.0586	5.90E-07	6.45E-06	5.09E-07	0.0586	0.0586	5.94E-07	5.86E-06	4.23E-05	0.0586	0.0586	5.94E-07	5.86E-06	4.23E-05	0.0586	0.0586	5.86E-07	6.15E-06

Table D-4. MCC-1 Leach Test 90°C Data Conversion (Cont.)

g sol'n/g glass	% in glass 0.0629 corrected Mg	g/cm2	#gms in sol'n	g sol'n/g glass
0.0036	0.0036	3.57E-08	3.79E-07	1.04E-06
0.0036	0.0036	3.55E-08	3.79E-07	1.01E-06
0.0036	0.0036	3.52E-08	4.14E-07	9.85E-07
0.0036	0.0036	3.58E-08	3.78E-07	1.01E-06
0.0036	0.0036	3.53E-08	3.79E-07	9.92E-07
0.0036	0.0036	3.55E-08	3.79E-07	1.00E-06
0.0036	0.0036	3.67E-08	3.79E-07	1.03E-06

g sol'n/g glass	% in glass 0.0901 Corrected Mg	g/cm2	#gms in sol'n	g sol'n/g glass
0.0036	0.0036	3.63E-08	3.96E-07	7.17E-07
0.0036	0.0036	3.61E-08	3.24E-07	7.43E-07
0.0036	0.0036	3.57E-08	3.96E-07	7.59E-07
0.0036	0.0036	3.63E-08	3.96E-07	8.50E-07
0.0036	0.0036	3.57E-08	3.96E-07	8.79E-07
0.0036	0.0036	3.68E-08	3.96E-07	9.33E-07
0.0036	0.0036	3.78E-08	3.96E-07	7.58E-07

g sol'n/g glass	% in glass 0.0629 corrected Mg	g/cm2	#gms in sol'n	g sol'n/g glass
0.0036	0.0036	3.65E-08	3.60E-07	1.06E-06
	0.0036	3.63E-08	3.60E-07	1.03E-06
0.0036	0.0036	3.58E-08	4.50E-07	1.06E-06

g sol'n/g glass	% in glass 0.0358 Corrected Mg	g/cm2	#gms in sol'n	g sol'n/g glass
0.0036	0.0036	3.62E-08	3.96E-07	1.96E-06
0.0036	0.0036	3.58E-08	3.78E-07	1.91E-06
0.0036	0.0036	3.68E-08	3.96E-07	2.00E-06
0.0036	0.0036	3.57E-08	3.60E-07	1.74E-06
0.0036	0.0036	3.54E-08	3.42E-07	1.57E-06
0.0036	0.0036	3.56E-08	3.42E-07	1.86E-06
0.0036	0.0036	3.61E-08	3.96E-07	2.01E-06

g sol'n/g glass	% in glass 0.0936 Corrected Mg	g/cm2	#gms in sol'n	g sol'n/g glass
0.0036	0.0036	3.54E-08	3.78E-07	6.83E-07
0.0036	0.0036	3.60E-08	3.42E-07	7.55E-07
0.0036	0.0036	3.55E-08	3.96E-07	6.63E-07
0.0036	0.0036	3.61E-08	3.96E-07	6.80E-07
0.0036	0.0036	3.60E-08	3.96E-07	6.78E-07
0.0036	0.0036	3.63E-08	3.96E-07	6.90E-07
0.0036	0.0036	3.66E-08	3.96E-07	6.98E-07

Appendix E

SAFETY AND RELATED TOPICS IN GLASS MAKING

It is important that anyone continuing to work at MIT's glass laboratory located in building NW13-235 know several aspects about making glass that should not be repeated. In other words, the mistakes made during past experiments can be avoided. The most important knowledge is related to safety when working with glass, a hot furnace, and acid baths.

When pouring glass, keep the crucible lip as close to the graphite as possible and cover the crucible when done with a slab of fire brick. It is best to have two people involved with pouring the glass; one to pour the glass and the other to open and close the furnace door. The furnace can ignite clothing if too close to the oven door. To test this theory, place a piece of clothing attached to the crucible tongs near the furnace and see how close you can get before igniting the clothing. This is an excellent experiment for convincing novice glass makers that the furnace is not just bright, but dangerous.

Glass is a very dangerous object to touch when hot. This is because it can be 600°C and look the same as when it is at room temperature. The same thing goes for crucibles, graphite, and firebrick. To avoid burning the hands on hot surfaces, gloves (not plastic) should be worn at the appropriate times. If you are not sure if something is hot, use the back of the hand to test for heat about one inch away. Do not use water to see if it will boil off hot glass. This has been tried and usually the thermal stress on the glass causes it to explode.

Other explosions have taken place in two other circumstances; when annealing glass billets and when cutting glass billets. When the glass is being annealed, it is best to have the furnace at around 100°C or less to avoid thermal shock to the glass which causes the glass to explode or crack. Then the temperature can be increased to 500°C. Make sure the glass billet is inside a crucible and covered so that in case the glass does crack or explode, pieces will not go under the ceramic plate by the bottom of the heating elements. When this happens, the furnace has to be completely cooled down to room temperature so that the plate can be taken out and the bottom of the furnace vacuumed. If a glass billet is cut before being annealed, the thermal stresses in the glass will cause the it to explode. Typically, these explosions have been violent enough to cause physical harm to the eyes and cause scars to skin. To avoid this, all glass should be annealed before cutting on the diamond saw. When cutting or polishing glass, a particulate mask should be worn along with a lab coat, goggles, and plastic gloves.

The furnace itself goes through about one heating element every month. To avoid the wear and tear on the furnace, it should be left between 800°C and 1000°C. If the furnace is not being used for longer than 48 hours, it is best to turn the furnace off. When replacing heating elements, they can be ordered and delivered in about three days. Unplug the furnace before taking the back plate off to avoid a large shocking experience causing death. Also, the heating elements and furnace should be cooled to room temperature before replacing. Never look into the furnace without eye protection above 800°C. Always wear gloves and the asbestos apron when taking crucibles in or out of the furnace. Also where durable shoes jeans and a lab coat. The crucibles should be resting on a thin layer of firebrick while inside the furnace in case any of the chemicals inside manage to ooze over the edges. When molten glass escapes out of the crucible, a corrosion process begins whereby the glass eats through much like an acid until the ceramic plate, firebrick, or heating element are destroyed. In all cases use common sense.

When cleaning Teflon containers, try not to splash any of the liquid around. This is done by slowly sinking the container into the solution. The Teflon sample bottle should be tilted when lowered. Use gloves that are talc free when handling all glass samples and Teflon containers.

When making new acid solution, have about 1 kg of sodium bicarbonate ready to buffer the solution. Add the chemical slowly in small spoonfuls because if too much is added at one time, a large froth of acid will come out of the container and contaminate the area around the hood. Always have the hood "on" when mixing chemicals. Large objects should be near the ends of the hood and nothing should block the way in the center. It should be noted that the hood sucks in air from the bottom of the hood and not at the top the best.

Appendix F

CURVE FIT RESULTS

F.1 Appendix Summary

This Appendix presents the results generated from the RS/1 curve fitting program. Normalized leach test results of silicon and sodium were fitted for this analysis. Each table contains two sub-tables, the parameter table and the AOV table. The parameter table shows parameters A and B, and B and C, for diffusion and saturation equations, respectively. The T value is also given which provides a confidence value of the fit to the individual data points. The AOV table presents the statistical data. The most important numbers are the F value and the square of the regression coefficient. The diffusion and saturation limit equations were represented by Leach Rate = $A*(time)^B$ and Leach Rate = C(1-exp(-B*time)), respectively.

Table F-1. Room Temperature Diffusion Curve Fit Results

Batch	Element	Parameter	Final Value	T Value	F Value	Mult R-SQ
29	Si	A	4.1E-5	17.6	2218	0.9995
		B	0.3327	16.2		
29	Na	A	2.7E-5	10.7	949	0.9989
		B	0.413	12.5		
32	Si	A	3E-7	4.7	195	0.997
		B	0.5357	7.6		
32	Na	A	8E-6	2.4	30	0.988
		B	0.3306	2.2		
56	Si	A	1.7E-5	2.34	92	0.995
		B	0.4476	4.3		
56	Na	A	7E-6	1.6	42	0.988
		B	0.4518	2.9		
59	Na	A	3E-6	3.0	194	0.9974
		B	0.5811	2.3		

Table F-2. Room Temperature Saturation Limit Curve Fit Results

Batch	Element	Parameter	Final Value	T Value	F Value	Mult R-SQ
29	Si	C B	1.19E-4 0.177	13.6 4.5	205	0.995
29	Na	C B	1.07E-4 0.125	10.0 3.8	151	0.993
31	Si	C B	3E-6 1.023	3.1 0.210	6.3	0.863
31	Na	C B	3E-5 0.677	5.9 0.78	24	0.9595
32	Si	C B	2E-6 0.0942	423 175	275200	0.9999
32	Na	C B	2.4E-5 0.185	15 5.5	206	0.998
35	Si	C B	1.72E-4 0.0246	1.2 0.87	59	0.983
35	Na	C B	3.52E-4 0.011	0.38 0.33	40	0.975
37	Si	C B	1E-7 0.599	15.6 2.48	172	0.994
37	Na	C B	2E-6 0.549	6.6 1.15	31	0.969
52	Si	C B	5E-6 0.193	1.02 0.11	0.9	0.632
52	Na	C B	2.4E-2 3.5E-5	0.019 0.018	17.7	0.972
56	Si	C B	1.33E-4 0.0347	25.7 10.6	920	0.9995
56	Na	C B	5.7E-5 0.0349	10.2 4.16	143	0.997
59	Si	C B	9.6E-3 3.6E-5	0.018 0.017	15.7	0.970
59	Na	C B	4.2E-5 0.021	4.6 2.3	69	0.993
61	Si	C B	1.01E-2 6.8E-5	0.01 0.01	5.7	0.919
61	Na	C B	5.85E-3 6.9E-5	0.012 0.011	6.9	0.932

Table F-3. 90°C Diffusion Curve Fit Results

Batch	Element	Parameter	Final Value	T Value	F Value	Mult R-SQ
56	Si	A	1.08E-4	2.9	135	0.992
		B	0.384	5.1		
56	Na	A	1.8E-5	2.7	290	0.997
		B	0.729	9.6		
59	Si	A	2.04E-4	13.8	2856	0.9997
		B	0.344	21.8		
59	Na	A	1.41E-4	21.1	7851	0.9999
		B	0.410	40.4		

Table F-4. 90°C Saturation Limit Curve Fit Results

Batch	Element	Parameter	Final Value	T Value	F Value	Mult R-SQ
52	Si	C	3.02E-4	14.9	170	0.994
		B	0.0711	3.9		
52	Na	C	3.05E-4	14.6	163	0.994
		B	0.0699	3.8		
56	Si	C	7.4E-4	5.7	31	0.969
		B	0.0277	1.9		
56	Na	C	1.3E-3	2.1	110	0.991
		B	0.005	1.4		
58	Si	C	2.88E-4	9.0	82	0.994
		B	0.084	2.6		
58	Na	C	3.04E-4	9.2	86	0.994
		B	0.0706	2.9		
59	Si	C	1.14E-3	11.4	112	0.991
		B	0.032	3.7		
59	Na	C	1.14E-3	9.3	94	0.989
		B	0.0236	3.2		
61	Si	C	3.46e-4	13.6	143	0.993
		B	0.0495	4.0		
61	Na	C	1.92E-4	14.4	158	0.994
		B	0.0745	3.6		

Appendix G

SEM-EDAX RESULTS

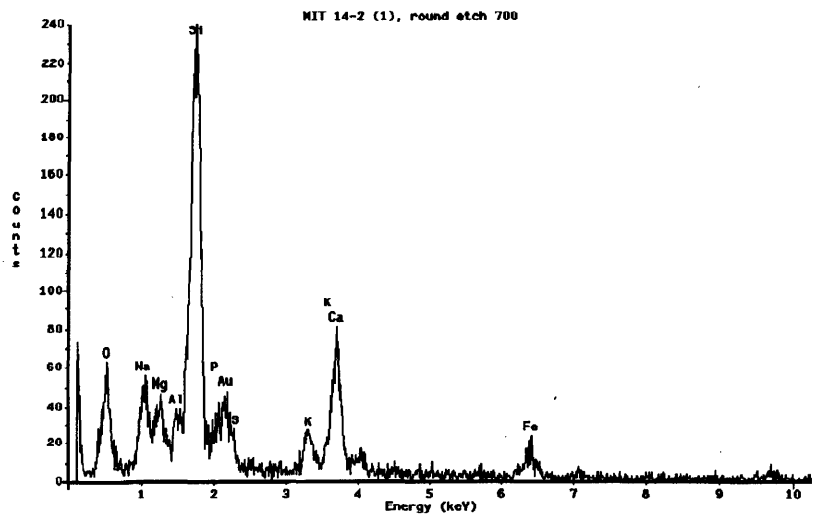

(a)

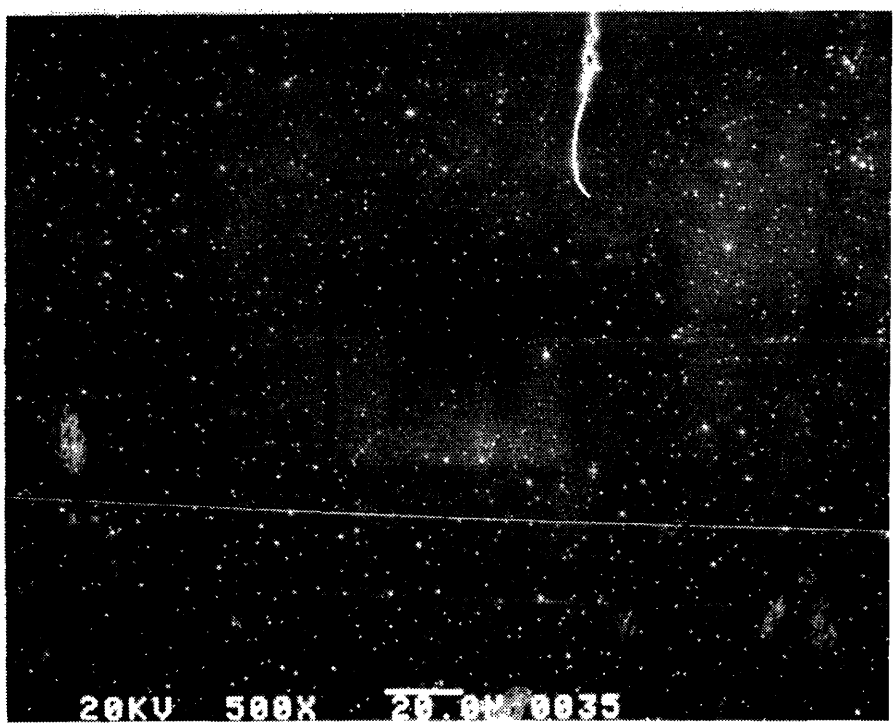

(b)

Fig. G-1. (a) EDAX point analysis of sharp edge of b. (b) Scanning electron micrograph of batch 37 after annealing and before MCC-1 leach test initiation showing smooth surface of glass at 500 magnification.

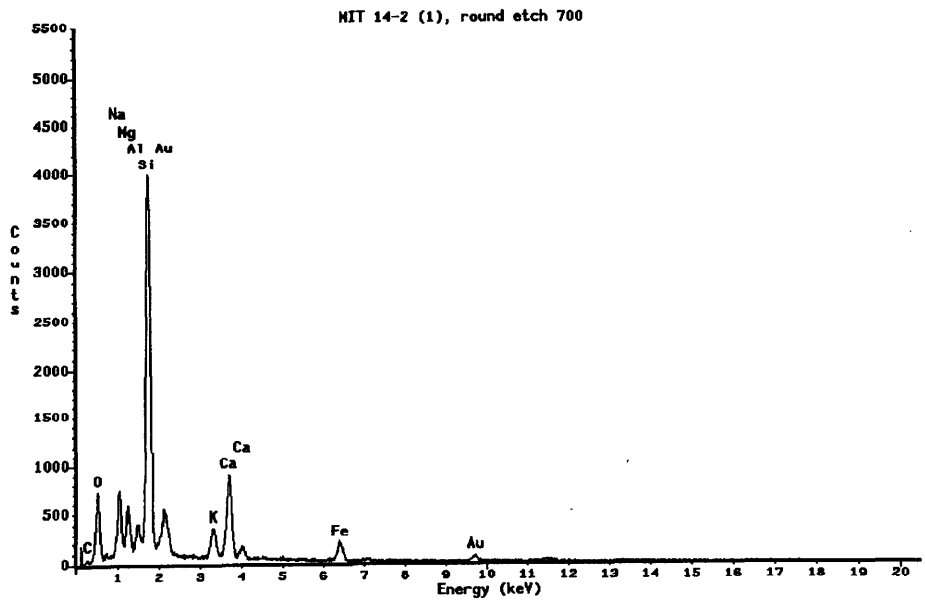

(a)

(b)

Fig. G-2. (a) EDAX analysis of point source on large chunk of b. (b) Scanning electron micrograph of batch 61 at 750 magnification showing large chunk of glass on smooth surface after annealing and before MCC-1 leach test analysis.

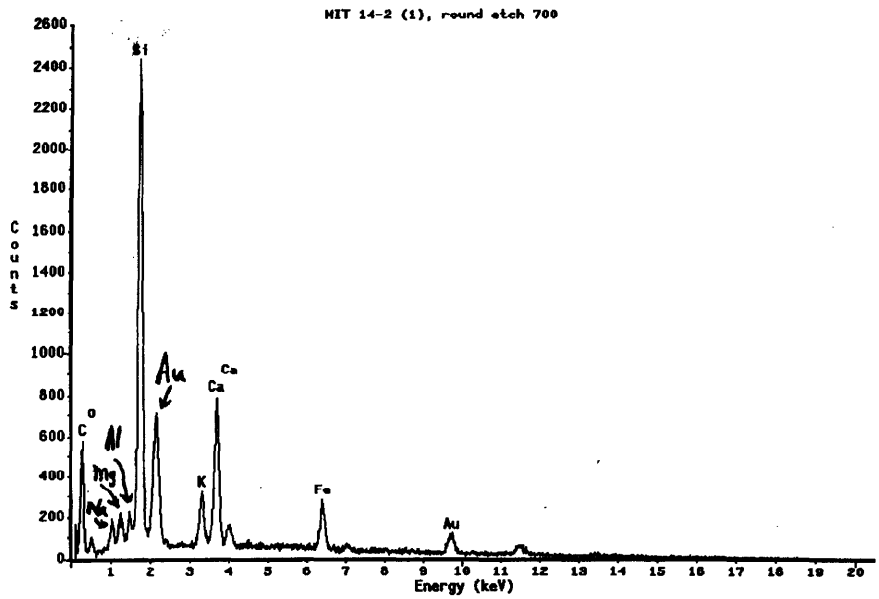

(a)

(b)

Fig. G-3. (a) EDAX analysis of tears in glass of picture b. (b) Scanning electron micrograph of batch 37 at 1000 magnification after annealing and before MCC-1 leach test analysis. Small holes and tears are present on the otherwise smooth glass surface.